TECHNICAL REPORT ARBRL-TR-02503

EXPERIMENTAL AND COMPUTATIONAL MODELING OF RAREFACTION WAVE ELIMINATORS SUITABLE FOR THE BRL 2.44 m SHOCK TUBE

George A. Coulter
Gerald Bulmash
Charles N. Kingery

June 1983

US ARMY ARMAMENT RESEARCH AND DEVELOPMENT COMMAND
BALLISTIC RESEARCH LABORATORY
ABERDEEN PROVING GROUND, MARYLAND

Destroy this report when it is no longer needed.
Do not return it to the originator.

Additional copies of this report may be obtained from the National Technical Information Service, U. S. Department of Commerce, Springfield, Virginia 22161.

The findings in this report are not to be construed as an official Department of the Army position, unless so designated by other authorized documents.

The use of trade names or manufacturers' names in this report does not constitute indorsement of any commercial product.

UNCLASSIFIED
SECURITY CLASSIFICATION OF THIS PAGE *(When Data Entered)*

REPORT DOCUMENTATION PAGE		READ INSTRUCTIONS BEFORE COMPLETING FORM
1. REPORT NUMBER TECHNICAL REPORT ARBRL-TR-02503	2. GOVT ACCESSION NO. AD A131 894	3. RECIPIENT'S CATALOG NUMBER
4. TITLE *(and Subtitle)* EXPERIMENTAL AND COMPUTATIONAL MODELING OF RAREFACTION WAVE ELIMINATORS SUITABLE FOR THE BRL 2.44 m SHOCK TUBE		5. TYPE OF REPORT & PERIOD COVERED Final 6. PERFORMING ORG. REPORT NUMBER
7. AUTHOR(s) George A. Coulter, Gerald Bulmash, Charles N. Kingery		8. CONTRACT OR GRANT NUMBER(s)
9. PERFORMING ORGANIZATION NAME AND ADDRESS US Army Ballistic Research Laboratory ATTN: DRDAR-BLT Aberdeen Proving Ground, MD 21005		10. PROGRAM ELEMENT, PROJECT, TASK AREA & WORK UNIT NUMBERS 1L162618AH80
11. CONTROLLING OFFICE NAME AND ADDRESS US Army Armament Research and Development Command US Army Ballistic Research Laboratory (DRDAR-BLA-S) Aberdeen Proving Ground, MD 21005		12. REPORT DATE June 1983 13. NUMBER OF PAGES 117
14. MONITORING AGENCY NAME & ADDRESS*(if different from Controlling Office)*		15. SECURITY CLASS *(of this report)* UNCLASSIFIED 15a. DECLASSIFICATION/DOWNGRADING SCHEDULE

16. DISTRIBUTION STATEMENT *(of this Report)*

Approved for public release; distribution unlimited.

17. DISTRIBUTION STATEMENT *(of the abstract entered in Block 20, if different from Report)*

18. SUPPLEMENTARY NOTES

19. KEY WORDS *(Continue on reverse side if necessary and identify by block number)*

Blast Rarefaction	Pressure-Time Records
Blast Reflection	Rarefaction Wave Eliminator
Blast Simulator	Shock Tube
Hydrocode	NASA-Ames Code
Negative Pressure	

20. ABSTRACT *(Continue on reverse side if necessary and identify by block number)*

Three general types of rarefaction wave eliminators, RWEs (solid plate, vented plate, and lattice) were tested on a 1/48th scale model of the BRL 2.44 m shock tube. Pressures were monitored along the test section with piezoelectric transducers to determine effectiveness of the RWEs tested. All types were found to be equally effective in reducing the rarefactions but the lattice type was most difficult to use. The solid plate and vented plate RWEs would both be suitable for the 2.44 m shock tube. Predictions

DD FORM 1 JAN 73 1473 EDITION OF 1 NOV 65 IS OBSOLETE

UNCLASSIFIED
SECURITY CLASSIFICATION OF THIS PAGE *(When Data Entered)*

are produced using the NASA-Ames one-dimensional computer hydrocode. The hydrocode can be used effectively to model a RWE for the 2.44 m shock tube. Experimental and computational results are compared.

TABLE OF CONTENTS

BLANK PAGE

LIST OF ILLUSTRATIONS

LIST OF ILLUSTRATIONS (Continued)

LIST OF ILLUSTRATIONS (Continued)

LIST OF ILLUSTRATIONS (Continued)

LIST OF TABLES

I. INTRODUCTION

The general objective of the test series presented in this report was to determine a concept of a rarefaction wave eliminator suitable for use on the Ballistic Research Laboratory's (BRL) 2.44 m shock tube/blast simulator. The necessary parameters for the rarefaction wave eliminator were to be determined from both scaled (1/48th) shock tube experiments and from results of predictions obtained by the NASA-Ames one-dimensional computer hydrocode.[1]

The study included three general types of rarefaction wave eliminators (RWEs). The first, Type A, consisted of a solid reflecting plate[2] placed outside the open end of the test section of the scaled shock tube. The standoff distance of the RWE was varied as a function of the input shock overpressure. The second RWE, Type B, consisted of vented plates[3,4] also combined with standoff distances. The third RWE type tested, Type C, consisted of lattice strips across the end of the test section. No standoff distance was used for this type of RWE.

The hydrocode was utilized to simulate a RWE on a computer generated 1/48 scale model of the BRL 2.44 m shock tube. This computational RWE represents a solid plate with one circular vented area in the center of the plate and no standoff. It most closely resembles experimental Type B, without standoff.

II. EXPERIMENT

This section describes the shock tube used for the tests, the associated instrumentation, and a description of the three general types of rarefaction wave eliminator models tested.

A. Modified 5.08 cm Inside Diameter Shock Tube

The BRL standard calibration shock tube[5] was modified in both driver and test section lengths so as to model at 1/48th scale the BRL 2.44 m

---

[1] *Andrew Mark, "Computational Design of Large Scale Blast Simulators," AIAA 19th Aerospace Sciences Meeting, January 12 - 15, 1981, St. Louis, MO.*

[2] *J. J. Yagla, and others, "The Waves System in Explosively Driven Conical Shock Tubes," Second MABS, DNA 2275P, The Naval Weapons Laboratory, Dahlgren, VA, 2 - 5 November 1970.*

[3] *J. R. Crosnier and J. B. G. Monsac, "Large Diameter High Performance Blast Simulators," Fifth MABS, Stockholm, May 23 - 26, 1977.*

[4] *W. Haverdings, "Preliminary Design of the 2.0 m Diameter FOE - Driven Blast Simulator," Seventh MABS, Medicine Hat, Alberta, Canada, 13 - 17 July 1981.*

[5] *George A. Coulter, "Dynamic Calibration of Pressure Transducers at the BRL Shock Tube Facility," BRL Memorandum Report 1843, May 1967 (AD 654508).*

shock tube.[6] See Figure 1 for a sketch of this shock tube. Figure 2 shows a sketch of the 5.08 cm shock tube as modified to give the 1/48th scale desired.

The shock tube was operated in an air-air mode with the downstream test section end modified for the RWEs. The different types of the rarefaction wave eliminators were tested for effectiveness as compared with the open end test results. The diaphragms were chosen to burst at the driver pressure necessary to cover the desired input shock overpressure range of 25 (3.6 psi) to 125 (18 psi) kPa. This range would include the most useful range of tests at the BRL 2.44 m shock tube.

Four transducer stations were located at the distances from the diaphragm section as shown on Figure 2. These stations' locations, when scaled up, corresponded to the present test stations for the full-sized shock tube (2.44 m diameter). The pressure transducers and associated electronics are described in the next section.

B. Instrumentation

A schematic of the data acquisition-reduction system is shown in Figure 3. Piezoelectric quartz transducers were used in the shock tube test section to monitor the shock wave interactions. The effects on the wave system caused by the different rarefaction wave eliminators were evaluated for effectiveness from the pressure transducer results.

The transducers were coupled through a power supply and data amplifiers to a digitizing oscilloscope. Onsite comparisons of the results were made directly from the oscilloscope. Final data processing was completed with the computer, printer, and plotter. Tables and plots of pressure-time records for the various test stations are presented for comparison of the results.

C. Types of Rarefaction Wave Eliminators

Three general types of rarefaction wave eliminators (RWE) were modeled for the present test series. They are shown in Figure 4 and listed in the data tables as Types A, B, and C.

The least complicated RWE, Type A, consisted simply of a solid circular reflecting plate spaced at varying distances from the open end of the shock tube test section. The second type of RWE, Type B, consisted also of a circular plate with a standoff distance, but the plate was, in addition, vented. Variations of the shape of the vented opening were tested. A single rectangular hole, a single circular hole, and a number of circular holes were tried for a given standoff distance. Both shape and percentage RWE opening were varied to determine the effectiveness of the RWEs. The third type of RWE, Type C,

[6] *Brian P. Bertrand, "BRL Dual Shock Tube Facility," BRL Memorandum Report 2001, August 1969 (AD 693264).*

NOTES:

1. DIAMETER NOT TO SCALE
2. DIMENSIONS IN METRES

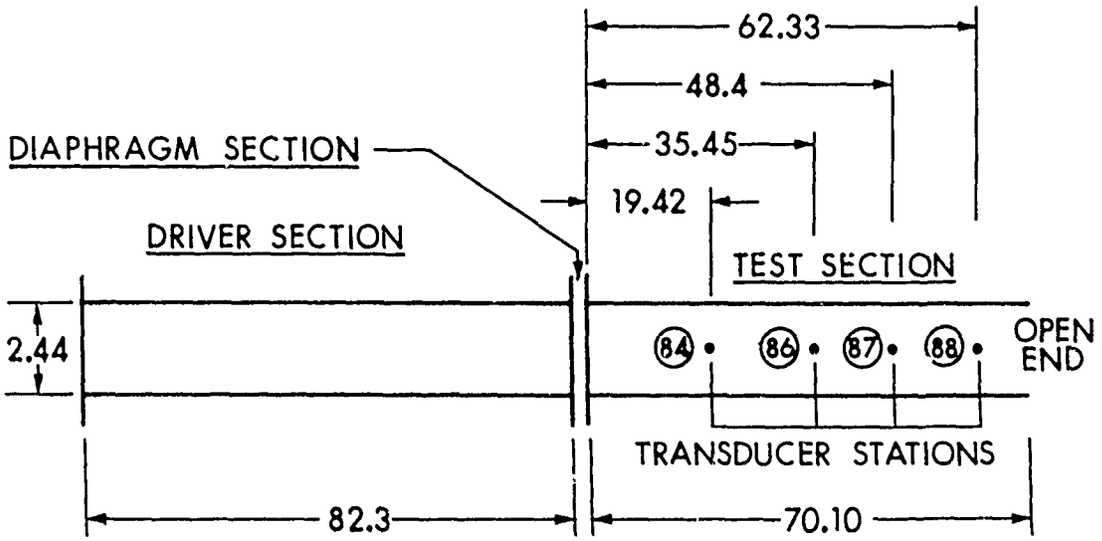

Figure 1. Sketch of BRL 2.44 m shock tube

NOTES:

1. DIAMETER NOT TO SCALE
2. DIMENSIONS IN METRES

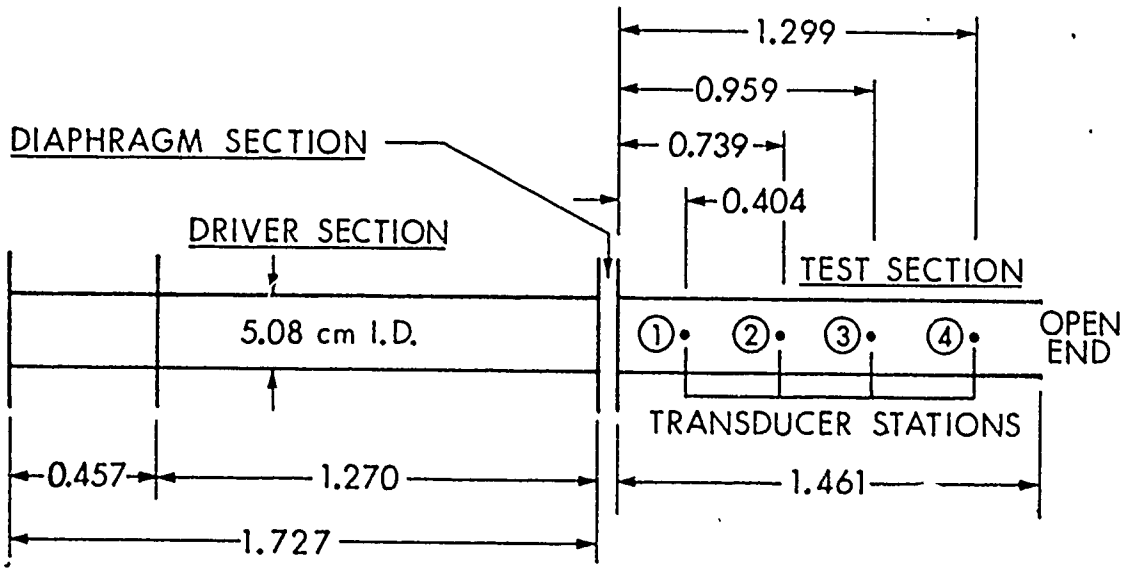

Figure 2. Sketch of modified 5.08 cm inside diameter shock tube

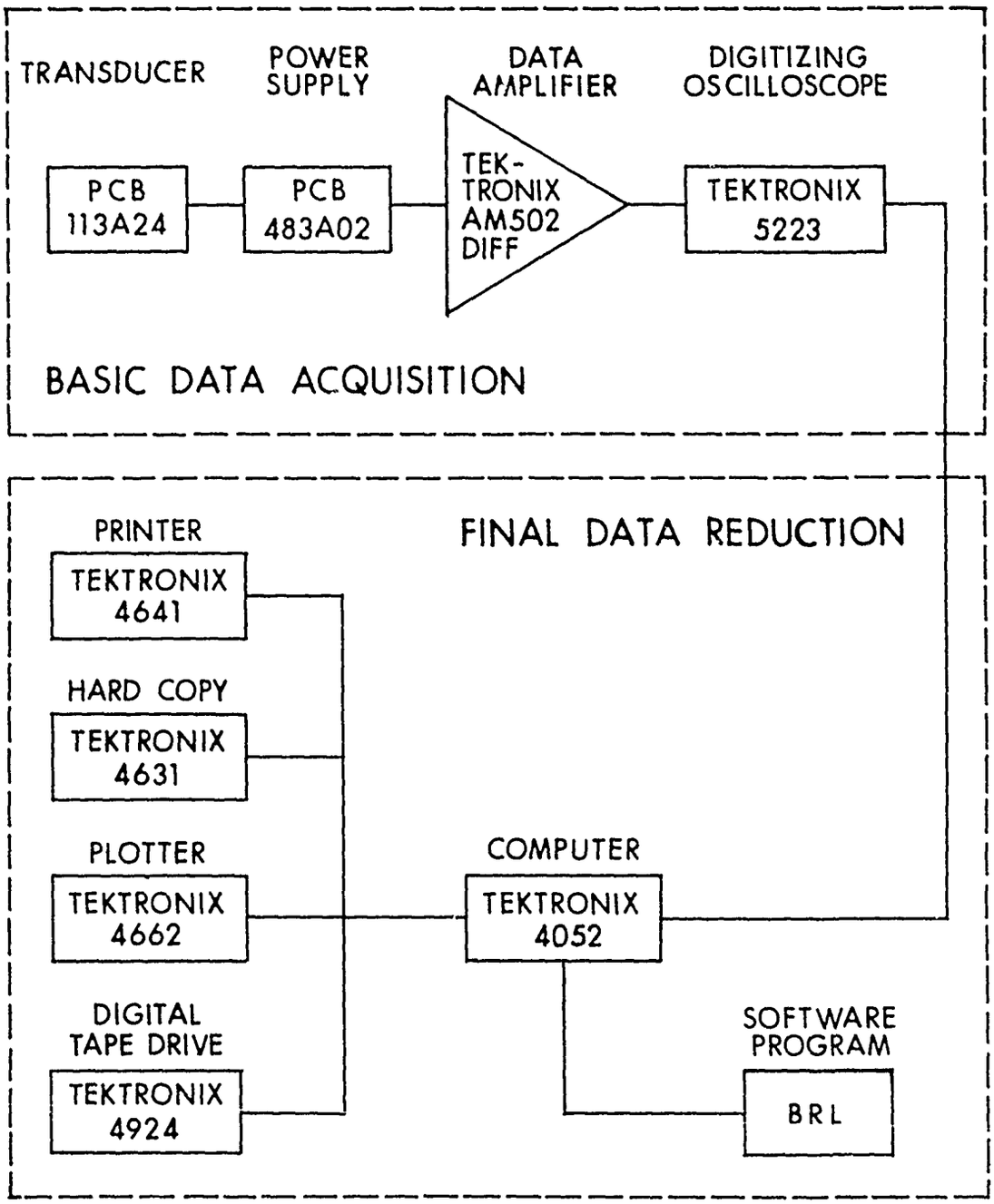

Figure 3. Schematic of data acquisition-reduction system

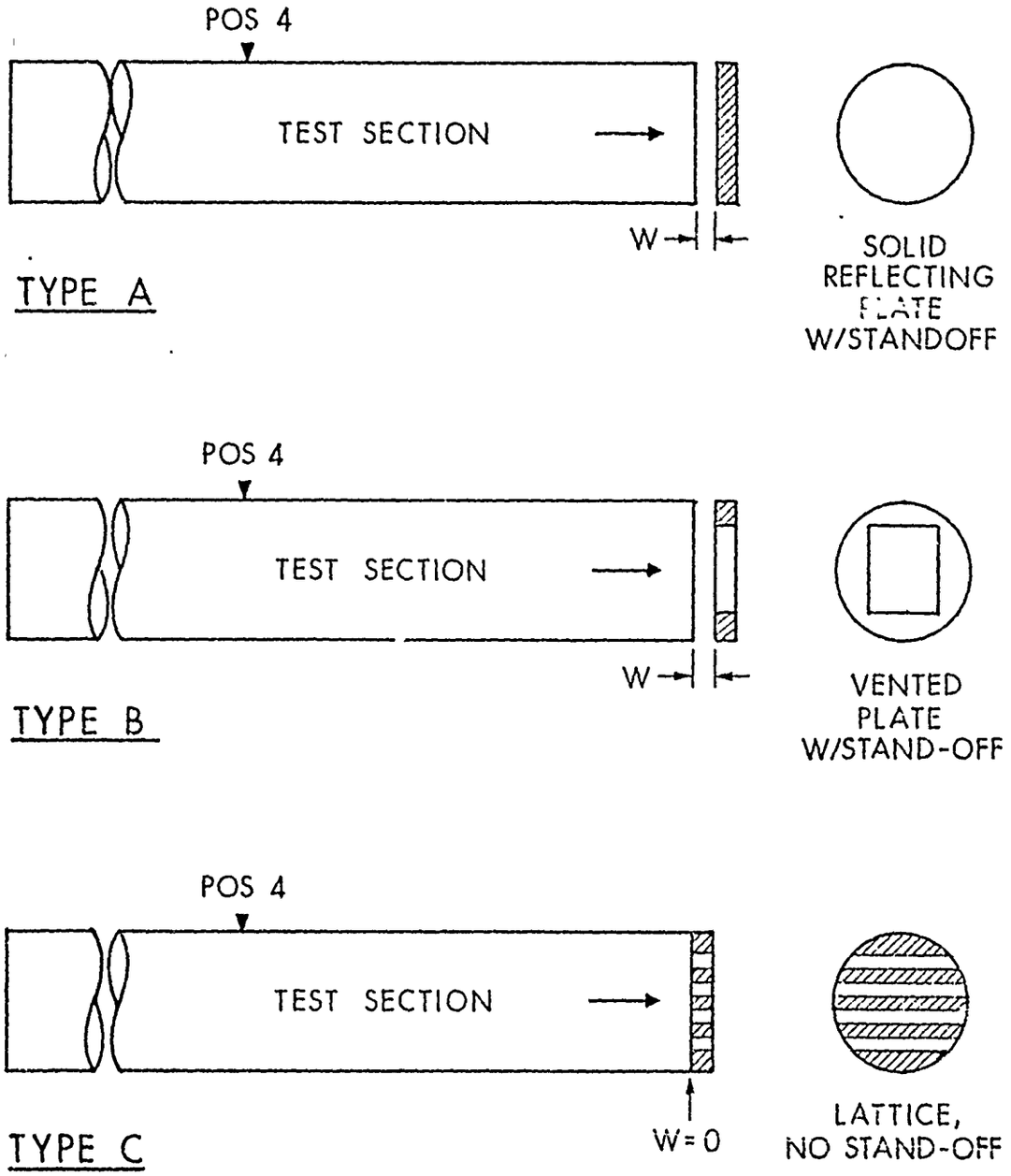

Figure 4. Types of rarefaction wave eliminators

was a very simple version of one used at the French[7] blast simulator facility at Gramat, France. The programable moving venetian blind type lattice used there, although effective, was thought not to be cost effective for use at the BRL 2.44 m shock tube. Instead a simple fixed lattice RWE was used as a substitute in the present tests. Lattice slats were removed to vary the venting area.

III. RESULTS

The results are summarized in the data tables and with pressure-time records to illustrate the effectiveness of the three general types of rarefaction wave eliminators tested.

A. Data Table

The pertinent shot parameters are listed in Table 1 for the types of RWEs tested and the input shock pressure level used. Table 1 also summarizes the parameters pertinent to the individual RWEs, such as standoff distance and ratio of vented opening to total shock tube cross section.

Presented also are the standoff distances necessary to eliminate the rarefactions as completely as possible for a Type A RWE for the range of input pressures from 23 to 124 kPa. The vented area listed in all cases is the effective area. Obstruction of fasteners used to mount the RWE was subtracted out of the vent area. The listed effective vented ratio varied from about 21 percent to 81 percent over the pressure range tested.

Also shown is a comparison of the Type B vented plate RWEs with standoff distances which were used to furnish part of the vented area. Again the input pressure versus effective vented area appeared similar to the solid plate. Vent area ratios range from 43 to 84 percent.

The lattice RWE was used without a standoff distance. The braces used to combine shots in Table 1 indicate an interpolation between shots to find the listed input pressure for the given vented area ratio. The lattice RWE is more cumbersome and less accurate to use for this reason. If the vented area is too large for a specific shock overpressure the reflected wave moving back up the tube will be too small and rarefaction effects will not be completly eliminated. Conversely, a vented area too small will reflect a shock which will be too large and again the loading on the target will not be realistic.

B. Pressure-Time Records without RWE

The first series of records shown in Figures 5 - 8 illustrate the pressure-time waveforms obtained for four side-on overpressure levels at the

---

[7] *C. Languin, "Simulation of Shock and Blast Expansion Wave Compensator for 2.40 m Diameter Shock Tube, Description, Report of Its Behavior in Response to Blast Waves," Centre d'Etudes de Gramat, Technical Note T-76-29, May 1976.*

Written material continued on page 29.

TABLE 1. SHOT PARAMETERS

Shot and Station No.	No.	Shock Over-pressure kPa	Type RWE	Standoff Distance cm	Vent Area Ratio	Comment
2-82-8	1	23.9	none	NA	1.00	Open tube
	2	23.9				
2-82-2	3	25.2				
	4	23.2				
2-82-7	1	54.5	none	NA	1.00	Open tube
	2	54.5				
2-82-1	3	55.3				
	4	51.7				
2-82-6	1	84.1	none	NA	1.00	Open tube
	2	87.2				
2-82-3	3	91.7				
	4	84.1				
2-82-5	1	116.7	none	NA	1.00	Open tube
	2	118.6				
2-82-4	3	122.0				
	4	110.3				
2-82-24	2	25.0	none	NA	1.00	Open tube
	3 Stag	29.0				
2-82-23	2	58.6	none	NA	1.00	Open tube
	3 Stag	71.7				
2-82-22	2	91.4	none	NA	1.00	Open tube
	3 Stag	128.9				

TABLE 1. SHOT PARAMETERS (Continued)

Shot and No.	Station No.	Shock Over-pressure kPa	Type RWE	Standoff Distance cm	Vent Area Ratio	Comment
2-82-21	2	124.8	none	NA	1.00	Open tube
	3 Stag	182.7				
2-82-54	2	23.4	none	NA	1.00	Open tube
	3	25.5				
2-82-51	2	59.6	none	NA	1.00	Open tube
	3	62.7				
2-82-52	2	91.0	none	NA	1.00	Open tube
	3	94.5				
2-82-53	2	118.5	none	NA	1.00	Open tube
	3	125.0				
2-82-16	3	22.8	A - Solid Plate			
	4	23.4		0.47	0.212	
2-82-14	2	93.1	A			
	3	95.5		1.12	0.698	
2-82-15	2	118.9	A			
	3	124.1		1.30	0.811	
2-82-17	2	26.3	A			
	3 Stag	28.3		0.47	0.212	
2-82-18	2	58.6	A	0.90	0.557	
	3 Stag	72.4				

TABLE 1. SHOT PARAMETERS (Continued)

Shot and Station No.	Station No.	Shock Over-pressure kPa	Type RWE	Standoff Distance cm	Vent Area Ratio	Comment
2-82-19	2	90.7	A			
	3 Stag	122.4		1.12	0.698	
2-82-20	2 Stag	123.1	A			
	3	177.9		1.30	0.811	
2-82-97	3	25.2	A	0.67	0.253	
2-82-100	3	39.6	A	0.80	0.415	
2-82-101	3	65.1	A	1.00	0.541	
2-81-102	3	75.6	A	1.10	0.603	
2-82-104	3	100.0	A	1.30	0.727	
2-82-32	2	24.5	B Hole Size			
	3	26.5	2.54 x 3.49 cm	0.0	0.438	
2-82-31	2	56.9	B Hole Size			
	3	59.6	2.54 x 3.49 cm	0.30	0.540	
2-82-30	2	95.8	B Hole Size			
	3	99.3	2.54 x 3.49 cm	0.60	0.729	
2-82-29	2	123.4	B Hole Size			
	3	129.6	2.54 x 3.49 cm	0.75	0.820	

TABLE 1. SHOT PARAMETERS (Continued)

Shot and No.	Station No.	Shock Over-pressure kPa	Type RWE	Standoff Distance cm	Vent Area Ratio	Comment
2-82-25	2	25.0	B Hole Size			
	3 Stag	30.0	2.54 x 3.49 cm	0.0	0.438	
2-82-26	2	57.9	B Hole Size			
	3 Stag	71.7	2.54 x 3.49 cm	0.30	0.540	
2-82-27	2	94.5	B Hole Size			
	3 Stag	127.6	2.54 x 3.49 cm	0.60	0.729	
2-82-28	2	123.4	B Hole Size			
	3 Stag	179.3	2.54 x 3.49 cm	0.75	0.820	
2-82-34	2	25.3	B Hole Size			
	3	26.5	3.33 cm Dia.	0.0	0.431	
2-82-35	2	58.6	B Hole Size			
	3	60.3	3.33 cm Dia.	0.30	0.533	
2-82-36	2	91.7	B Hole Size			
	3	95.1	3.33 cm Dia.	0.60	0.722	
2-82-37	2	121.3	B Hole Size			
	3	122.4	3.33 cm Dia.	0.75	0.815	
2-82-49	2	25.5	B Hole Size			
	3 Stag	29.6	3.33 cm Dia.	0.0	0.431	
2-82-48	2	56.5	B Hole Size			
	3 Stag	71.0	3.33 cm Dia.	0.30	0.533	

TABLE 1. SHOT PARAMETERS (Continued)

Shot and No.	Station No.	Shock Over-pressure kPa	Type RWE	Standoff Distance cm	Vent Area Ratio	Comment
2-82-47	2	93.1	B Hole Size			
	3 Stag	129.6	3.33 cm Dia.	0.60	0.722	
2-82-46	2	125.5	B Hole Size			
	3 Stag	186.2	3.33 cm Dia.	0.75	0.815	
2-82-41	2	24.8	B 10 Holes			
	3	26.2	1 cm Dia.	0.0	0.452	
2-82-40	2	58.6	B 10 Holes			
	3	59.3	1 cm Dia.	0.30	0.554	
2-82-39	2	95.3	B 10 Holes			
	3	100.0	1 cm Dia.	0.60	0.743	
2-82-38	2	120.0	B 10 Holes			
	3	123.4	1 cm Dia.	0.75	0.836	
2-82-42	2	25.2	B 10 Holes			
	3 Stag	29.6	1 cm Dia.	0.0	0.452	
2-82-43	2	54.5	B 10 Holes			
	3 Stag	68.3	1 cm Dia.	0.30	0.554	
2-82-44	2	98.3	B 10 Holes			
	3 Stag	138.6	1 cm Dia.	0.60	0.743	
2-82-45	2	124.1	B 10 Holes			
	3 Stag	184.8	1 cm Dia.	0.75	0.836	

TABLE 1. SHOT PARAMETERS (Continued)

Shot and Station No.	No.	Shock Over-pressure kPa	Type RWE	Standoff Distance cm	Vent Area Ratio	Comment
2-82-56	2	24.7	C Lattice			
	3	26.7	5 Slats	0.0	0.465	
2-82-57	2	45.0	C Lattice			
	3	47.6	5 Slats	0.0	0.465	
2-82-58	2	58.6	C Lattice			
	3	61.7	2 Slats	0.0	0.716	
2-82-59	2	105.5	C Lattice			
	3	111.7	2 Slats	0.0	0.716	
2-82-60	2	92.4	C Lattice			
	3	95.8	1 Slat	0.0	0.868	
2-82-61	2	103.4	C Lattice			
	3	108.9	1 Slat	0.0	0.868	
2-82-62	2	124.0	C Lattice			
	3	130.3	1 Slat	0.0	0.868	
2-82-108	3	24.7	C Lattice 5 Slats	0.0	0.465	
2-82-109	3	38.7	C Lattice 5 Slats	0.0	0.465	

TABLE 1. SHOT PARAMETERS (Continued)

Shot and Station No.	Station No.	Shock Over-pressure kPa	Type RWE	Standoff Distance	Vent Area Ratio	Comment
2-82-110	3	63.6	C Lattice 4 Slats	0.0	0.597	
2-82-113	3	83.7	C Lattice 2 Slats	0.0	0.705	
2-82-116	3	171.5	C Lattice 1 Slat	0.0	0.879	

NOTES: 1 - Cross Sectional Area of Shock Tube is 20.26 cm^2

2 - Ambient Temperature Range 18.2 · 22.0 ^oC

3 - Ambient Pressure, 99.1 - 104.1 kPa

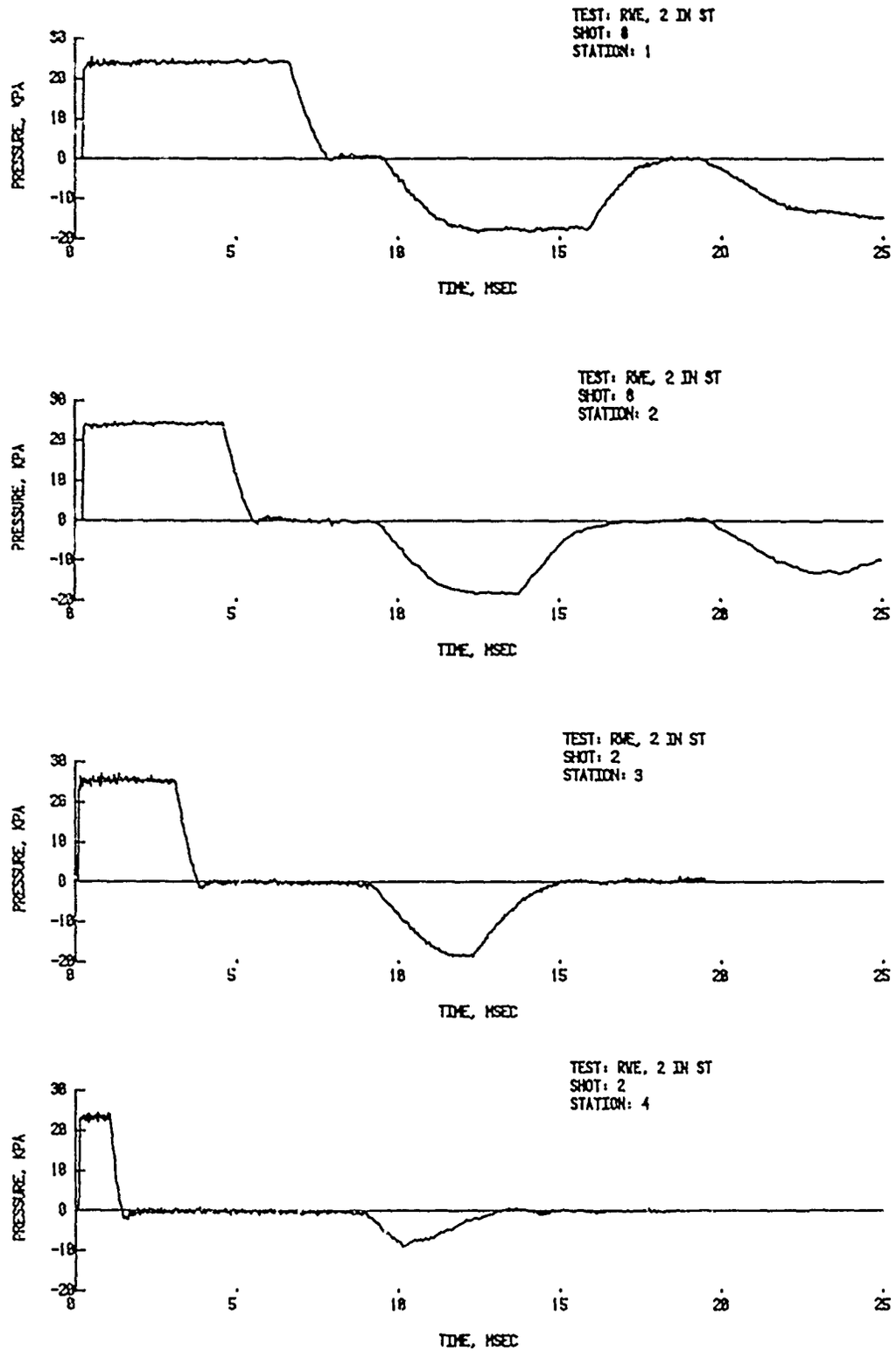

Figure 5. Pressure-time records - test section open, average input pressure 24.1 kPa

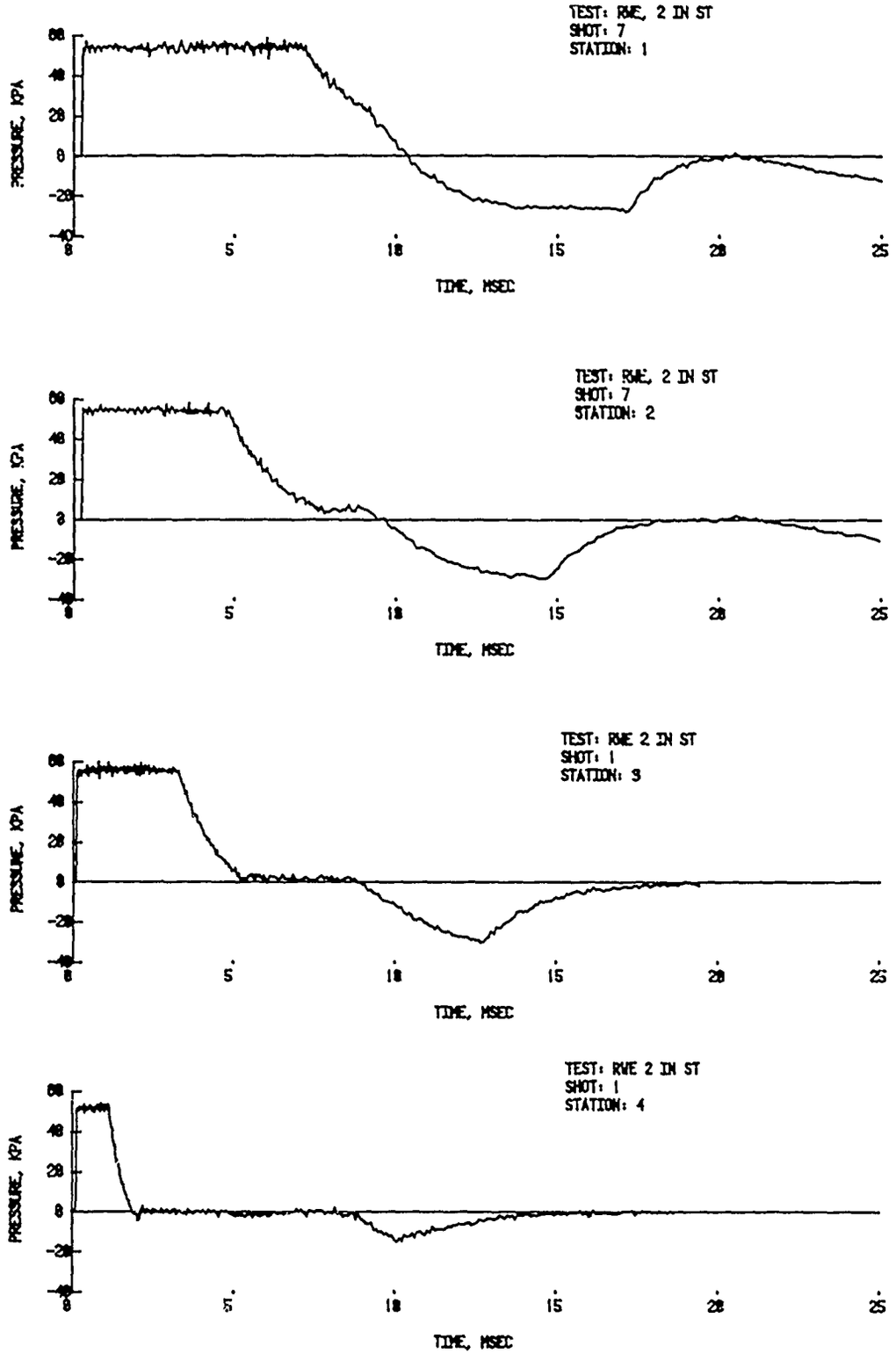

Figure 6. Pressure-time records - test section open, average input pressure 54.0 kPa

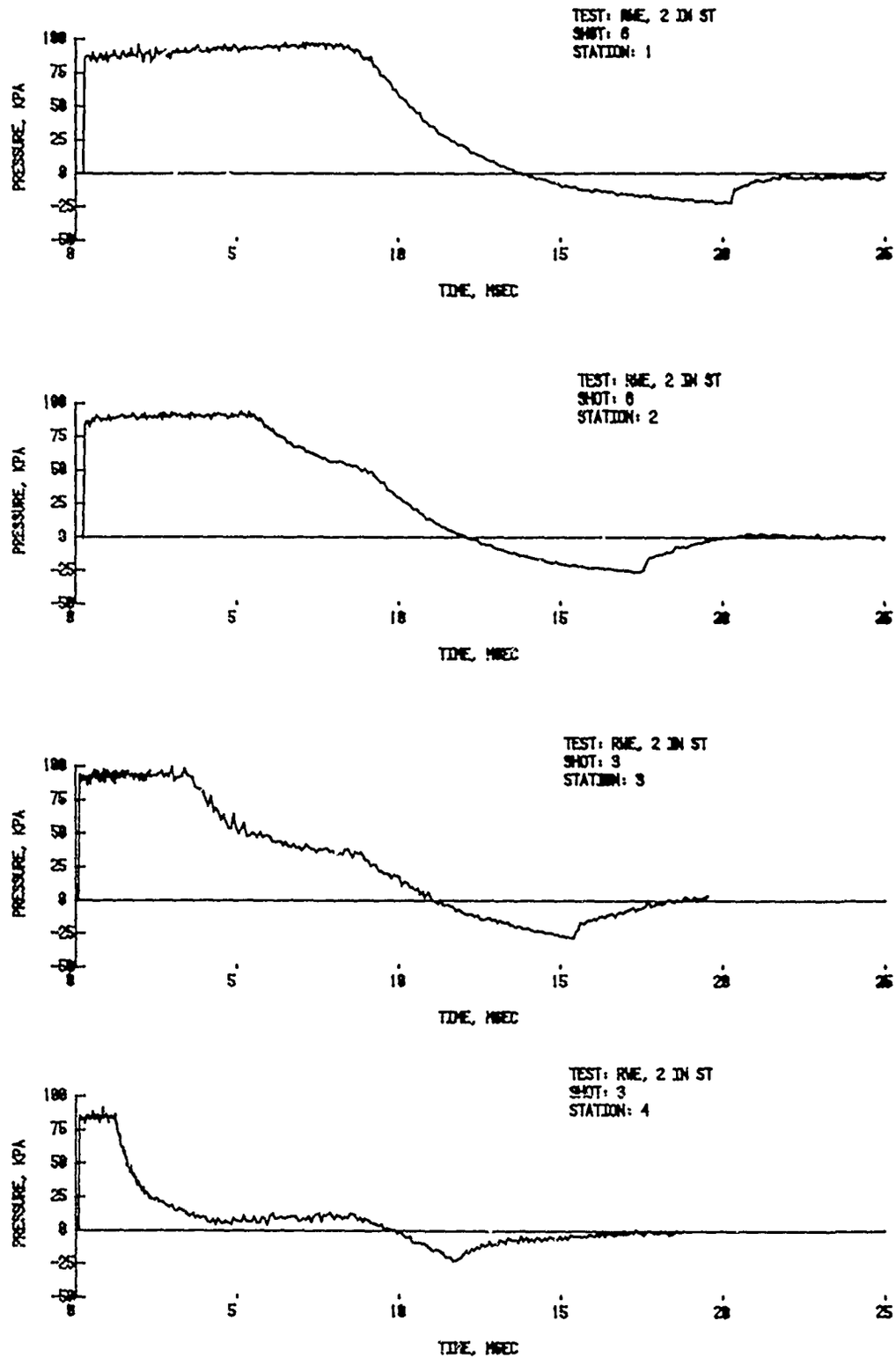

Figure 7. Pressure-time records - test section open, average input pressure 86.8 kPa

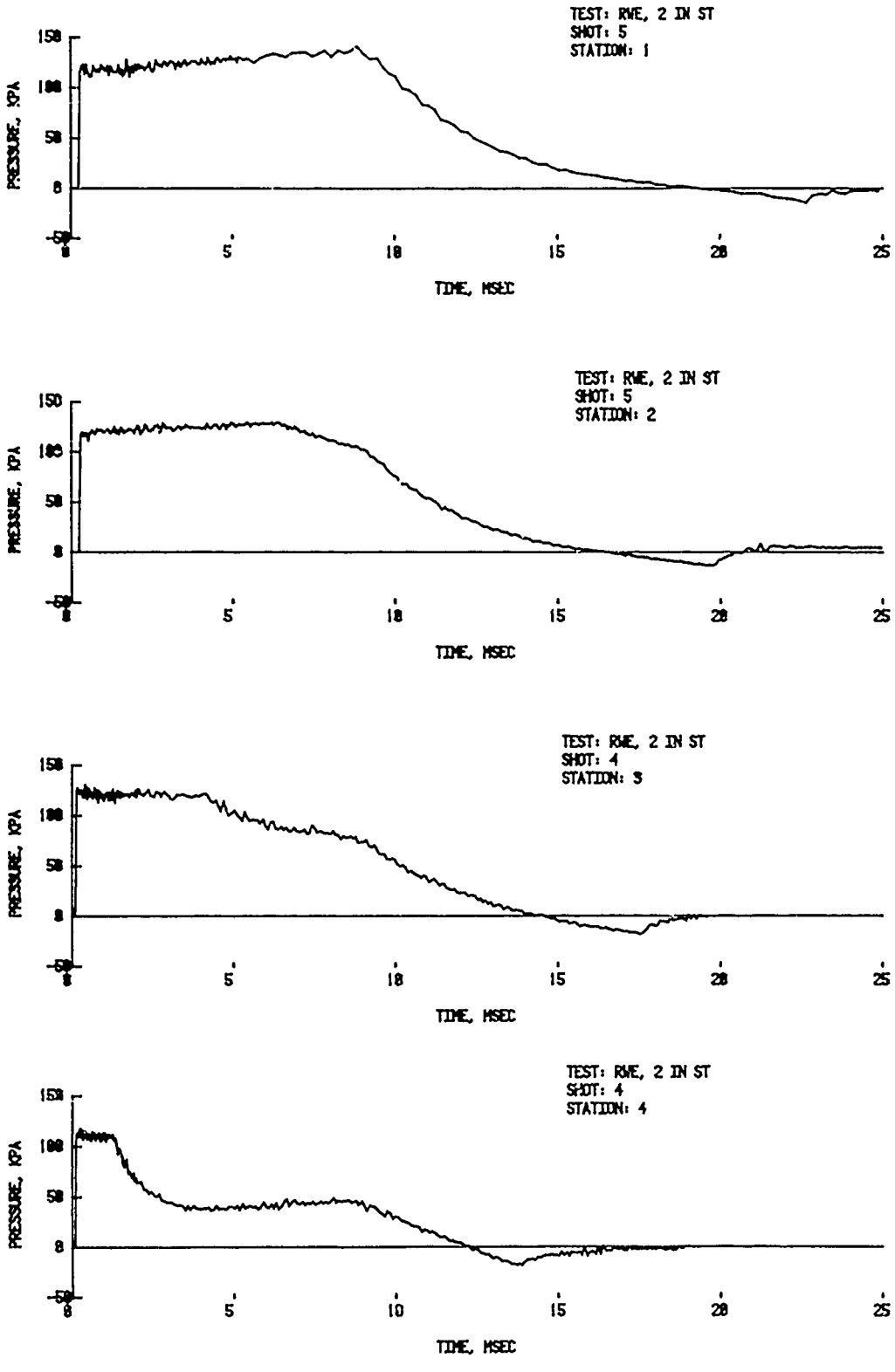

Figure 8. Pressure-time records - test section open, average input pressure 116.9 kPa

four test stations. These correspond to the current test stations (multiply time by 48) in the BRL 2.44 m shock tube. The effect of the two types of rarefaction wave can be traced from station to station. The first rarefaction following the flat part of the pressure records is the one propagated upstream from the open end of the test section. The second rarefaction arrives from the closed end of the driven section after about 10 ms. Both rarefaction waves degrade the positive wave duration and significantly change the flow conditions behind the shock front.

Test Station 3 (87 in the 2.44 m shock tube) was of the most interest since the large tube's test platform is located at this point. Therefore, stagnation records were also taken in the 5.08 cm shock tube corresponding to the test platform's location. Figure 9 shows these records from Station 3 over the input pressure range of the test.

Figures 10 - 13 (bottom traces) show records of subtractions of the side-on pressure from the stagnation pressure. This difference is a measure of the dynamic load (compressible Q) available to a test target. Figure 11 (bottom trace) illustrates the effects of the two rarefaction waves on the drag load. The dynamic pressure increases rapidly at the arrival of the open-end rarefaction wave $\sim$4 ms and decreased upon the arrival of the closed-end rarefaction wave $\sim$9 ms. At this input pressure level the drag load on the face of the test target will increase to over four times the desired load. The test target might, therefore, be over-ranged, making any given test on it invalid.

C Pressure-Time Records with RWE

The addition of a RWE on the open-end of the shock tube provides a reflected shock and a rarefaction wave. As the initial shock wave reaches the RWE, both the reflected shock which comes from the solid structure of the RWE, and the rarefaction wave which comes from the opening in the RWE, begin to travel up the tube against the flow. By adjusting the opening of the RWE the strength of both the reflected shock and the rarefaction wave can be tailored to minimize the flow perturbation in the test section. Figures 14 - 17 show records taken from Station 3 with a Type A solid plate RWE in place at the end of the test section. A comparison of Figure 15 with Figure 11 illustrates the smoothed drag loading and more correct input load for a test of a drag target, as well as a longer duration shock wave.

Figures 18 - 21 show the same range of tests and subtractions of records for a Type B, vented plate RWE. The pressure-time records do not look significantly different from those obtained using the Type A, a solid plate RWE. Both appear to be equally effective in eliminating the effects of the rarefaction wave.

The lattice RWE, Type C, was found to be difficult to adjust to just eliminate the rarefactions. Accordingly, no stagnation pressure-time records were taken with the lattice RWE. If the reflecting area of the RWE is too small then the reflected wave will be too small in magnitude and will appear as shown in Figure 22 on Shot 58. Conversely, if the reflecting area is too large then the reflected wave will be too large and will appear as shown in Shot 57 in Figure 22. The venting area at the end of the shock tube must be matched with the overpressure reaching the end of the tube in order to eliminate the effects of the rarefaction wave.

Written material continued on page 46.

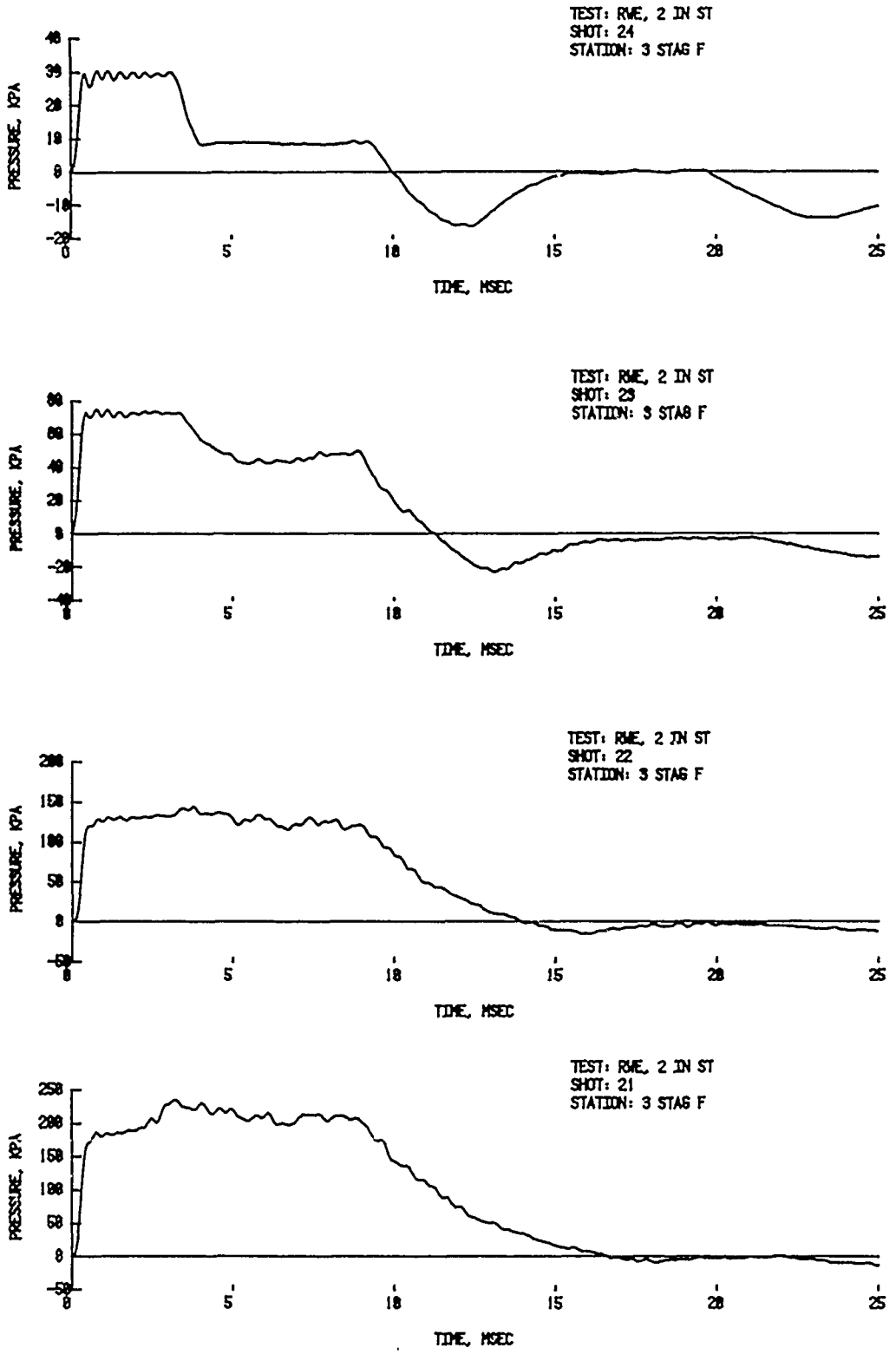

Figure 9. Stagnation pressure-time records - test section open, input pressures 25, 58.6, 91.4 and 124.8 kPa

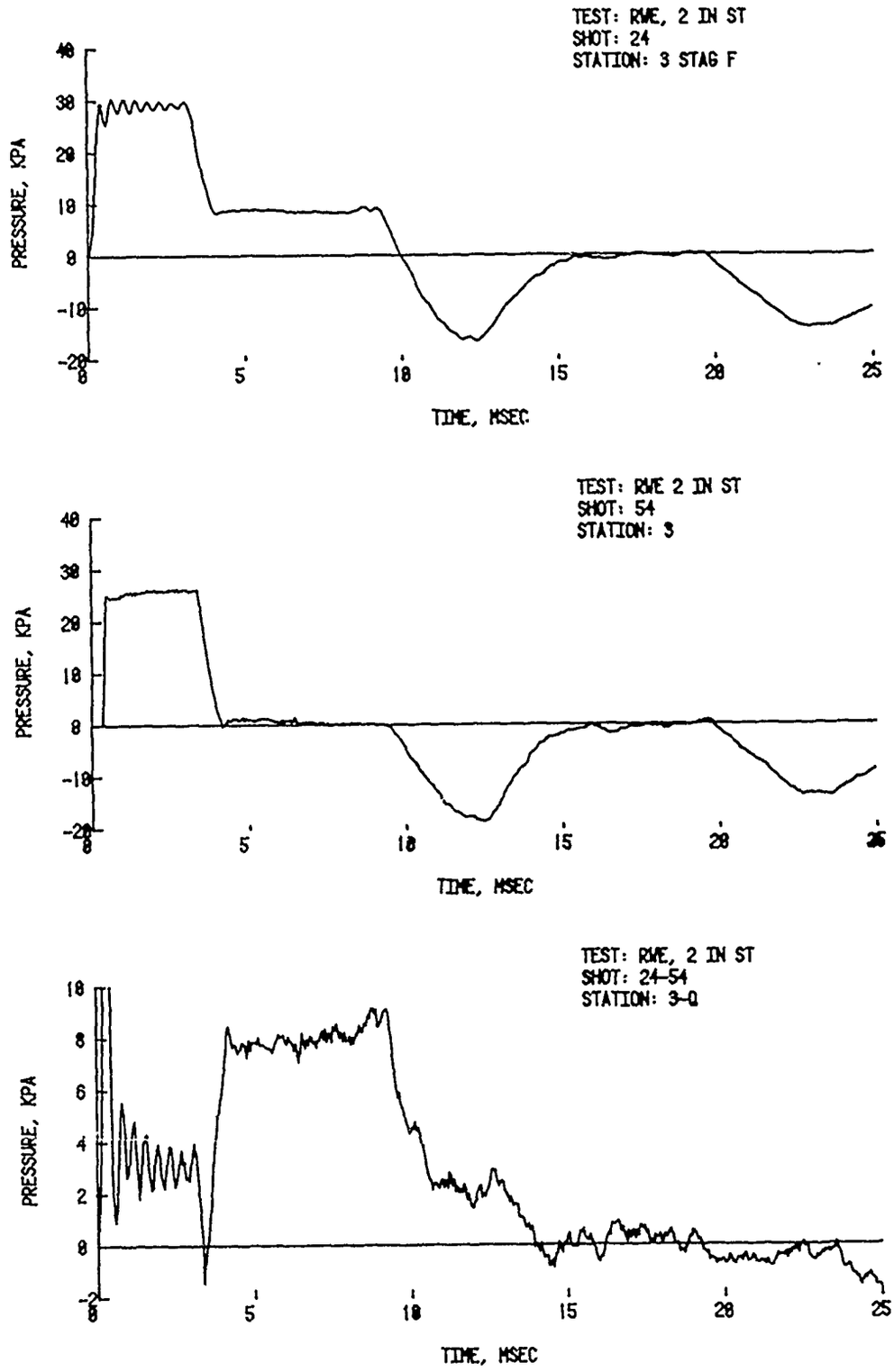

Figure 10. Stagnation pressure minus side-on - test section open, average input pressure 24.2 kPa

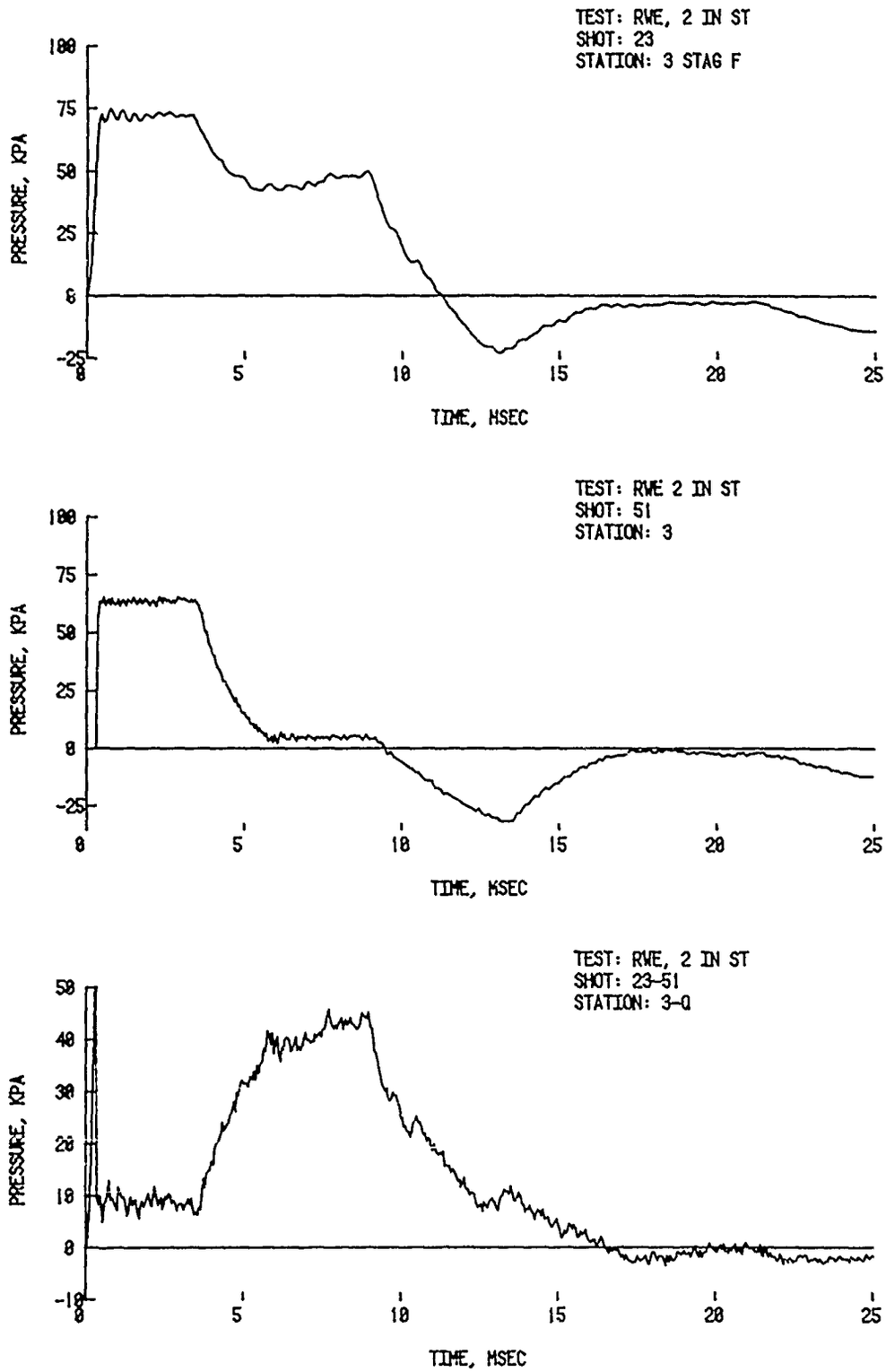

Figure 11. Stagnation pressure minus side-on - test section open, average input pressure 59.0 kPa

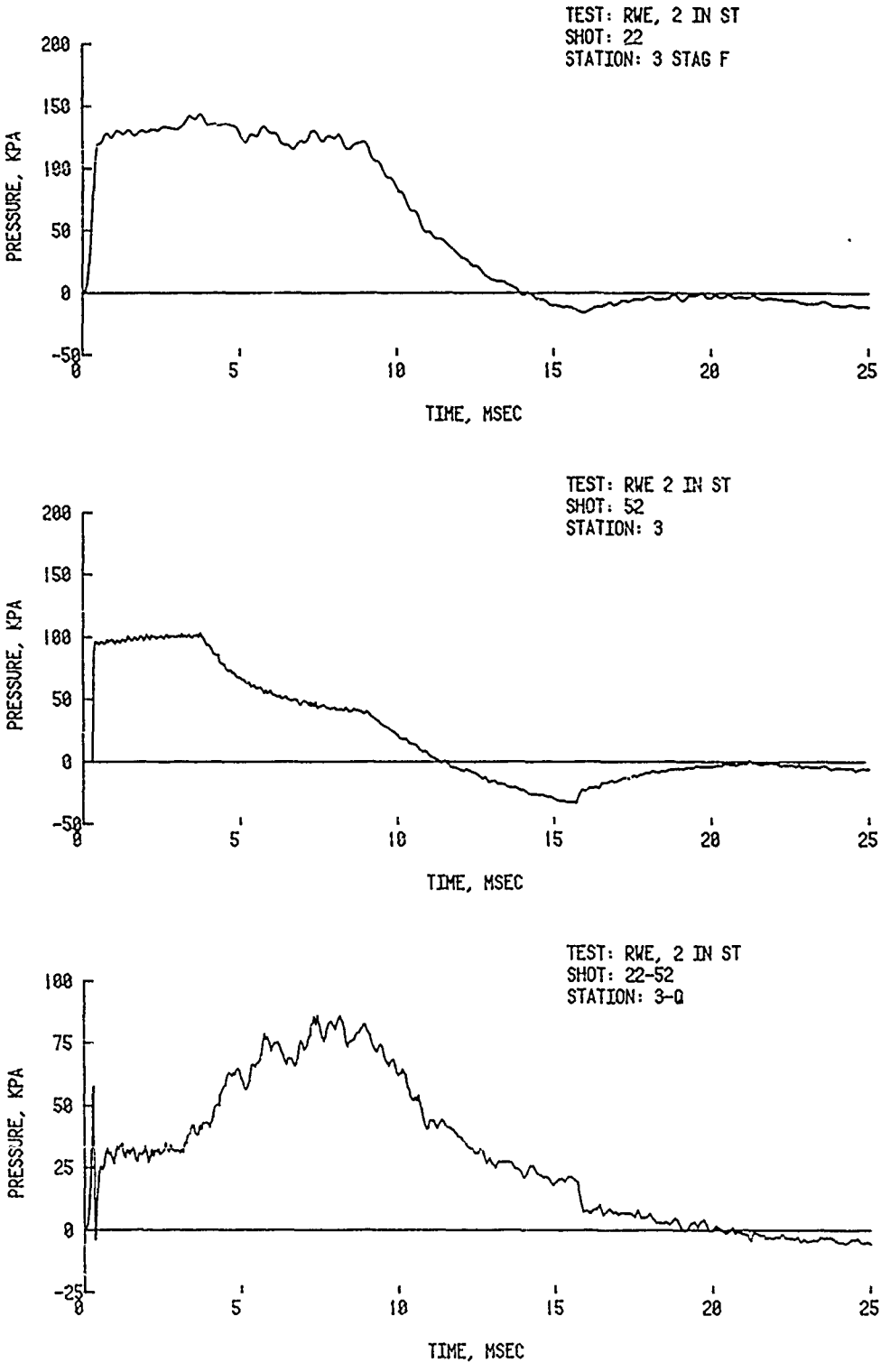

Figure 12. Stagnation pressure minus side-on - test section open, average input pressure 91.2 kPa

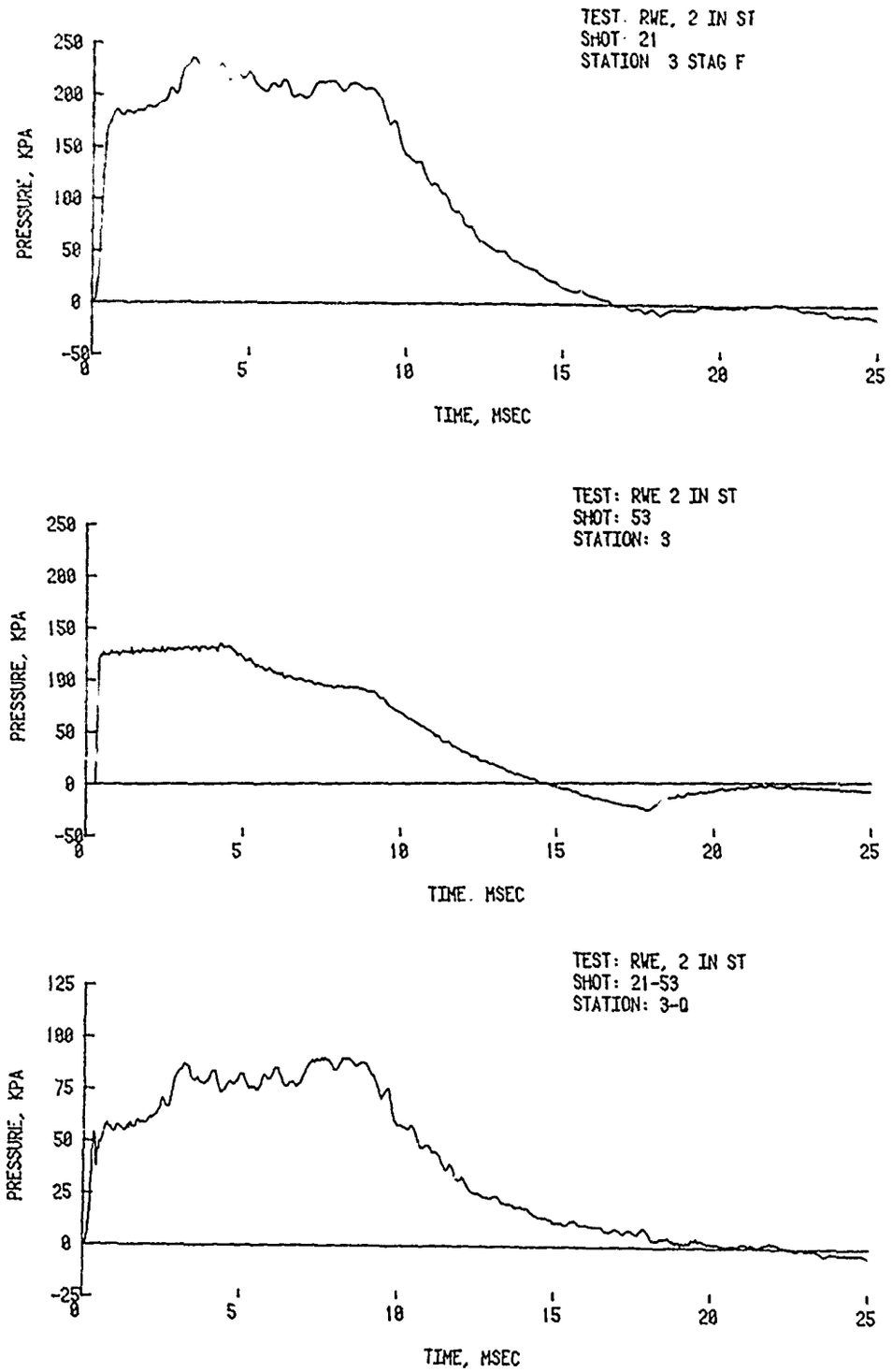

Figure 13. Stagnation pressure minus side-on - test section open, average input pressure 121.1 kPa

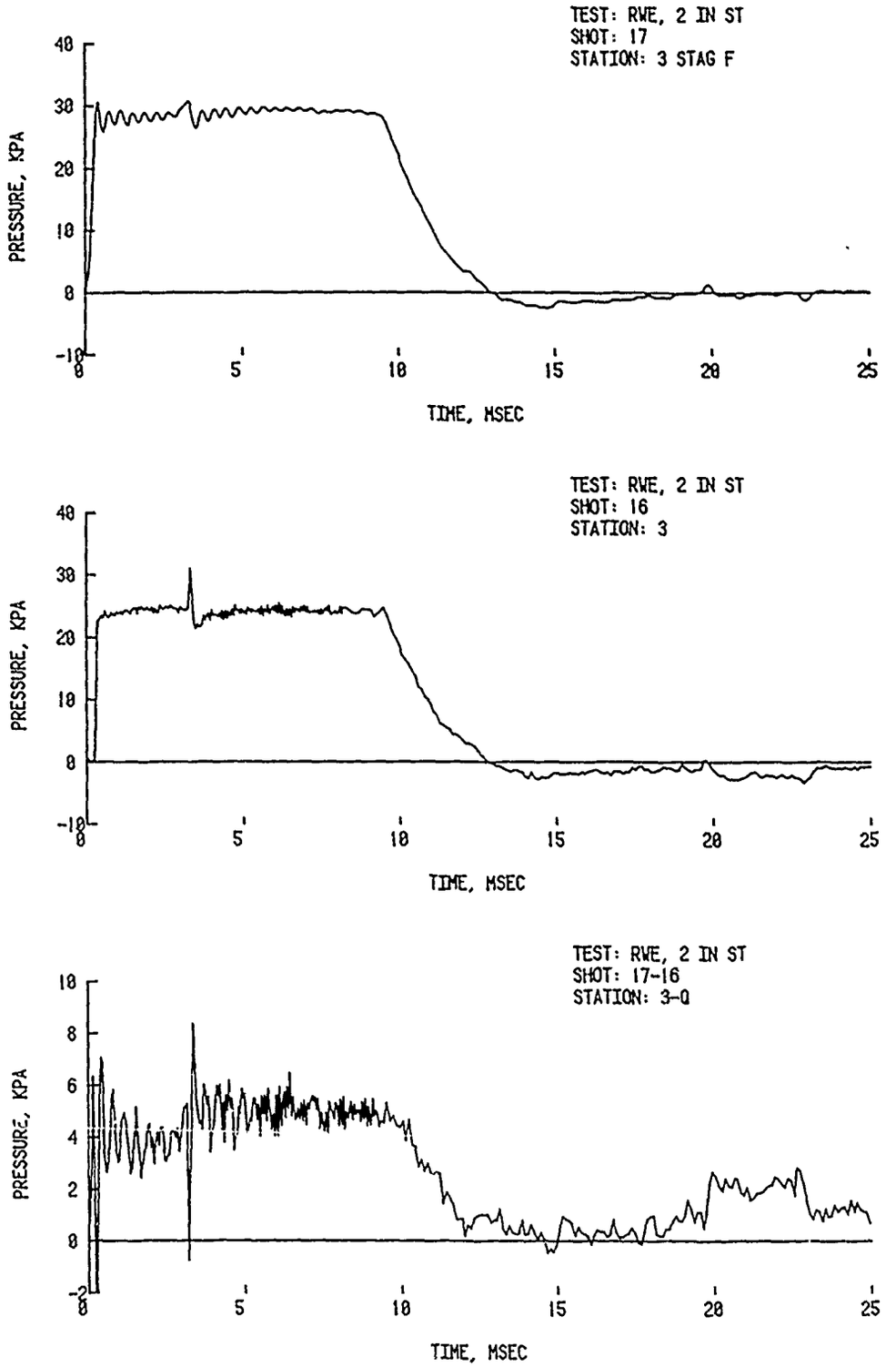

Figure 14. Stagnation pressure minus side-on - Type A solid plate RWE, average input pressure 24.5 kPa

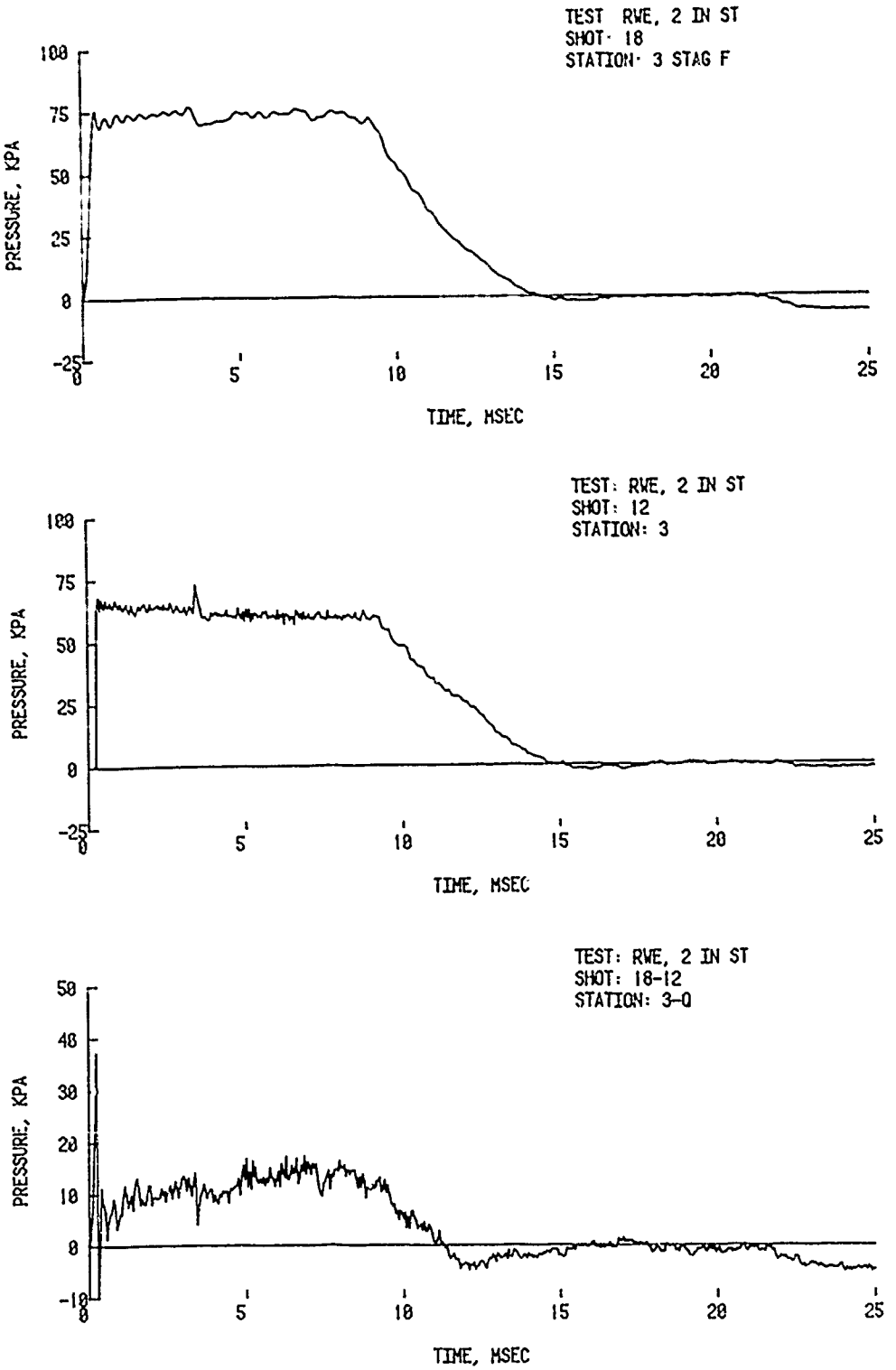

Figure 15. Stagnation pressure minus side-on - Type A solid plate RWE, average input pressure 62.4 kPa

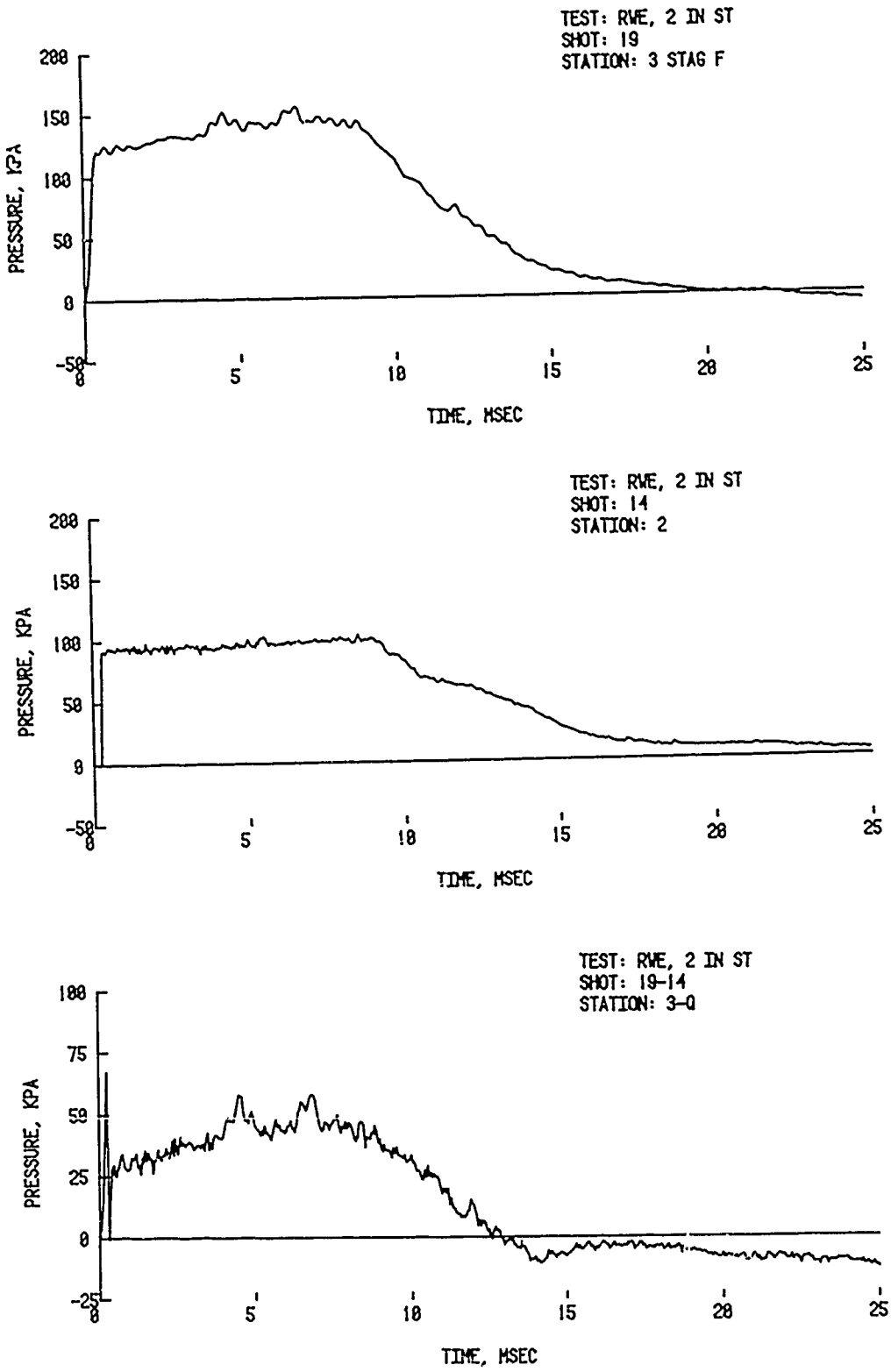

Figure 16. Stagnation pressure minus side-on - Type A solid plate RWE, average input pressure 91.9 kPa

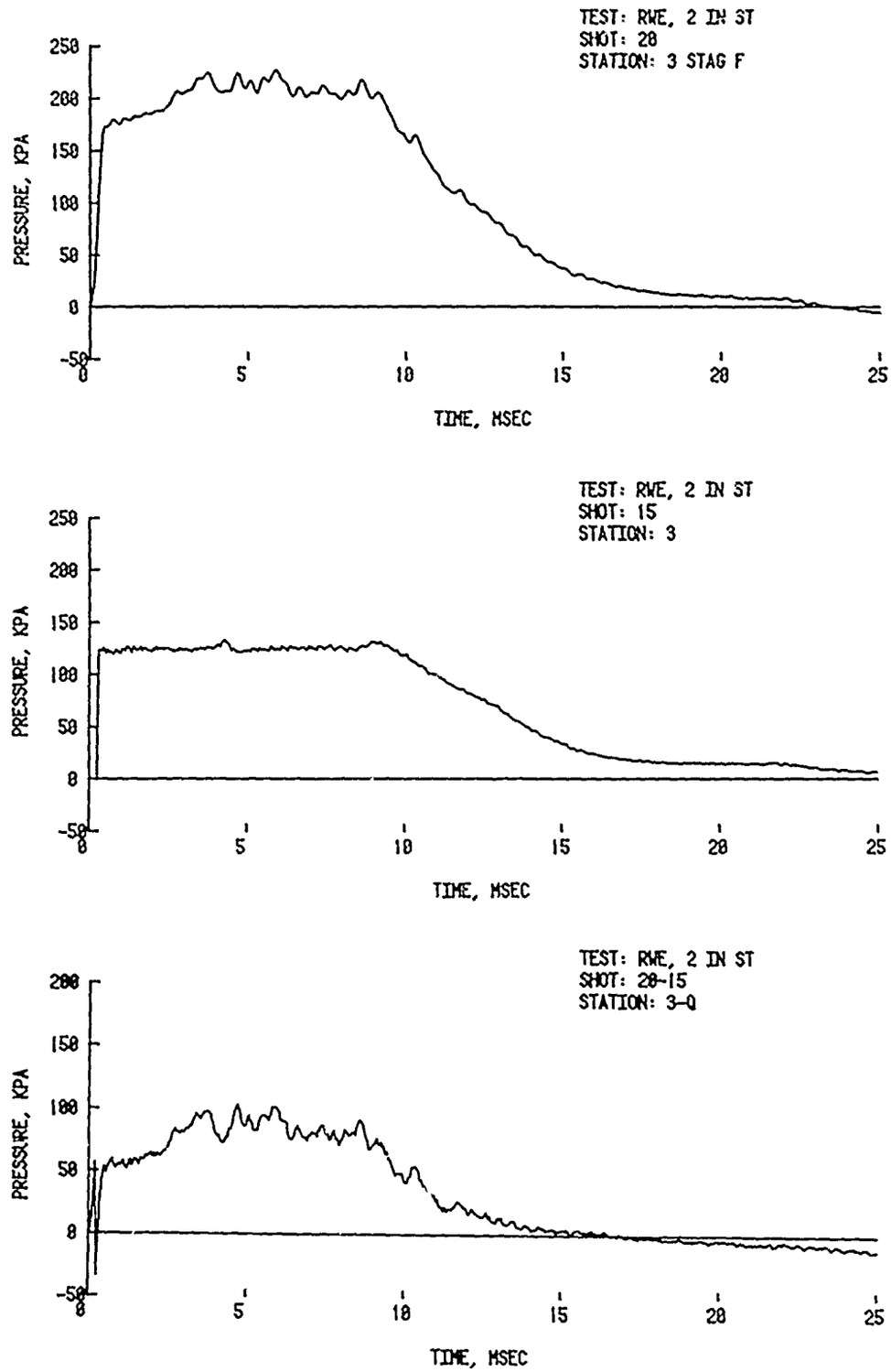

Figure 17. Stagnation pressure minus side-on - Type A solid plate RWE, average input pressure 121 kPa

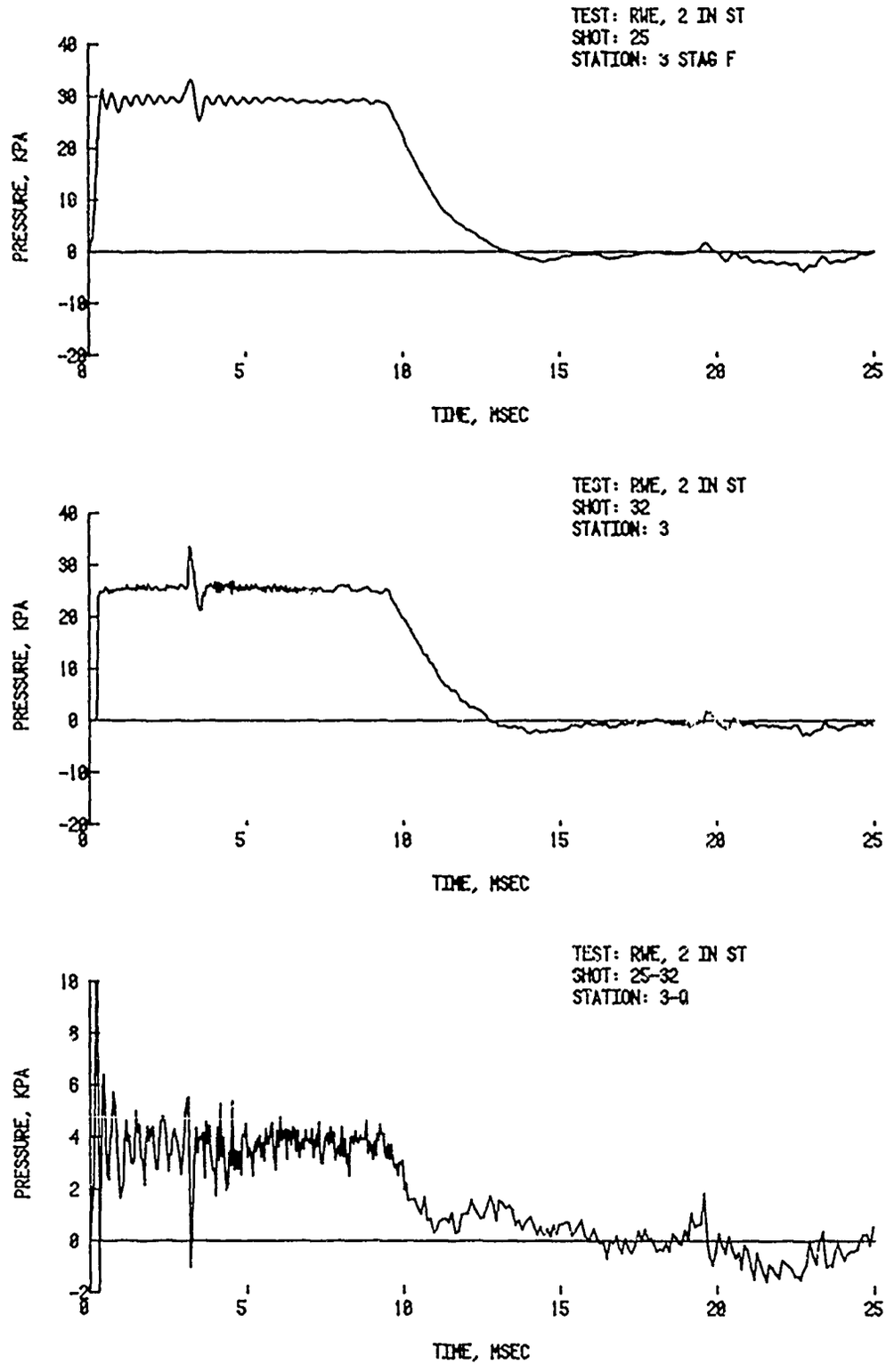

Figure 18. Stagnation pressure minus side-on - Type B vented plate RWE with a 2.54 x 3.49 cm hole, average input pressure 24.8 kPa

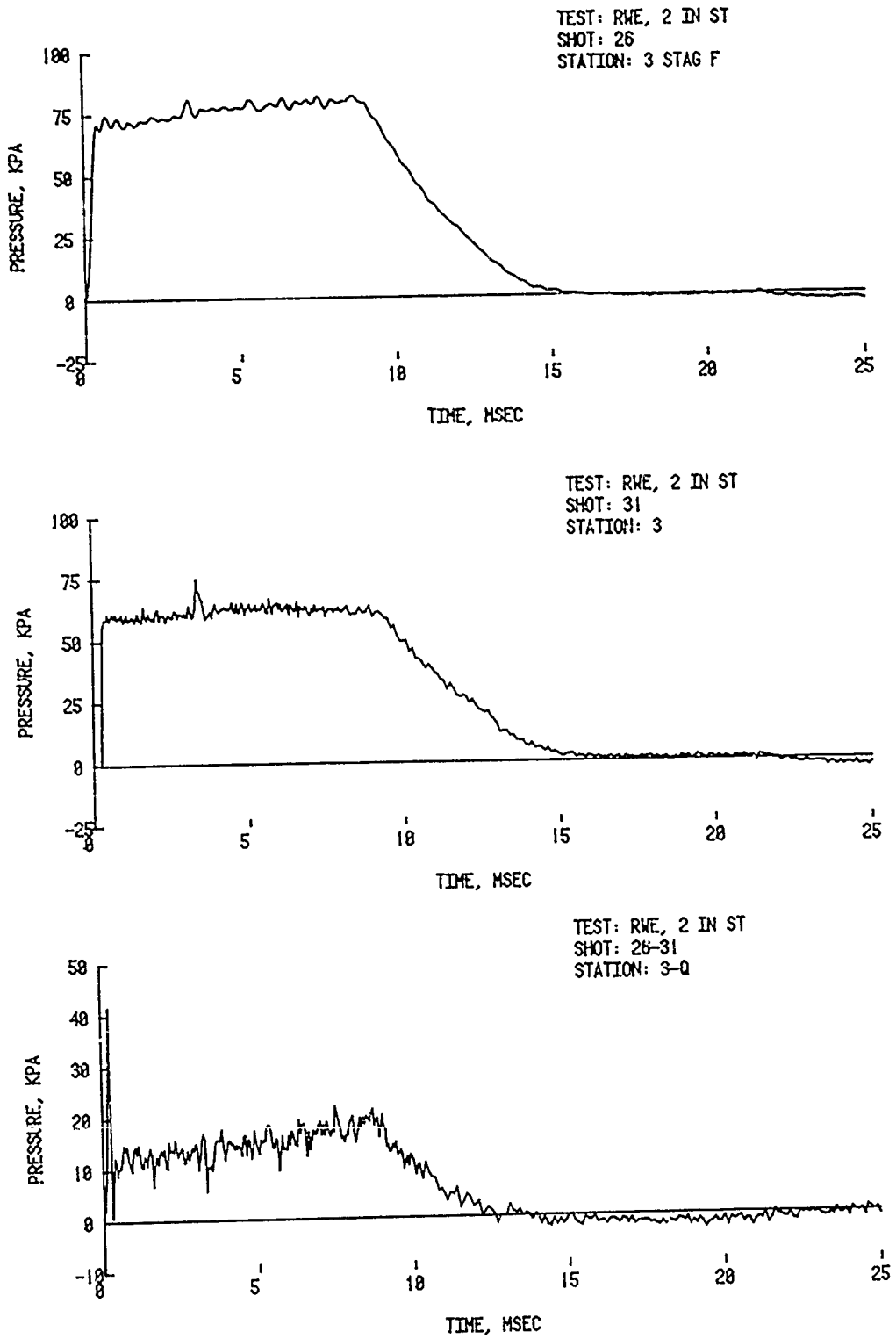

Figure 19. Stagnation pressure minus side-on - Type B vented plate RWE with a 2.54 x 3.49 cm hole, average input pressure 57.4 kPa

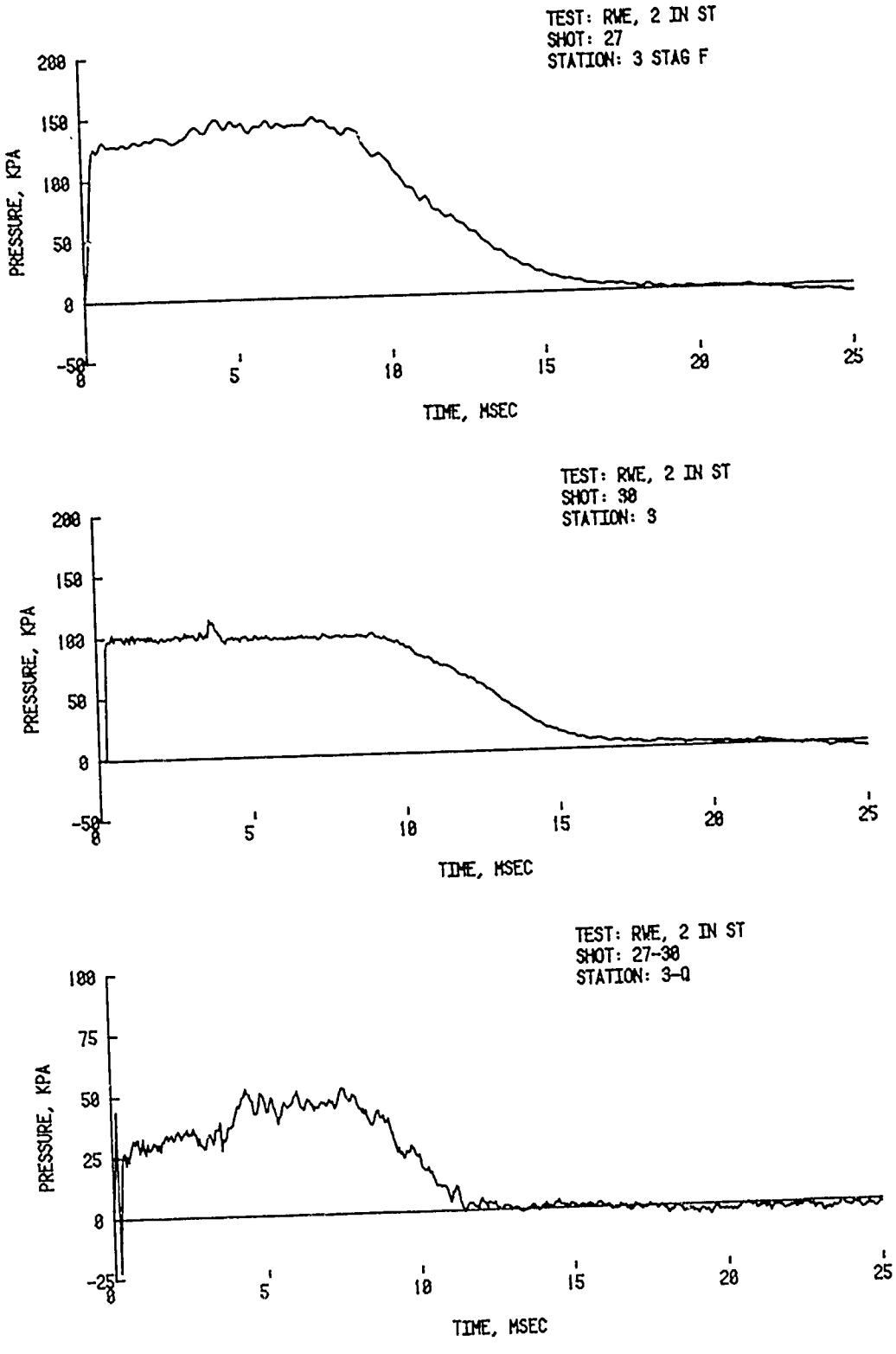

Figure 20. Stagnation pressure minus side-on - Type B vented plate RWE with a 2.54 x 3.49 cm hole, average input pressure 95.2 kPa

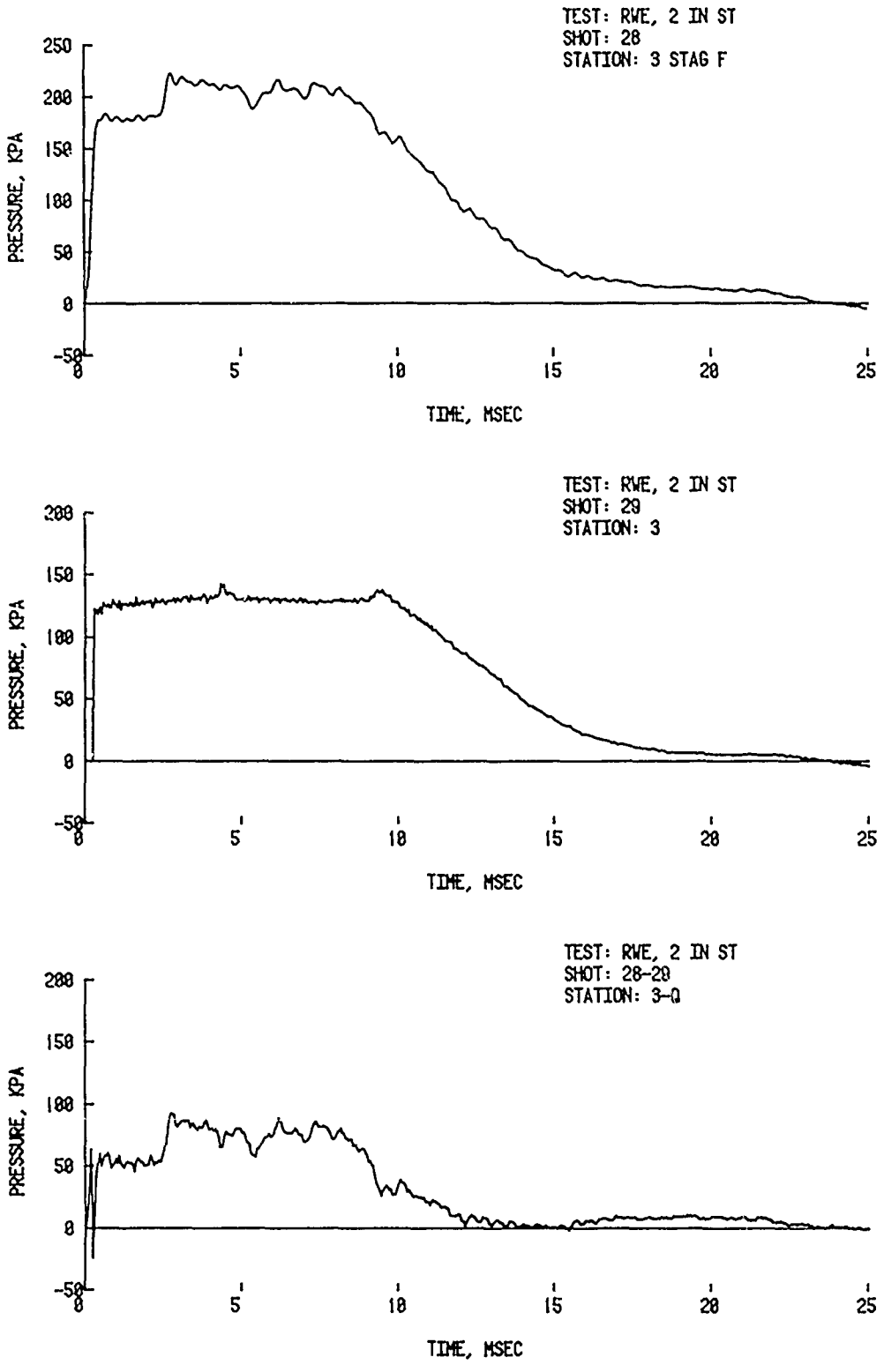

Figure 21. Stagnation pressure minus side-on - Type B vented plate RWE with a 2.54 x 3.49 hole, average input pressure 123.4 kPa

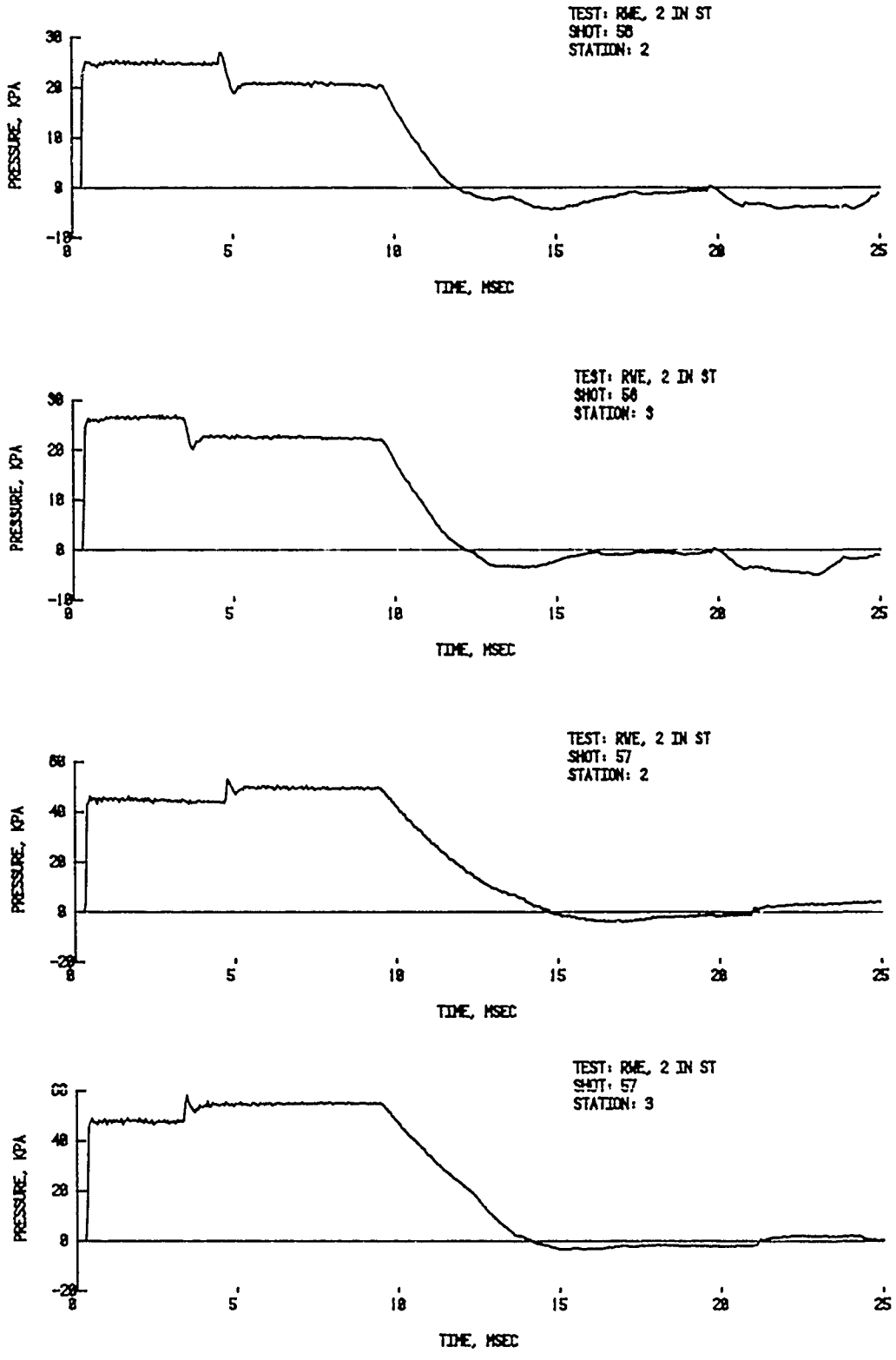

Figure 22. Pressure-time records for Type C lattice RWE

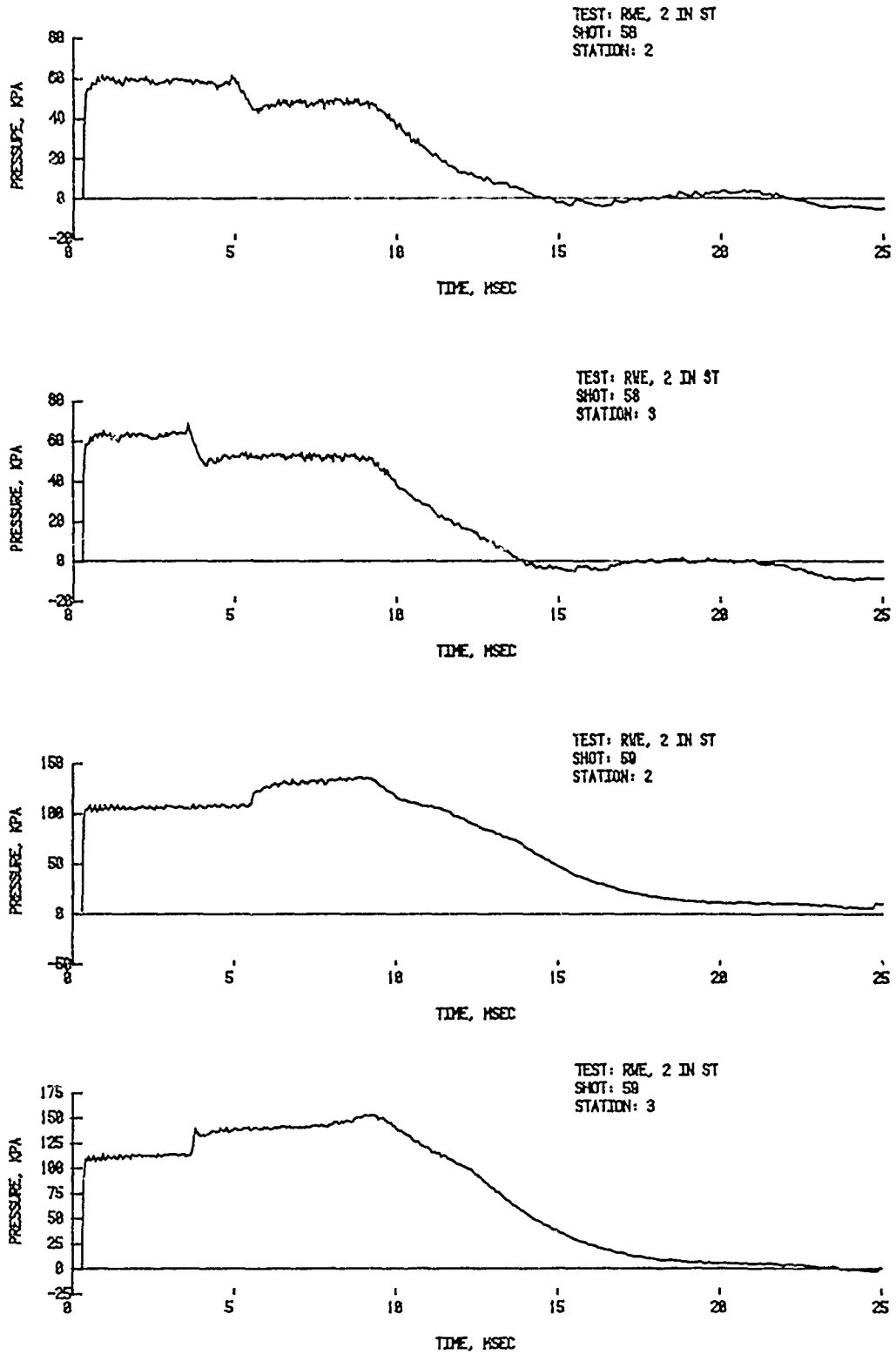

Figure 22. (continued) Pressure-time records for Type C lattice RWE

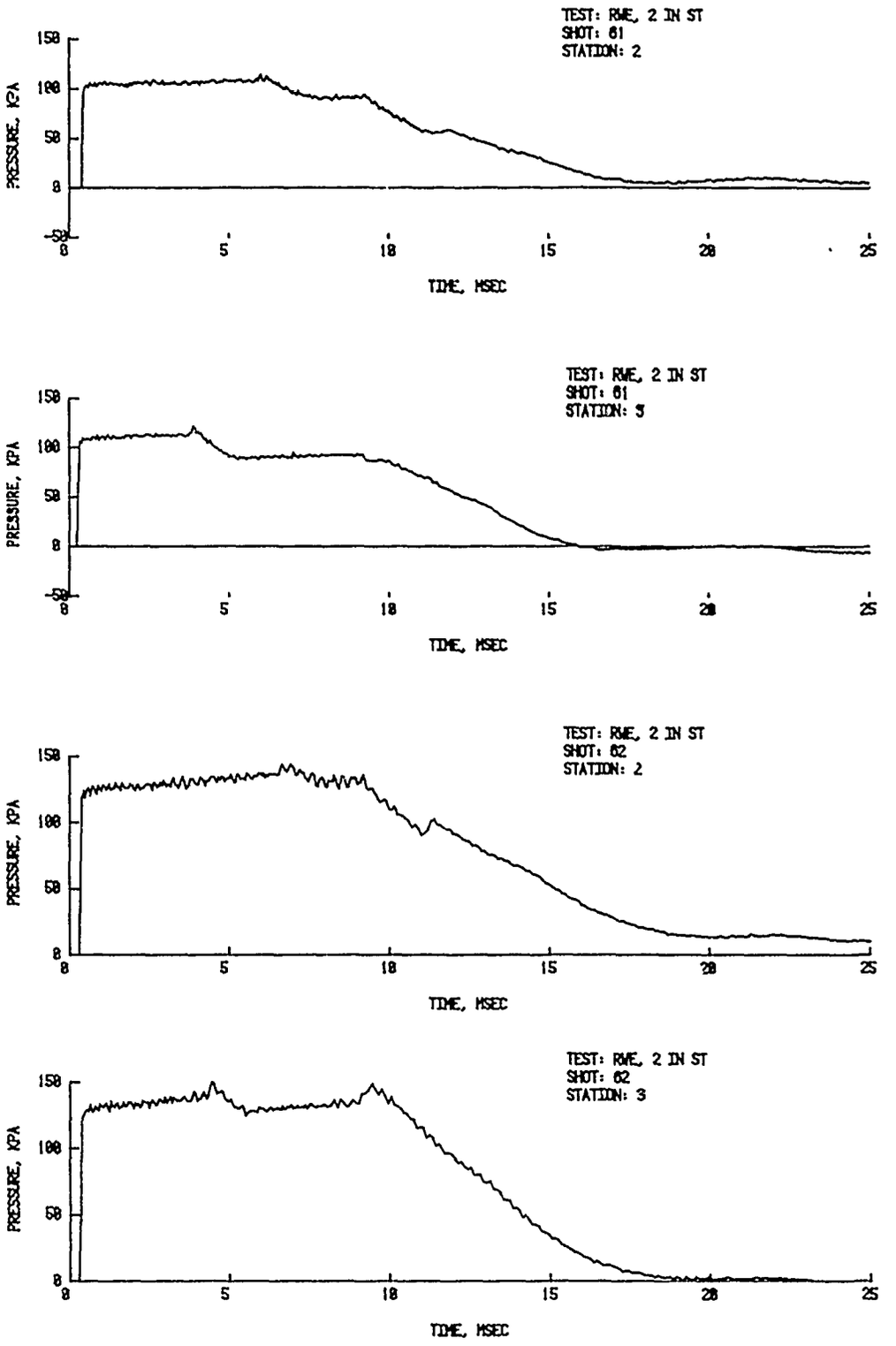

Figure 22. (continued) Pressure-time records for Type C lattice RWE

A comparison of records taken when various vented RWEs were in place with one taken when the solid plate RWE was in place is shown in Figure 23 for an intermediate input shock pressure. The vented plate RWE was varied; making use of a single rectangular opening, a single circular opening, and ten smaller holes. The vented opening was equal for all RWEs used to obtain the results shown in Figure 23. All RWEs appear to be equally effective. The lattice RWE was not compared here because of the previous difficulties in its use.

Additional pressure-time records for the different RWEs are shown in Appendix A.

IV. NASA-AMES COMPUTER CODE PREDICTIONS

A. Introduction

Utilizing a mainframe computer it is possible to simulate complicated fluid flow by employing a mathematical algorithm based on either the Lagrangian or Eulerian fluid mechanics model.[8] Detailed information describing field variables may be obtained at any spacial and temporal location which is essentially the computational equivalent of a fluid dynamics experiment. Although mathematically possible to perform this task without a computer it is impractical because of the large number of calculations required.

B. Theory

The NASA-Ames hydrodynamic code employed in this study is a one-dimensional, adiabatic, inviscid, Eulerian computer algorithm which was written by Dr. Andrew Mark* and modified by Mr. Klaus Opalka** of the Ballistic Research Laboratory.

The Euler equations for conservation of mass, momentum, and energy per unit volume are solved in differential form for the field variables: density, pressure, temperature, total energy, and a one-dimensional component of flow velocity using finite differencing formulations attributed to Beam and Warming.[9] The ideal gas equation of state, Equation 1, and the Euler equations, Equation 2,

---

[8] *Patrick J. Roache, Computational Fluid Mechanics, Hermosa Publishers, Albuquerque, NM, 1972, pp 2 - 12, 204 - 286.*

[9] *R. M. Beam and R. F. Warming, "An Implicit Factored Scheme for the Compressible Navier Stokes Equations," AIAA Journal, Volume 16, No. 4, April 1978, pp 393 - 402.*

* Private communication with Dr. Andrew Mark, Ballistic Research Laboratory, Jan 1982.

**Private communication with Mr. Klaus Opalka, Ballistic Research Laboratory, Jan 1982.

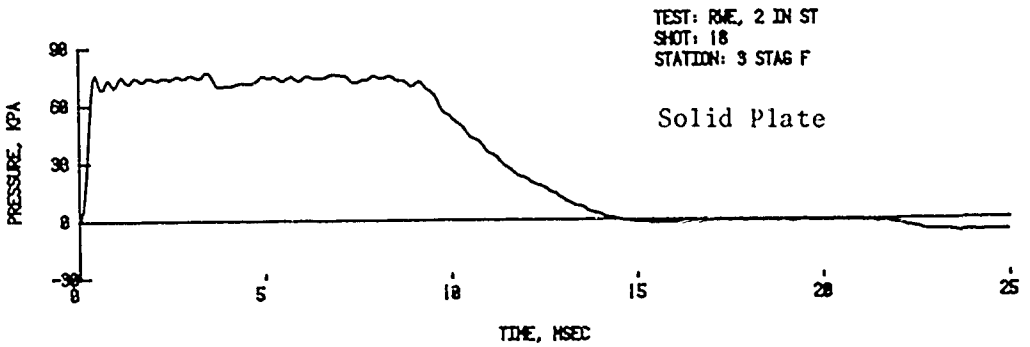

A. Solid plate RWE.

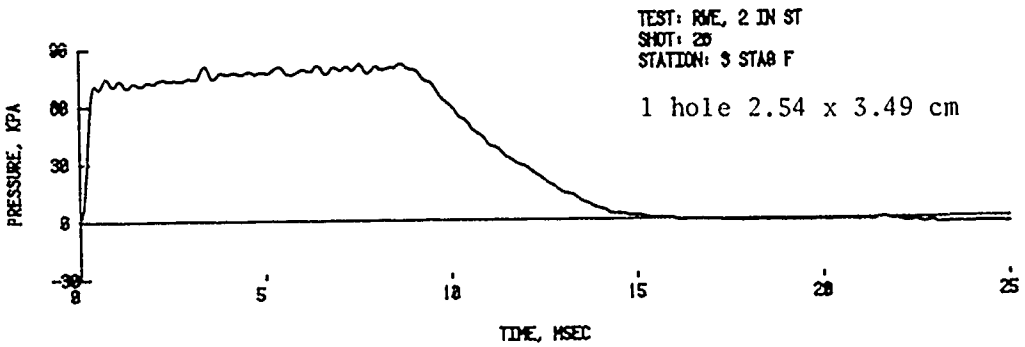

B. Rectangular vented RWE.

Figure 23. Comparison of the effectiveness of the Type A solid plate RWE with the Type B vented RWE

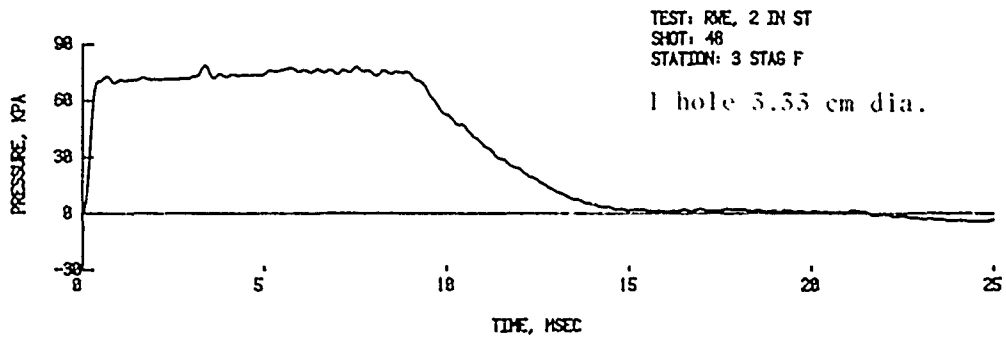

C. Circular vented RWE.

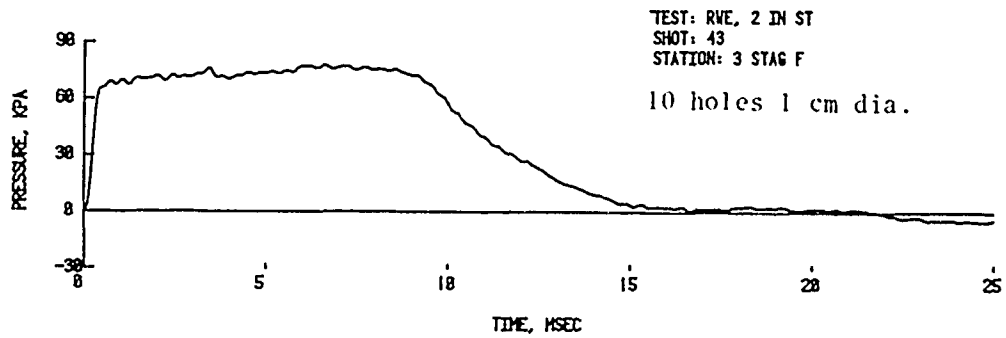

D. Multiple circular vented RWE.

Figure 23. (continued) Comparison of the effectiveness of the Type A solid plate RWE with the Type B vented RWE

are applied to a straight shock tube with a RWE placed at the open end.

$$p = (\gamma-1)\ (e-\tfrac{1}{2}\rho u^2), \tag{1}$$

$$\frac{\partial(\rho A)}{\partial t} + \frac{\partial}{\partial x}(\rho u A) = 0 \tag{2-a}$$

$$\frac{\partial(\rho u A)}{\partial t} + \frac{\partial[(\rho u^2 + p)A]}{\partial x} - p\frac{\partial A}{\partial x} = 0, \text{ and} \tag{2-b}$$

$$\frac{\partial(eA)}{\partial t} + \frac{\partial[uA(e+p)]}{\partial x} = 0, \tag{2-c}$$

where p = pressure, γ is the ratio of specific heats, e = total energy/volume, ρ = density, u = flow velocity, A = tube cross-sectional area, t = time, and x = distance.

The initial conditions are normalized. Variables at the closed end of the tube, i.e., the compression chamber backwall, are computed using image points. Variables of the open end are calculated by using backward differencing.

Independent variables (x,t) are transformed into a computational grid and the governing equations are solved at one-dimensional spacial grid points (x) as a function of time. Refer to Figure 24, a sketch of the computational shock tube. The distribution and total number of grid points are established as computer input parameters. Typically, the number of spacial grid points varies from 100 - 1000 with 200 - 400 providing adequate results.

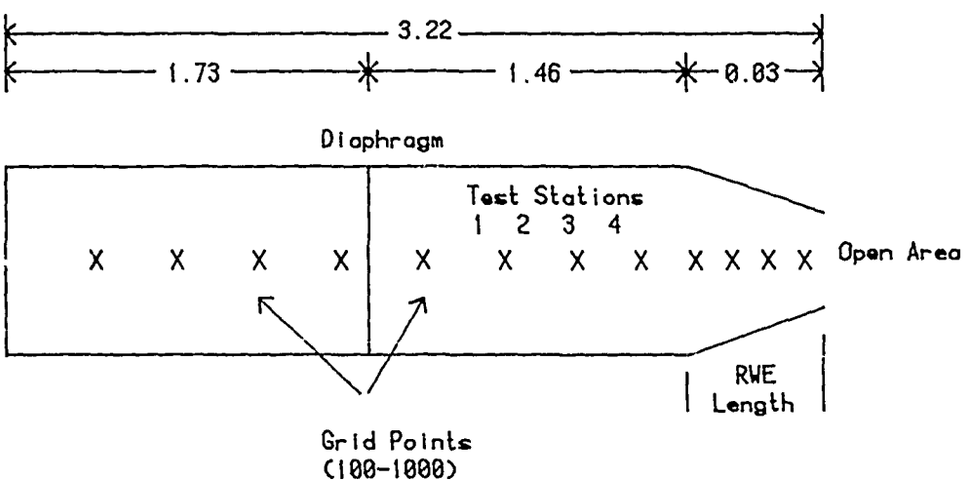

Figure 24. Sketch of computational shock tube.

The computational grid may be equidistantly partitioned along the tube length or clustered about a specified location utilizing the hyperbolic function incorporated in the code. Thus, a proportionally large number of grid points may be positioned where cross-sectional area changes occur, i.e., at the RWE.

The RWE positioned at the open end of the tube partially reflects the shock wave which decreases the magnitude and effect of the open-end rarefaction wave. The hydrocode models a RWE that is a flat circular plate of the same diameter as the shock tube. In this study the RWE has one circular hole of time-invariant cross-sectional area that allows for outflow. (The code also provides for a RWE that varies as a function of time; this feature was not utilized in the present study.) The RWE percent of vented area ratio (cross-sectional open area/total cross-sectional area X 100) is varied with each computational run depending upon the driver pressure.

There are several computational difficulties with the RWE model that do not have experimental counterparts. The RWE can never be truly perpendicular to the end of the shock tube. For if it were, then the last grid point would be dual valued. Therefore, the RWE is placed at a slight angle and the change in tube area occurs over a small distance x which is also an input parameter. This change in cross-sectional tube area, $\frac{dA}{dx}$, describes a parabolic arc, i.e., tube radius r is dependent on x, and A is proportional to r^2.

The computational scheme is sensitive to the number of grid points within the length of the RWE. Since $\frac{dA}{dx}$ is nonlinear, a large number of grid points is required to precisely define the continuous area change. Computational results approach an asymptotic value if 10 grid points are placed within the length of the RWE.

The imposition of an artificial length to the RWE changes slightly the physical dimensions of the tube which alters the normalized locations of the test stations. This effect is minimal; the RWE length was established as 1% of the tube length.

C. Results

The results apply equally to the 5.08 cm and 2.44 m shock tubes. Computational shock tube dimensions are identical to the 5.08 cm experimental tube. These dimensions are normalized by the computer code. Since the 5.08 cm tube is a 1/48th scale model of the 2.44 m tube, the normalized dimensions apply to both shock tubes. For the 2.44 m tube, time of arrival and shock duration must be increased by a factor of 48.

As indicated in the theory section, the code is sensitive to the number of points within the RWE length. By using as input parameters 404 grid points, a 1% RWE length, and a hyperbolic sine clustering factor $\beta = 5$, seven grid points were placed within the RWE length. Reported results are within 5% of results achieved with 10 grid points within the RWE length. (10 grid points provide a close approximation to the asymptotic value.)

Seven points were chosen to keep computer processing time and output file lengths within manageable limits while also maintaining accurate results.

Figure 25 displays hydrocode generated side-on and dynamic pressure ($q = \frac{1}{2}\rho u^2$) for an input pressure of 26.8 kPa at test stations 1, 2, 3, and 4 without a RWE. Manifestations of wave decay due to both rarefaction waves are present. Stations 1, 2, 3, and 4 correspond to experimental Stations 84, 86, 87, and 88, respectively, for the BRL 2.44 m shock tube. These results are quite similar to experimental results at a comparable imput pressure. Refer to Figure 5. Note the zero time on the experimental curve is the time of arrival at the station, while the zero time on the calculations starts at the break of the diaphragm. Direct computational and experimental comparisons for various conditions are reported in Section V.

Figure 26 shows results for 62.7, 91.7, and 122.0 kPa at Station 3 which corresponds to the primary test station in the 2.44 m tube. Again, no RWE is utilized and the rarefaction wave effects are evident. Refer to Figures 6, 7, and 8 for comparison with experiment.

The results displayed in Figures 27 through 31 show the effects of a RWE over a large range of input pressures, including input pressures used in Figure 26 for comparison. All data are computed at Station 3. These results are reported in tabular form in Table 2, which shows the appropriate vented area ratios needed to extend the shock wave duration as a function of input pressure at Station 3.

TABLE 2. VENTED AREA RATIO VERSUS INPUT SHOCK OVERPRESSURE - COMPUTER CODE

Input Pressure (kPa)	Vented Area / Total Area
2.5	.060
5.0	.100
9.8	.150
21.4	.250
26.6	.288
34.3	.339
40.9	.380
56.1	.470
61.4	.500
71.3	.550
79.9	.590
97.2	.663
119.6	.750
125.4	.770
142.4	.820

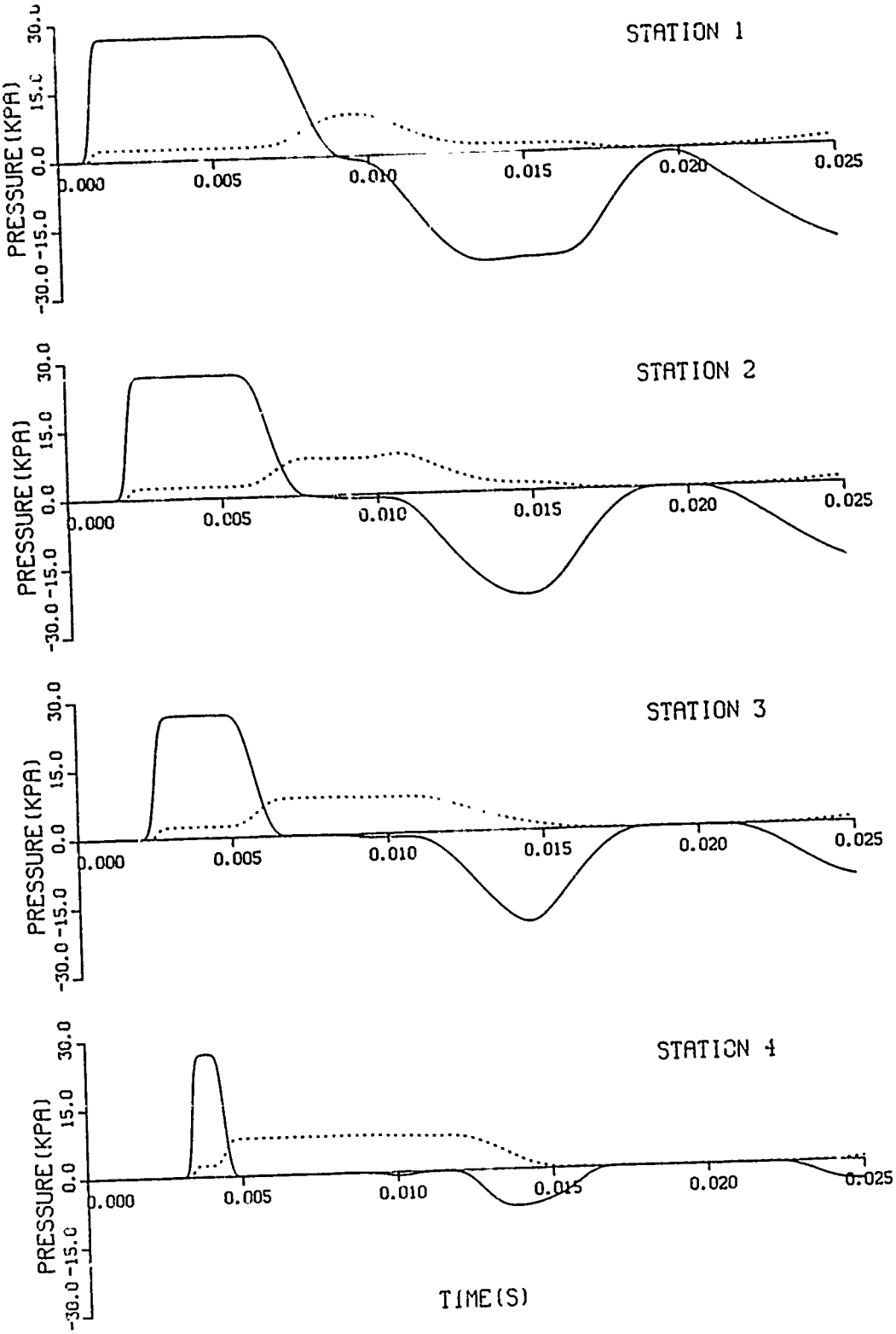

Figure 25. Computer side-on and dynamic pressure-time records, 26.8 kPa, no RWE, Stations 1, 2, 3, and 4

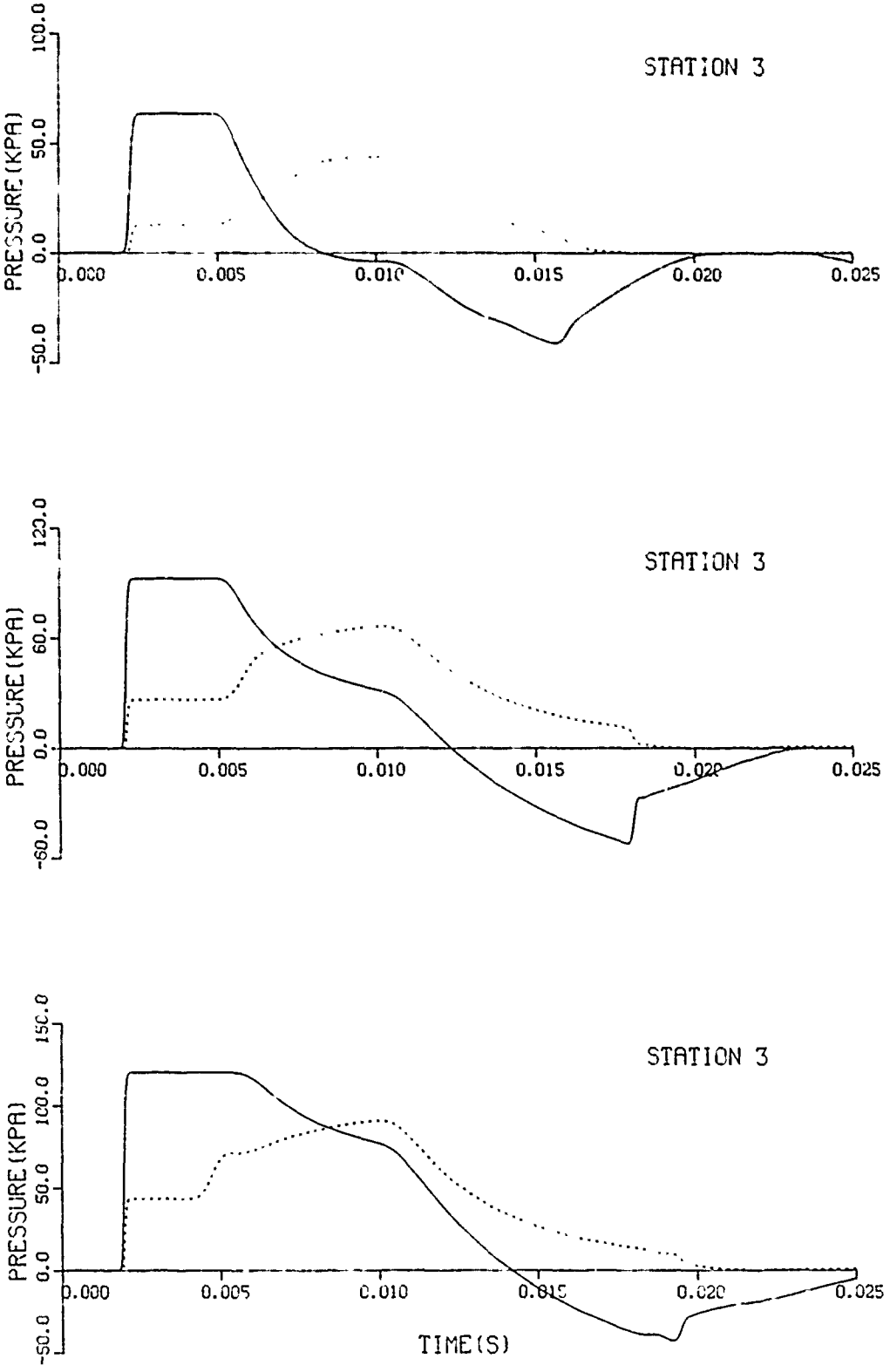

Figure 26. Computer side-on and dynamic pressure-time records, 62.7, 91.7, and 122.0 kPa, no RWE, Station 3

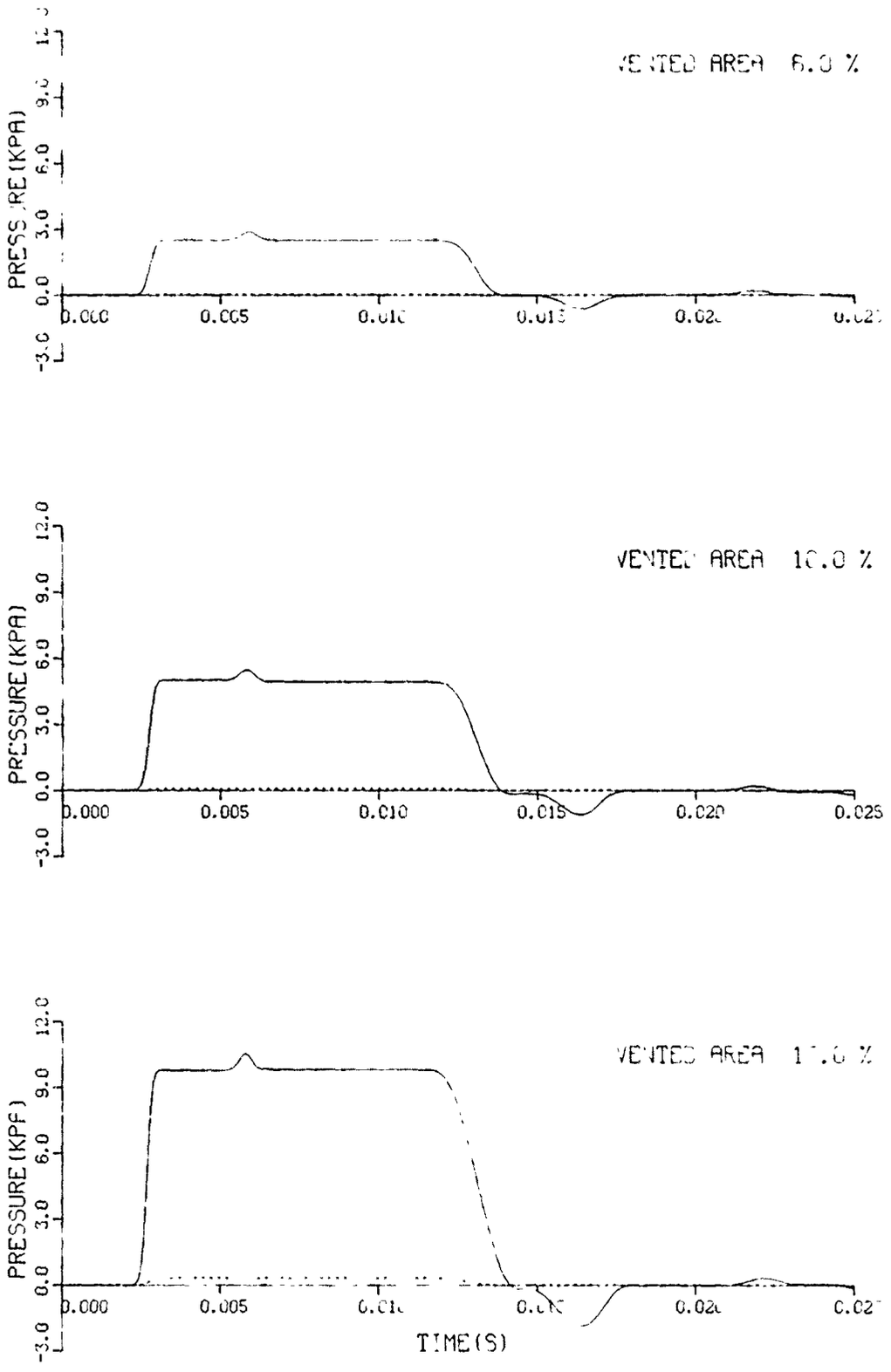

Figure 27. Computer side-on and dynamic pressure-time records, 2.5, 5.0, and 9.8 kPa, RWE, Station 3

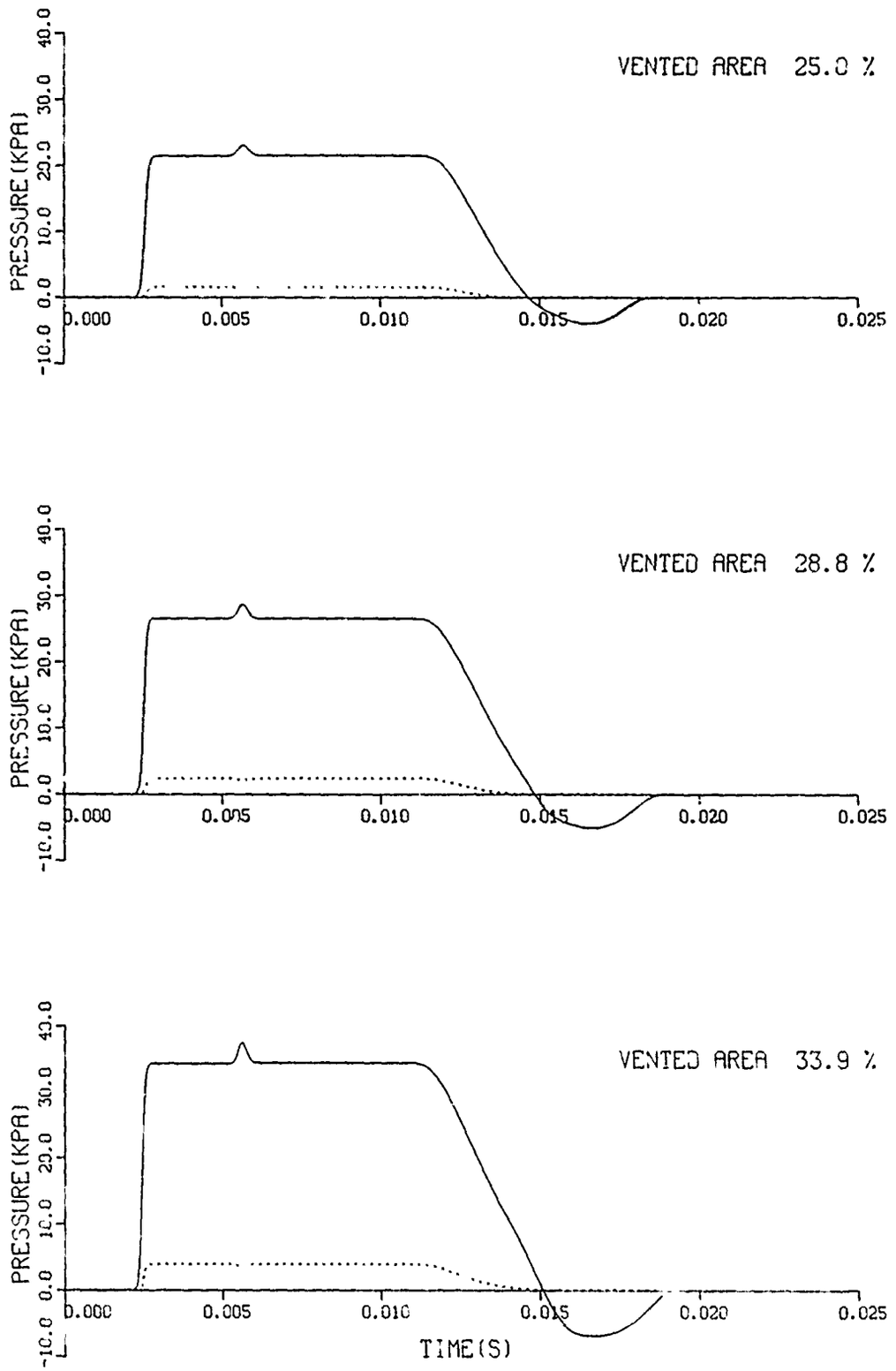

Figure 28. Computer side-on and dynamic pressure-time records, 21.4, 26.6, and 34.3 kPa, RWE, Station 3

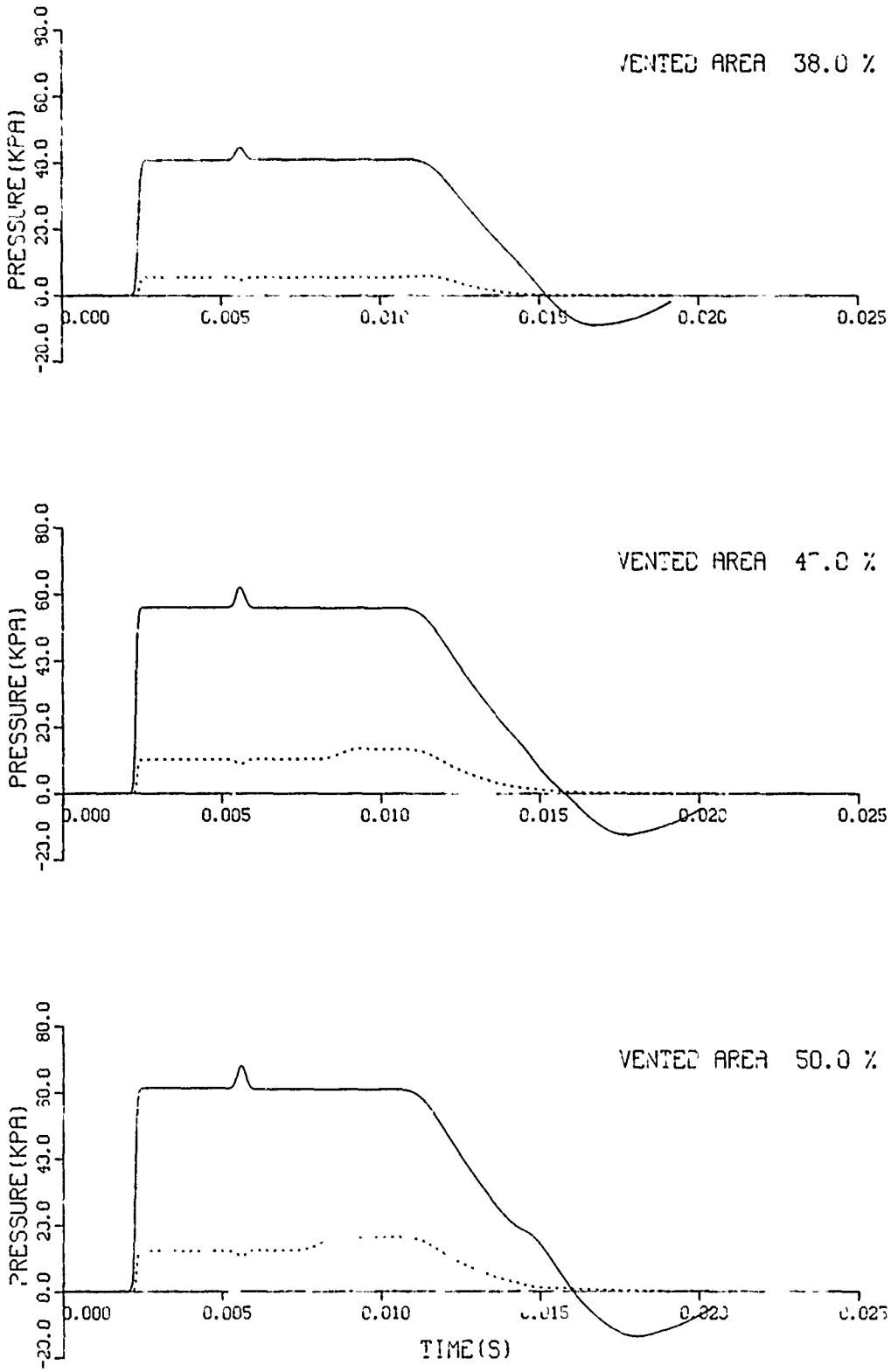

Figure 29. Computer side-on and dynamic pressure-time records, 40.9, 56.1, and 61.4 kPa, RWE, Station 3

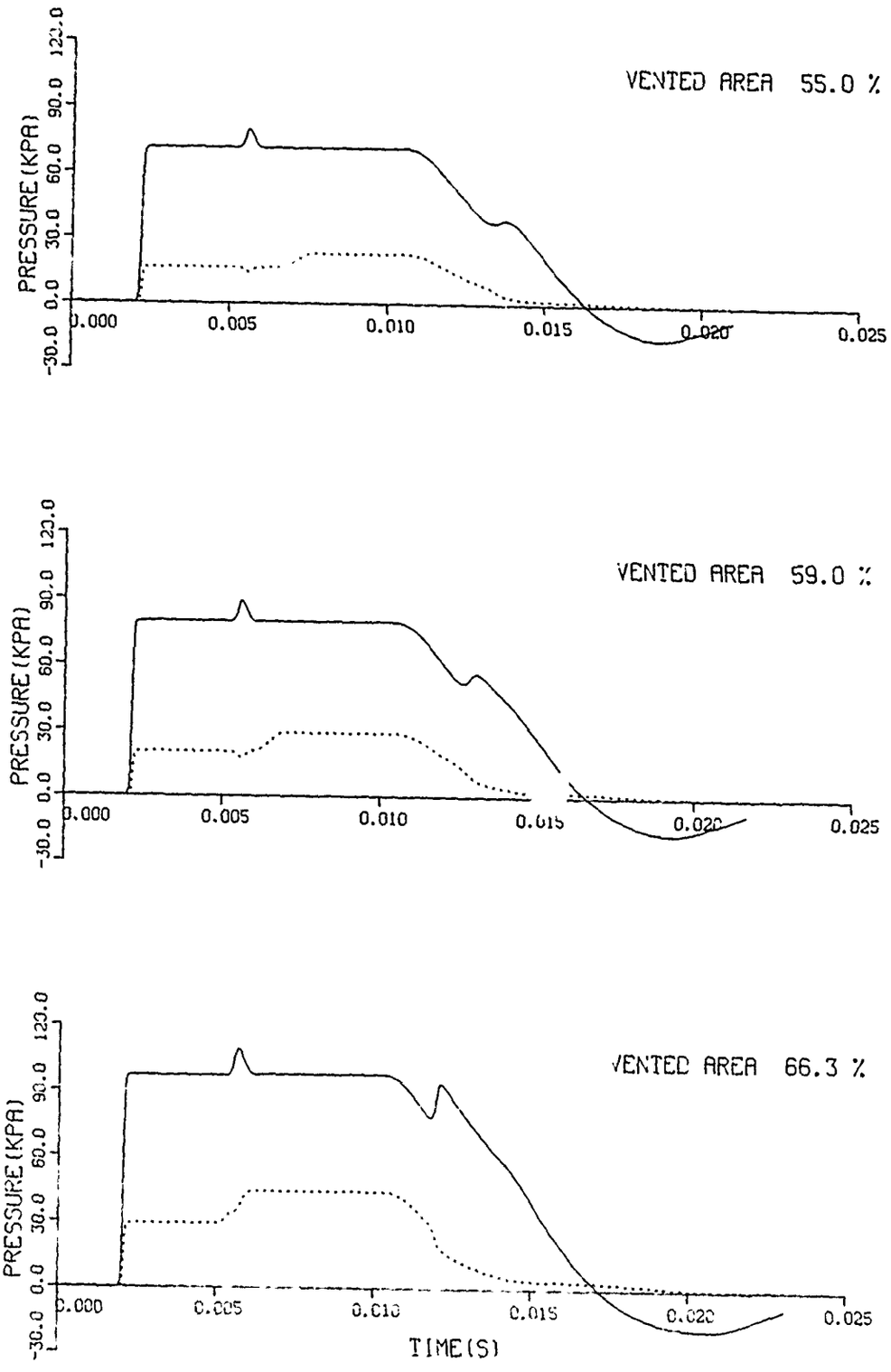

Figure 30. Computer side-on and dynamic pressure-time records, 71.3, 79.9, and 97.2 kPa, RWE, Station 3

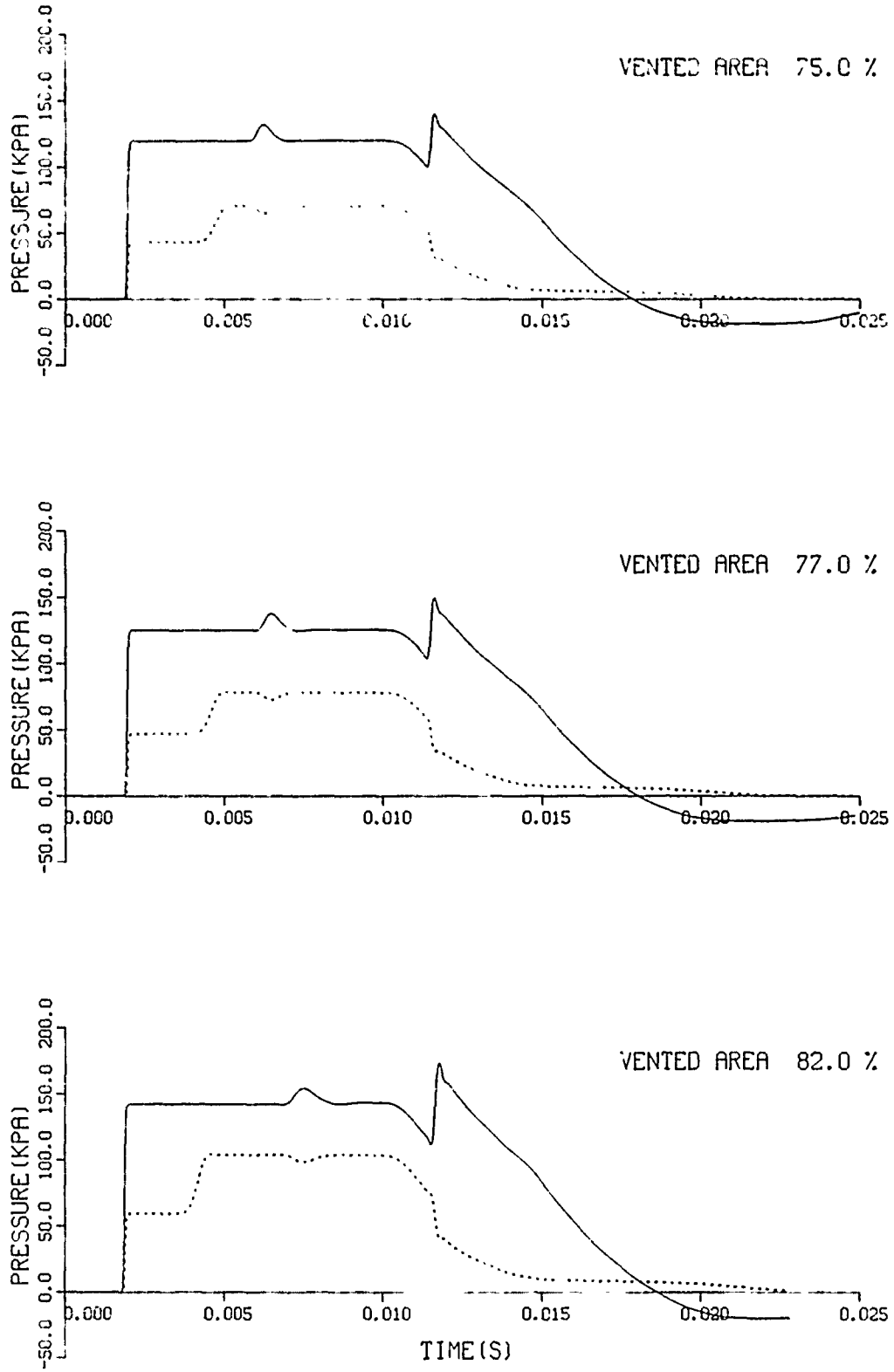

Figure 31. Computer side-on and dynamic pressure-time records, 119.6, 125.4, and 142.4 kPa, RWE, Station 3

A secondary wave* which first appears at a 50 percent vented area with input shock overpressure of 61.4 kPa is a compression wave propagating upstream. This wave is caused by the interaction of the contact surface with the open end of the tube. The time of arrival and magnitude is a function of vented area and shock overpressure. See Figures 30 and 31.

D. Discussion

For low to moderate pressure levels the RWE extends the duration of the square shock wave and reduces the dynamic pressure. Effects of the open end rarefaction wave are nullified. At higher pressure the RWE extends the duration of the square wave and continues to significantly decrease the dynamic pressure.

Figure 32 displays the RWE vented area ratio versus overpressure based on the data in Table 2. This curve can be used to predict the effects of a RWE, without standoff, by varying the circular opening.

V. ANALYSIS

The analysis section will treat the experimental results obtained from the tests in the 5.08 cm shock tube, determine the parameters needed to apply results to the BRL 2.44 m shock tube, and compare experimental results with predictions from the NASA-Ames one-dimensional hydrocode.

A. Data from 5.08 cm Shock Tube

Bertrand* found from experiments at the BRL 57.47 cm shock tube that a larger reflecting surface of a test target at the end of the open test section had the effect of a rarefaction wave eliminator. He found that the standoff distance and vented area needed to eliminate the rarefaction were related to the input shock overpressure. Accordingly, the data from the present experiments were plotted as input shock overpressure as a function of vented area ratio. Figure 33 shows the data plotted in this manner for the three general types of RWE tested. The asterisks are points from theory given in Reference 10 by Weidermann. As noted in Table 1 the vented plates with no standoff had a vented area ratio ranging from 43 to 45 percent, and it can be seen in Figure 33 that those data points do not fit the trend of data from RWEs with standoff distances. Figure 34 shows data from the solid plate RWE. Either of these curves (Figure 33 or 34) may be used to determine the parameters for a suitable rarefaction wave eliminator on the BRL 2.44 m shock tube.

B. Parameters for Rarefaction Wave Eliminator - 2.44 m Shock Tube

Both the solid plate RWE and the vented Plate RWE appeared suitable for use at the large shock tube. No attempt was made to adapt the lattice type of RWE to the large shock tube.

---

[10] *A. Weidermann, "Study of Grids in Shock Tubes," Proceedings of First Shock Tube Symposium, SWR-TM-57-2, Hq AFSWC, Kirtland Air Force Base, NM, 26-27 Feb 1957.*

*Private communication from Mr.Brian P.Bertrand, Ballistic Research Laboratory, July 1981 and June 1982.

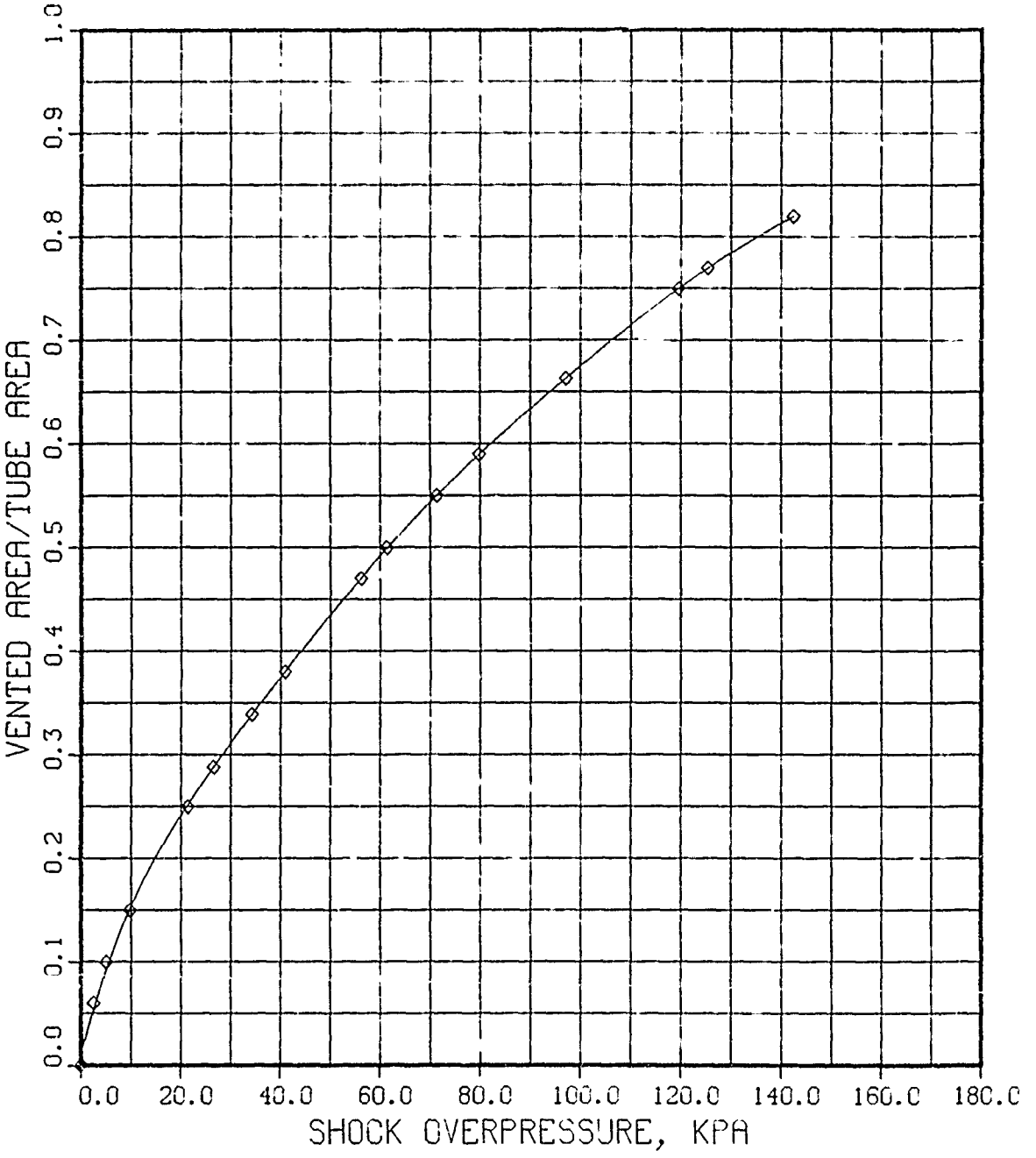

Figure 32. RWE vented area ratio versus input shock overpressure - computer code

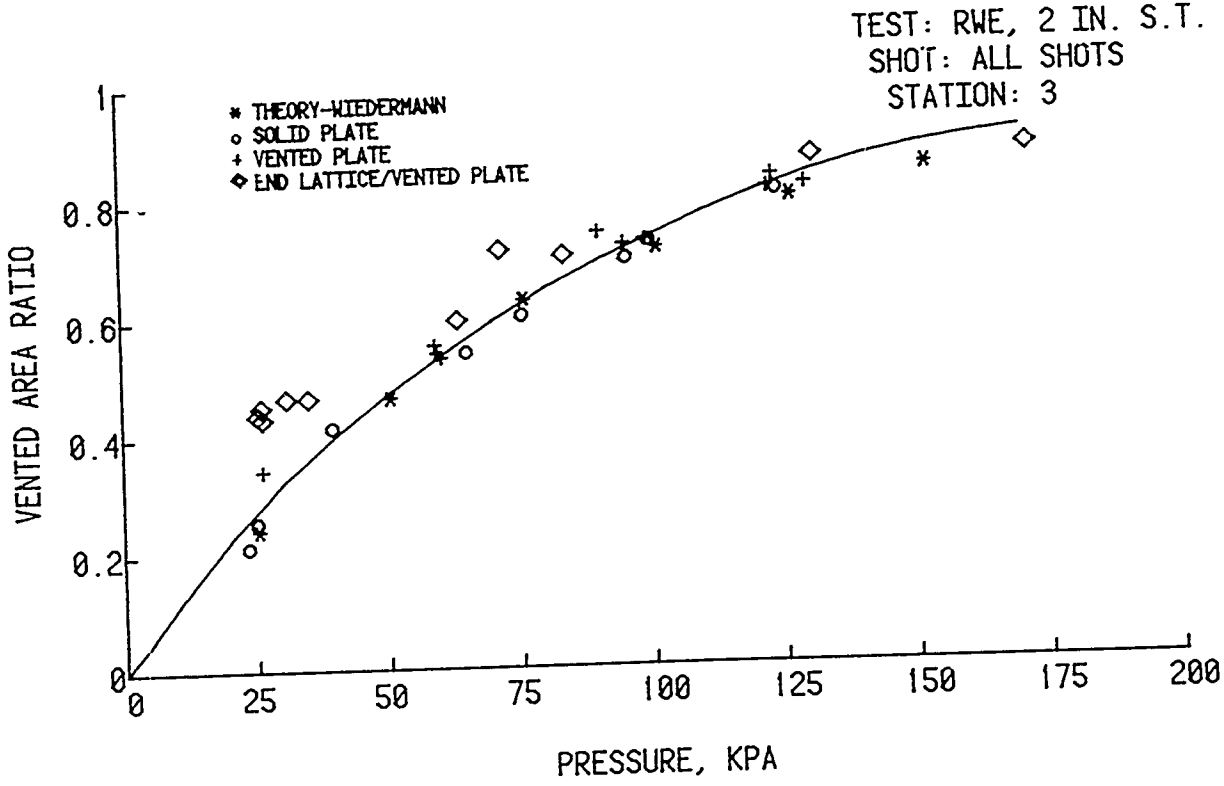

Figure 33. Vented area ratio of the RWEs as a function of shock input overpressure

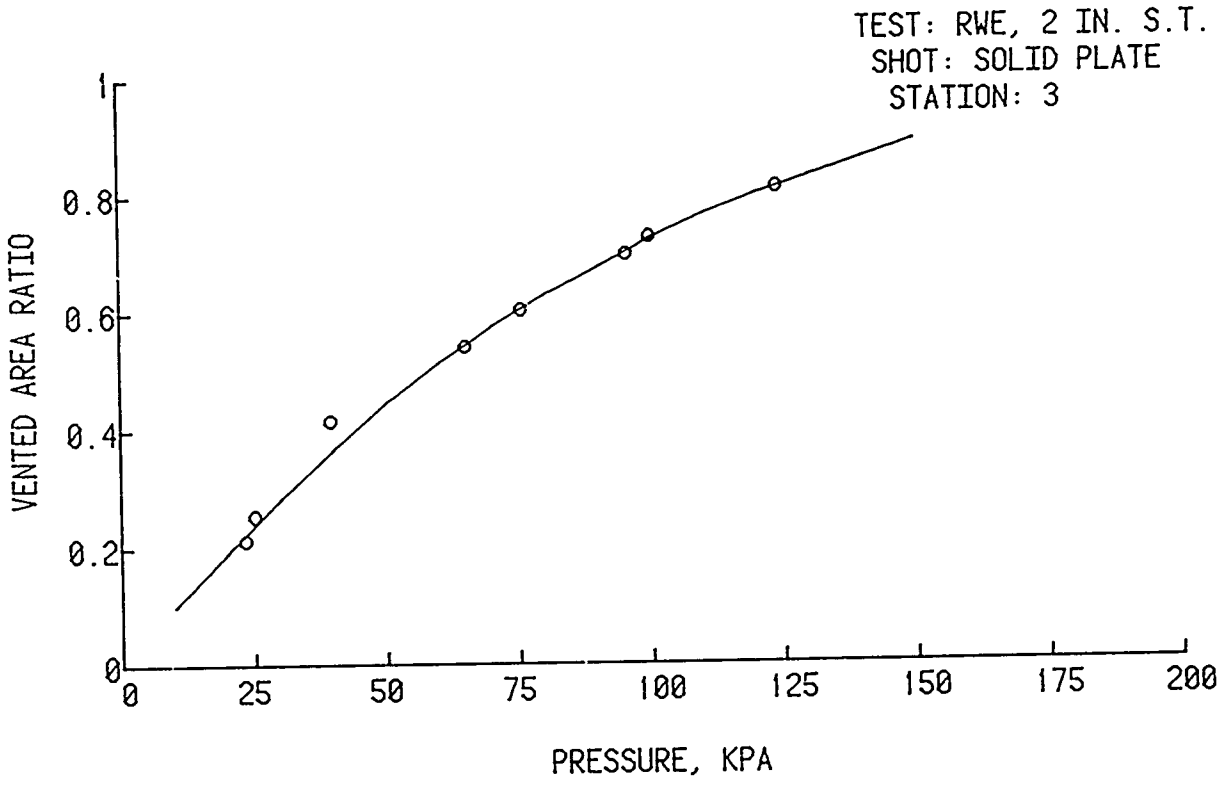

Figure 34. Vented area ratio for solid plate RWE as a function of input shock overpressure

The solid plate needs only one parameter - the standoff distance - to be varied to eliminate the rarefaction wave. The vented plate RWE needs two parameters - the vented area of the plate and the standoff distance.

Since, at present, the large shock tube has an end flange test stand assembly which has a 1.219 x 1.691 m rectangular opening, either a solid or vented RWE would be suitable using the available hardware. See Appendix B for drawing details of the flange.

Calculations of standoff distance, W, assumed twenty-one bolts/spacers of 4.76 cm dia. each. The area obstructed by the bolts in the standoff zone was subtracted from the total vented area (side vented area plus area of RWE plate hole). The effective vented area ratio was used as found from the small shock tube results. Working backwards from the given cross-section area, 4.669 m^2 (50.26 ft^2), of the 2.44 m shocks tube and required vented area ratio, the standoff was calculated for each RWE. If a circular RWE is assumed, simple relationships may be obtained.

Equations 3 - 5 below give the results for a solid plate RWE.

$$\frac{Av}{A_t} \equiv R, \tag{3}$$

the vented area ratio found in Tables 3 and 4 as functions of input shock pressure, where Av is the effective vented area and A_t is the total cross section of the shock tube.

$$Av = (\pi DW - A_{Bolts}) = RA_t, \tag{4}$$

the effective side vented area, where the area of the exposed bolts was subtracted. Assuming twenty-one bolts, Equation 4 becomes:

$$W = 0.701R, \text{ m.} \tag{5}$$

Using the same method and assumptions from above, the relationship for standoff for the end flange assembly's vented plate (2.043 m^2), is given in Equation 6.

$$W = 0.701R - .307, \text{ m.} \tag{6}$$

The limit of R at W = 0 is 0.438 corresponding to an input of 45 kPa. For values less than this, the given opening in the vented RWE plate will have to be reduced according to values listed in the bottom half of Table 4.

Figure 35 shows two sample curves plotted from Tables 3 and 4 for the RWEs used.

TABLE 3. STANDOFF DISTANCE VERSUS INPUT SHOCK OVERPRESSURE - SOLID PLATE RWE

Input Overpressure kPa	Overpressure psi	Vented Area Ratio	Standoff Distance* cm	Standoff Distance* in.
0	0	0	0	0
5	0.725	0.055	3.8	1.50
10	1.450	0.116	8.1	3.19
20	2.900	0.225	15.8	6.22
30	4.351	0.320	22.4	8.82
40	5.802	0.400	28.0	11.02
50	7.252	0.470	33.0	12.99
60	8.702	0.535	37.5	14.76
70	10.15	0.593	41.6	16.38
80	11.60	0.648	45.4	17.87
90	13.05	0.693	48.6	19.13
100	14.50	0.735	51.5	20.28
110	15.95	0.775	54.4	21.42
120	17.40	0.810	56.8	22.36
130	18.85	0.840	58.9	23.19
140	20.31	0.865	60.7	23.90
150	21.76	0.885	62.1	24.45
160	23.21	0.898	62.9	24.76
170	24.66	0.910	63.8	25.12

*Standoff was calculated from the vented area ratio based on shock tube internal diameter. Exposed bolts/spacers were subtracted from the vented area. Twenty-one bolt/spacers were assumed - 4.76 cm dia. each.

TABLE 4. STANDOFF DISTANCE VERSUS INPUT SHOCK OVERPRESSURE - VENTED PLATE RWE

Input kPa	Overpressure psi	Vented Area Ratio	Standoff Distance* cm	in	Area of Hole in Plate m^2	f^2
45	6.527	0.437	0	0	2.043	22.0
50	7.252	0.470	2.3	0.91		
60	8.702	0.535	6.8	2.68		
70	10.15	0.593	10.9	4.29		
80	11.60	0.648	14.7	5.79		
90	13.05	0.693	17.9	7.05		
100	14.50	0.735	20.9	8.23		
110	15.95	0.775	23.7	9.33		
120	17.40	0.810	26.1	10.28		
130	18.85	0.840	28.2	11.10		
140	20.31	0.865	30.0	11.81		
150	21.76	0.885	31.4	12.36		
160	23.21	0.898	32.3	12.72		
170	24.66	0.910	33.1	13.03		
0	0	0	0	0	0	0
5	0.725	0.055	0	0	0.257	2.764
10	1.450	0.116	0	0	0.542	5.831
20	2.900	0.225	0	0	1.051	11.31
30	4.351	0.320	0	0	1.494	16.09
40	5.802	0.400	0	0	1.868	20.11

*Standoff was calculated from the vented area ratio for a vented plate with one hole - 1.219 x 1.676 m. The ratio was based on the internal diameter of the shock tube. Exposed bolts/spacers were subtracted from total vented area. Twenty-one bolt/spacers were assumed - 4.76 cm dia. each.

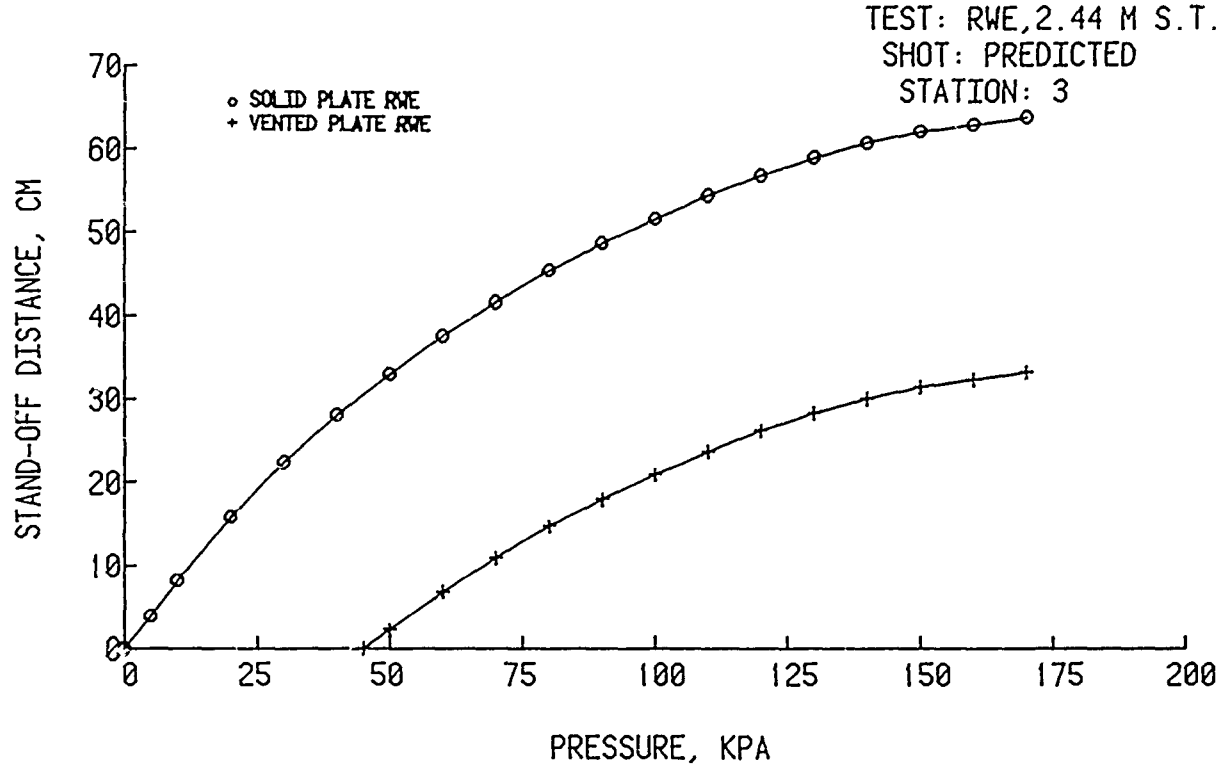

Figure 35. Predicted standoff distance for RWEs on 2.44 m BRL shock tube

C. NASA-Ames Computer Code Comparisons

Figures 36 - 41 on the following pages display comparisons between experimental and computational results for side-on and dynamic pressure at three pressure levels with and without a RWE. Results are for Station 3. Because the input pressure comparison cases are not identical, slight differences in pressure levels are evident.

The reader is advised to observe the general waveforms. It is apparent that both experimental and computational results may be used to model a RWE for the 2.44 m shock tube. There is a difference between the experimental and computational RWE vented areas used in Figures 37, 39, and 41. Comparisons of experimental (solid plate) and computational RWE vented area ratios as a function of input pressure are presented in Figure 42. The two curves are markedly different and this distinctness, which clearly is to be expected, is due to the geometrically different methods used to obtain vented areas. Experimentally a standoff distance is the RWE mechanism; this allows for outflow normal to the side of the shock tube. Computationally, the one-dimensional hydrocode, RWE model allows for outflow normal to the end of the tube.

Although the results are distinct, both methods of modeling a RWE are useful and if conjoined provide an efficient, cost-effective blast modeling technique. The experimental predictions may be used straightforwardly to forecast the appropriate RWE parameters for a specific shot in the 2.44 m tube. Or to save shot time and money a first approximation to experimental results may be obtained by running the hydrocode. Subsequently, Figure 42 provides a method for conversion from computational vented area to experimental vented area applicable to the 2.44 m shock tube.

D. Comparison of 1/48 Scale and Computer Results with Full-Scale Results

A calibration test was conducted in the full-size tube with the rarefaction wave elimination standoff distance established from the curve presented in Figure 35 for a side-on overpressure of 60 kPa. The results of this test are shown in Figure 43. The recorded side-on overpressure was 64.0 kPa which gave a higher reflected pressure on the RWE and therefore a higher reflected pressure moving back up the tube as shown on the records in Figure 43.

A computer run was made to predict the overpressure versus time and the dynamic pressure versus time at stations 84, 86, 87, and 88 in the full-size (2.44 m) shock tube with a rarefaction wave eliminator. These results are presented in Figure 44. The planned maximum side-on pressure was 64 kPa, but the rarefaction wave eliminator was set for a vent area/shock tube area ratio from Figure 32 for a 60 kPa overpressure to match the experimental conditions. Note that the reflected wave from the rarefaction wave eliminator is slightly higher than the side-on pressure as shown in Figure 43.

A computer run was also made for a 64 kPa side-on overpressure in the full-size tube without a rarefaction wave eliminator. The side-on overpressure and dynamic pressure versus time are presented for the four stations in Figure 45. A comparison of Figures 45 and 44 will show the improvement in the extended duration of the overpressure versus time and the realistic dynamic pressure when a rarefaction wave eliminator is applied.

In Figure 46 a comparison is made of the side-on overpressure and dynamic pressure at Station 87 for the 1/48 scaled shock tube model, the computer code run, and the full-size shock tube, without a rarefaction wave eliminator. All pressures are normalized to an input wave of 62 kPa for direct comparisons and the time scale of the record from the model was multiplied by 48. The three sets of records show excellent correlation.

A similar comparison is made in Figure 47 showing again the correlation at Station 87 between the two methods used to predict the effect of a rarefaction wave eliminator when placed to give the proper vent area.

Written material continued on page 81.

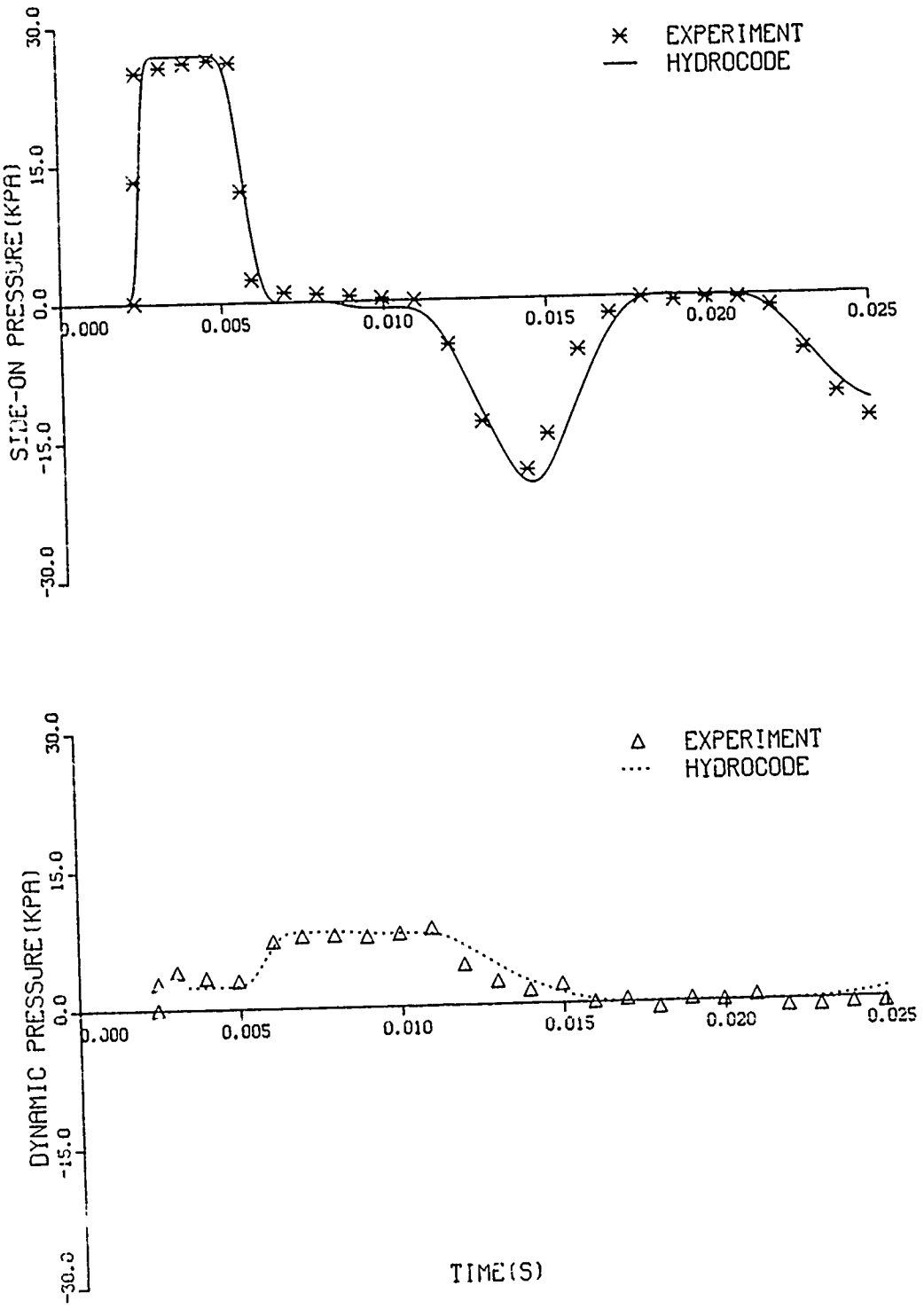

Figure 36. Comparison of experimental and computer side-on and dynamic records, 26.15 average kPa, no RWE, Station 3

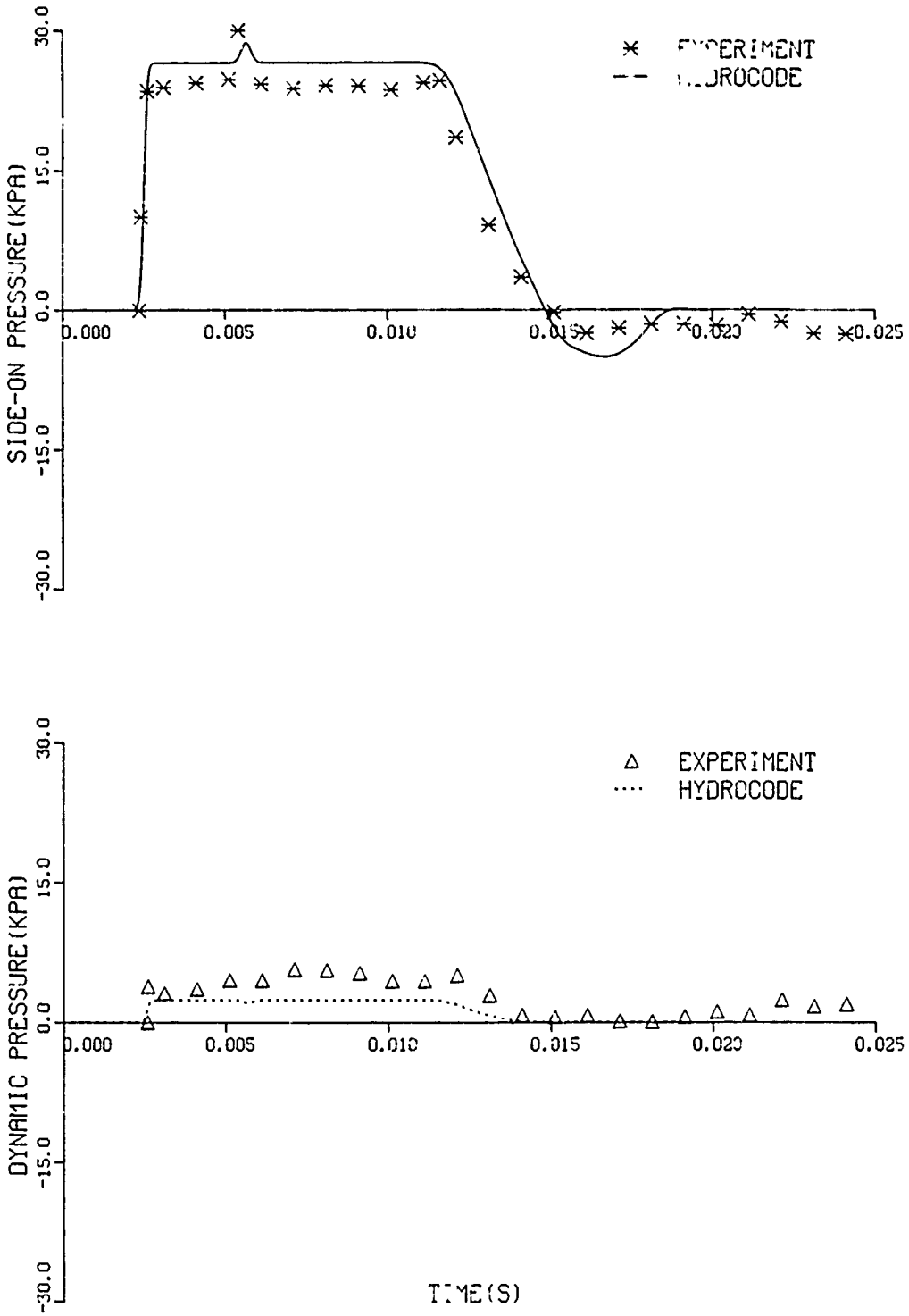

Figure 37. Comparison of experimental and computer side-on and dynamic records, 25.0 average kPa, RWE, Station 3

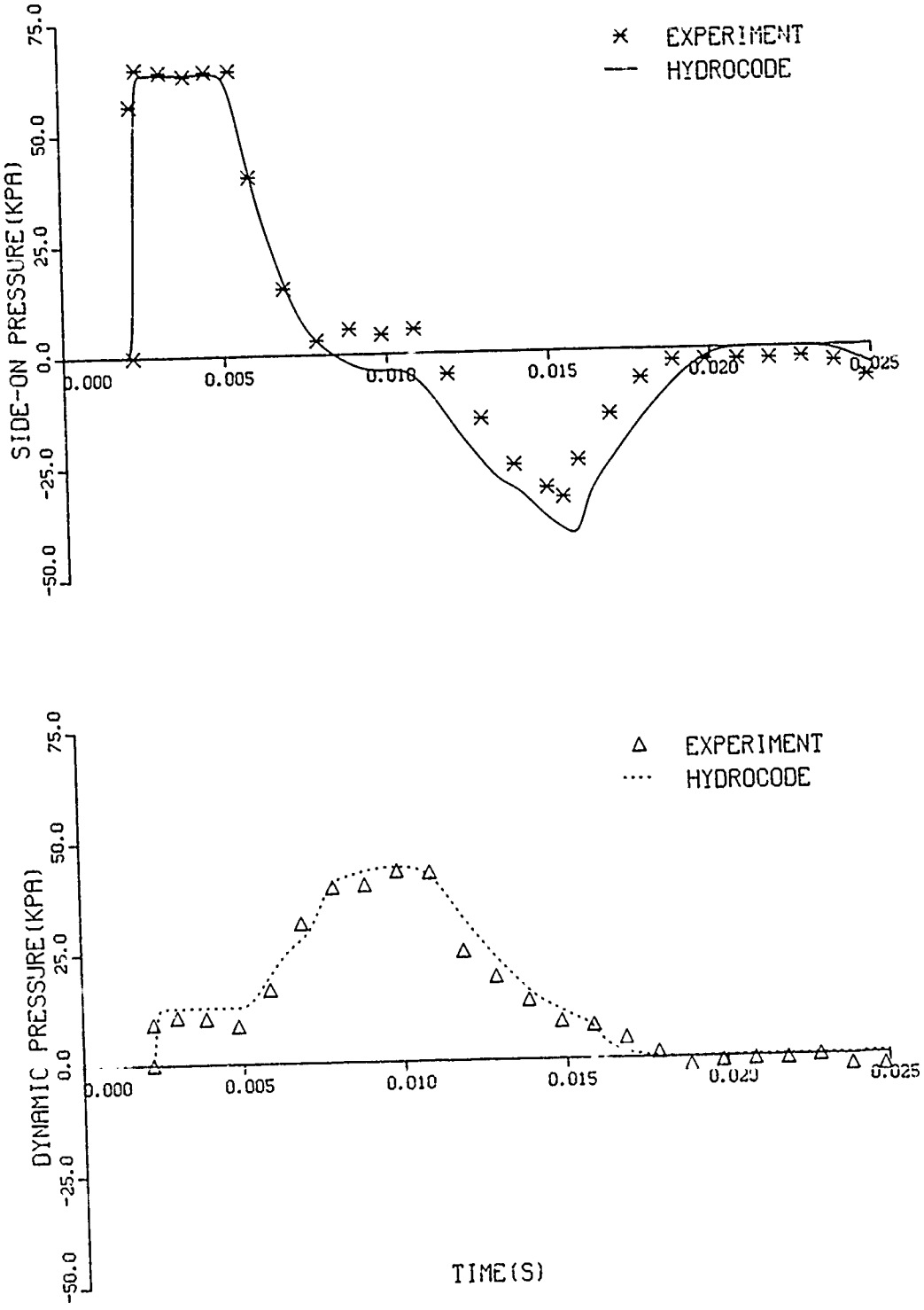

Figure 38. Comparison of experimental and computer side-on and dynamic records, 62.7 average kPa, no RWE, Station 3

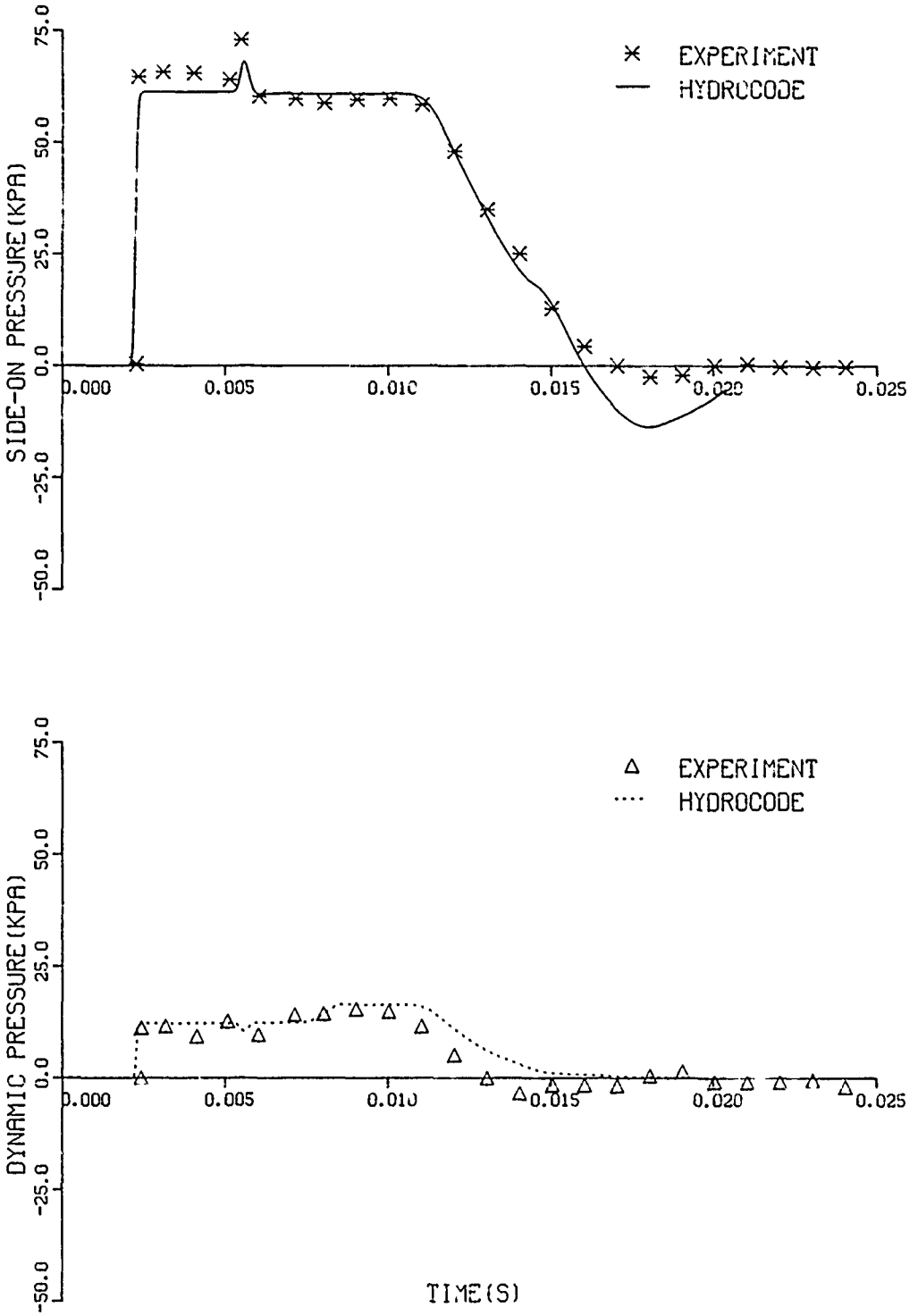

Figure 39. Comparison of experimental and computer side-on and dynamic records, 63.8 average kPa, RWE, Station 3

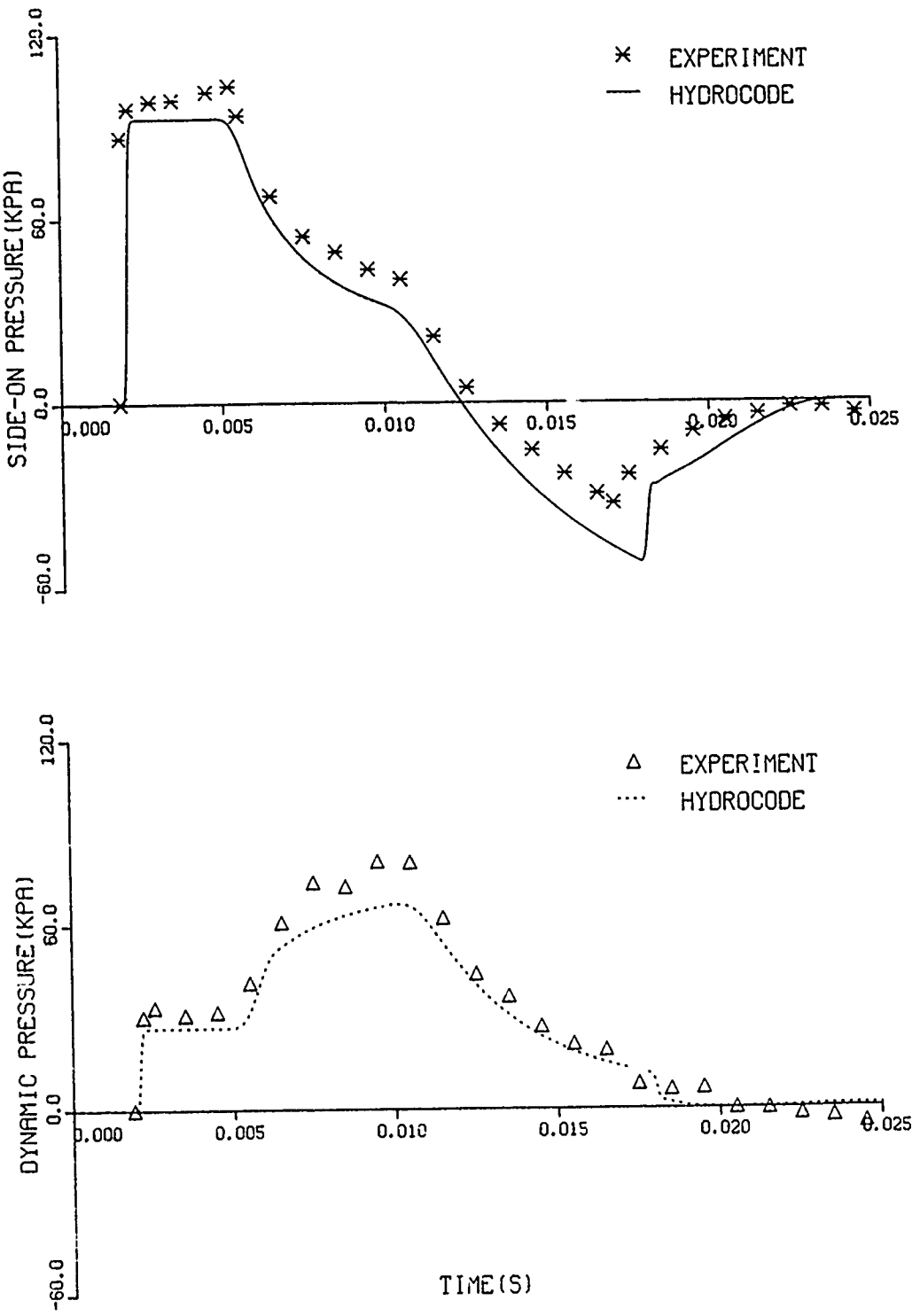

Figure 40. Comparison of experimental and computer side-on and dynamic records, 93.1 average kPa, no RWE, Station 3

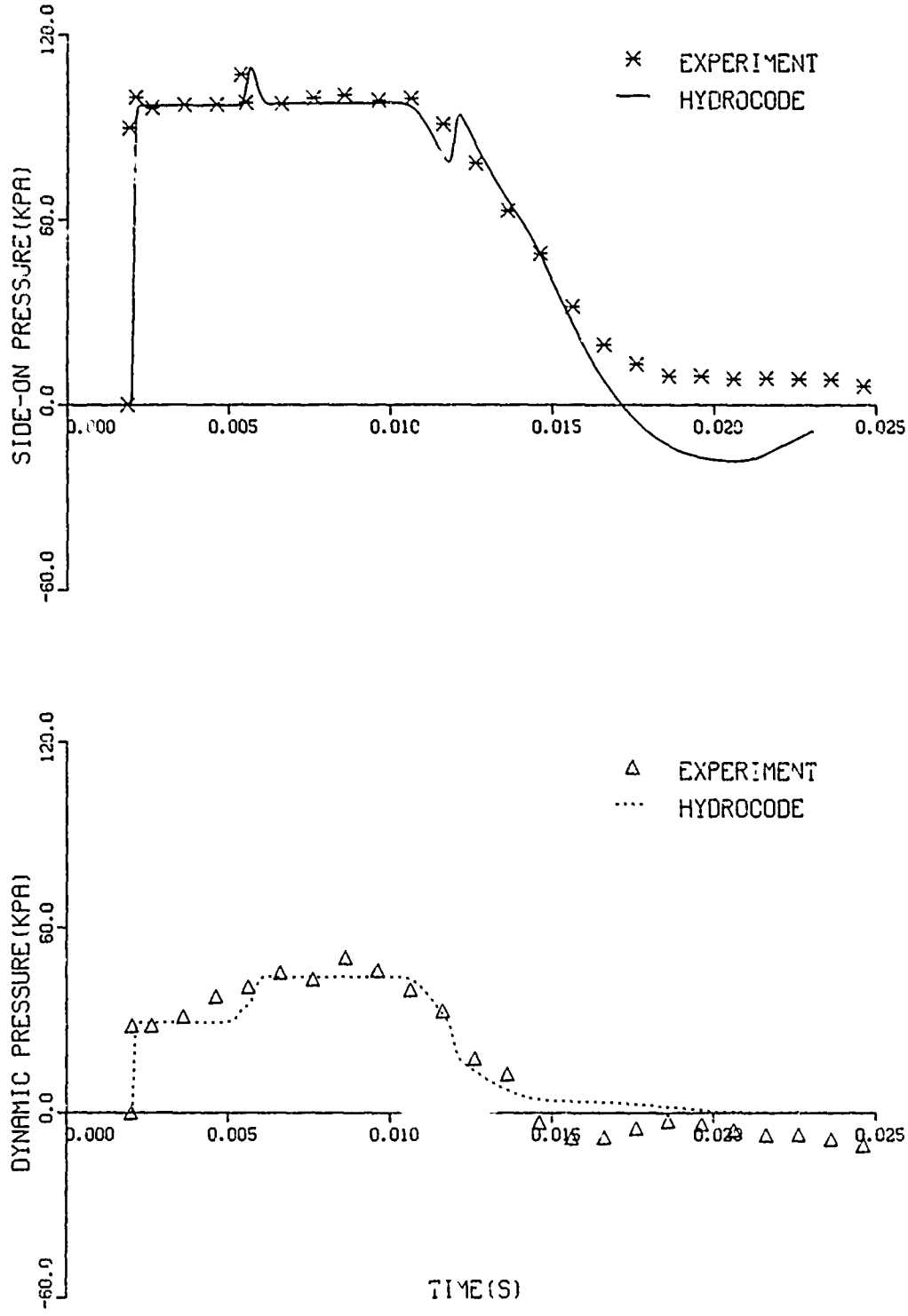

Figure 41. Comparison of experimental and computer side-on and dynamic records, 96.35 average kPa, RWE, Station 3

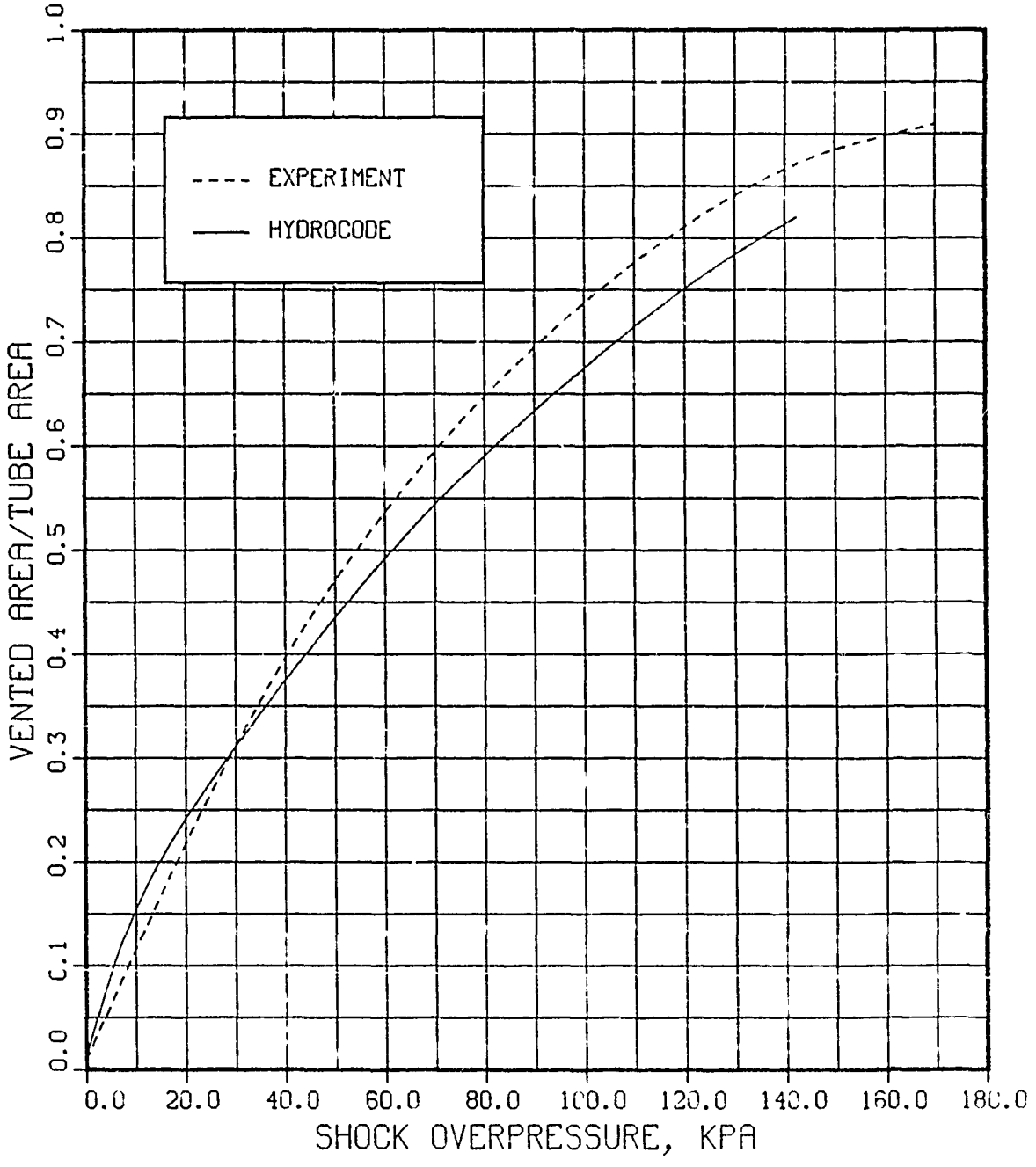

Figure 42. Comparison of experimental (solid plate) and computational predictions for vented area ratio versus input overpressure

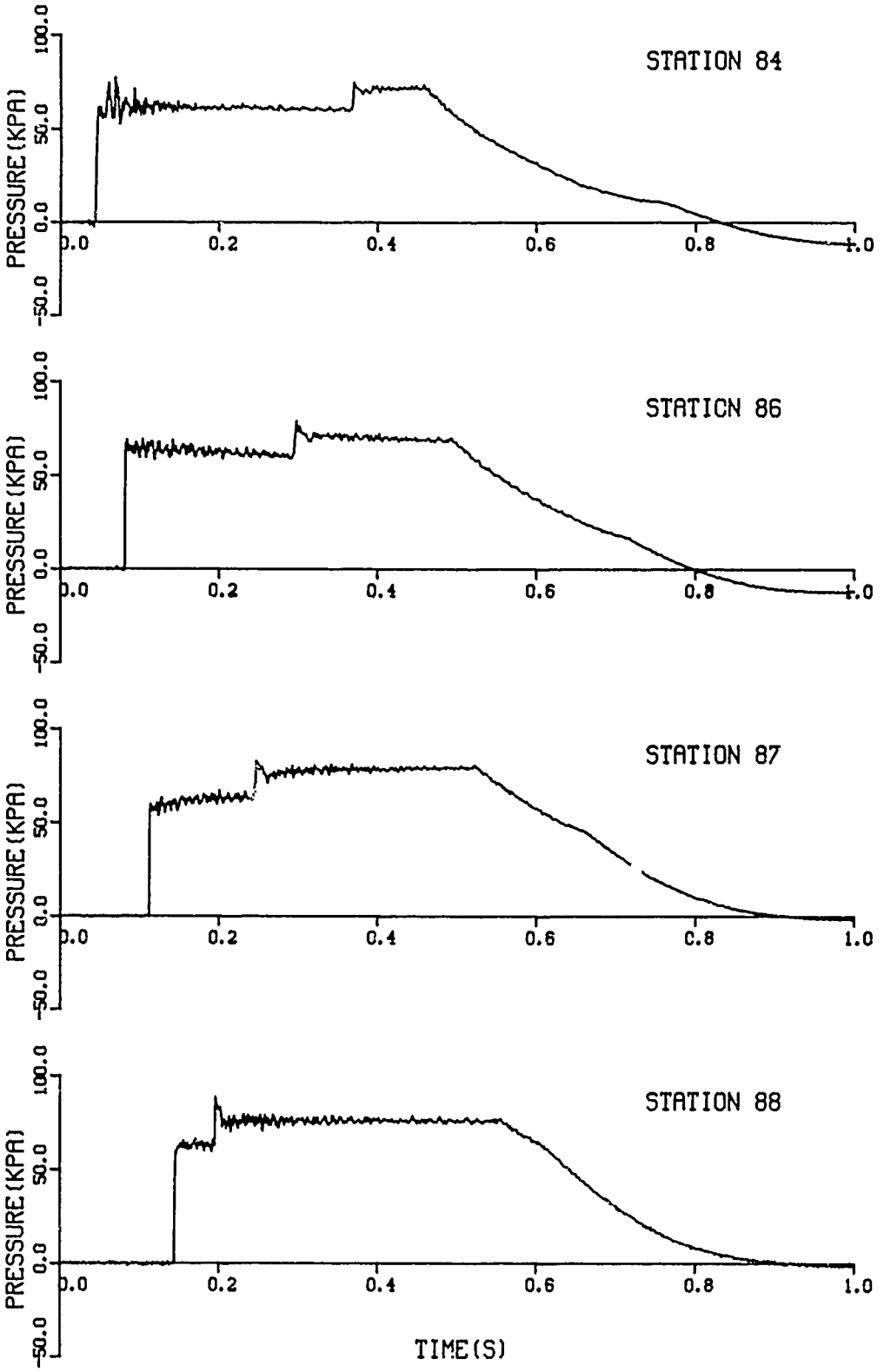

Figure 43. Overpressure versus time at four stations in the 2.44 metre shock tube with RWE.

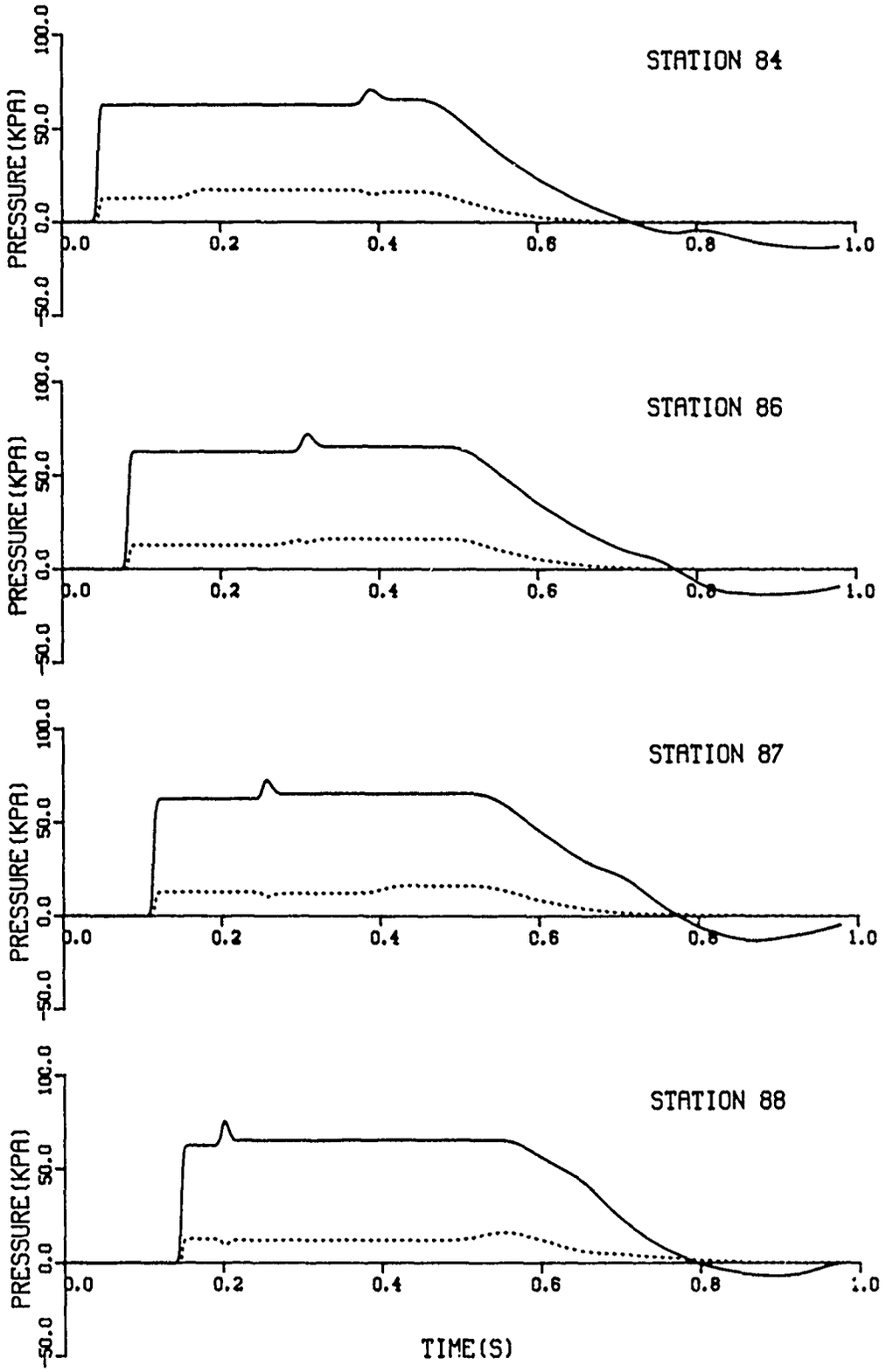

Figure 44. Overpressure and dynamic pressure versus time from NASA-Ames computer program for the 2.44 metre shock tube with RWE

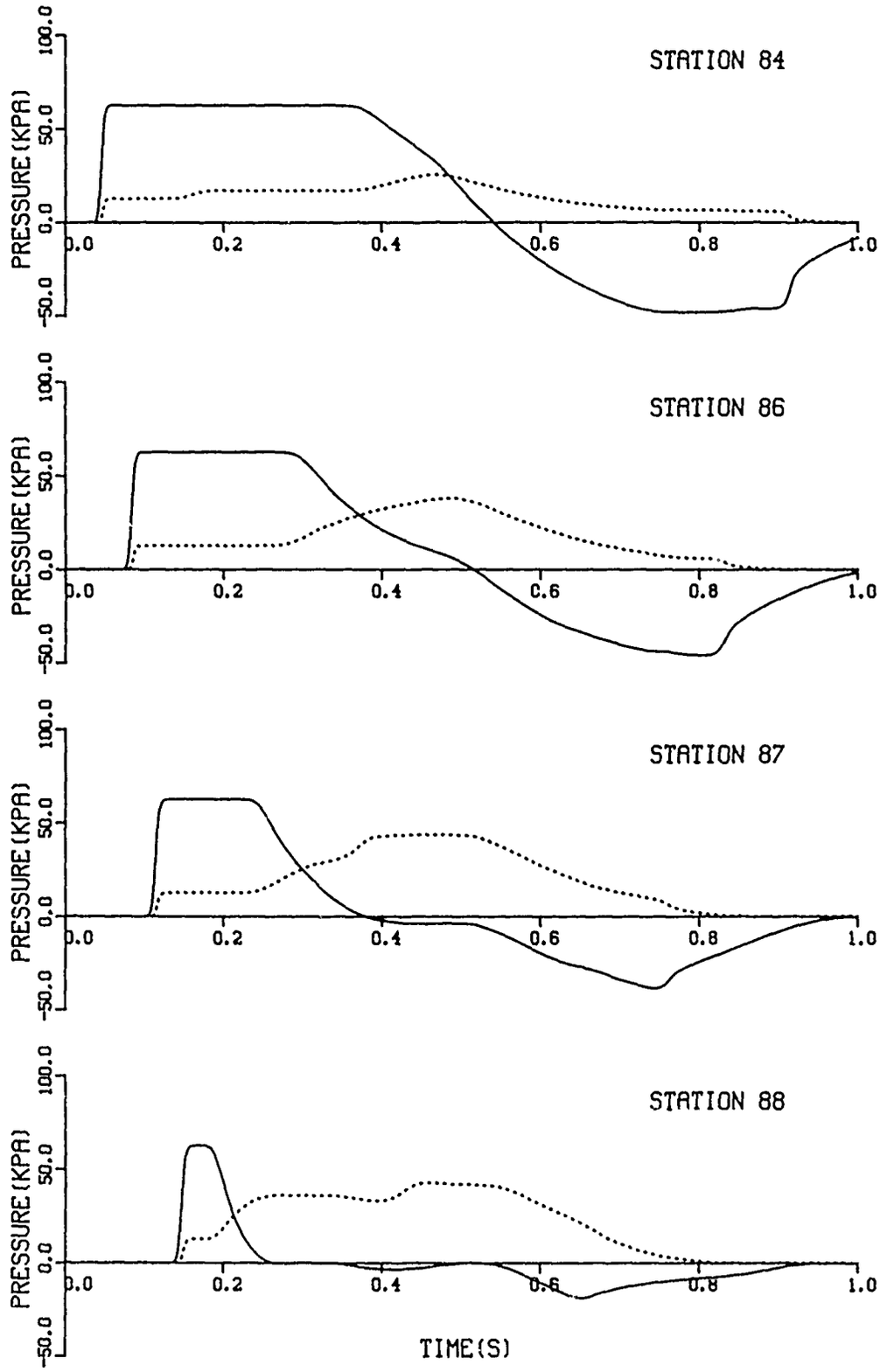

Figure 45. Overpressure and dynamic pressure versus time from NASA-Ames computer program for the 2.44 metre shock tube without RWE.

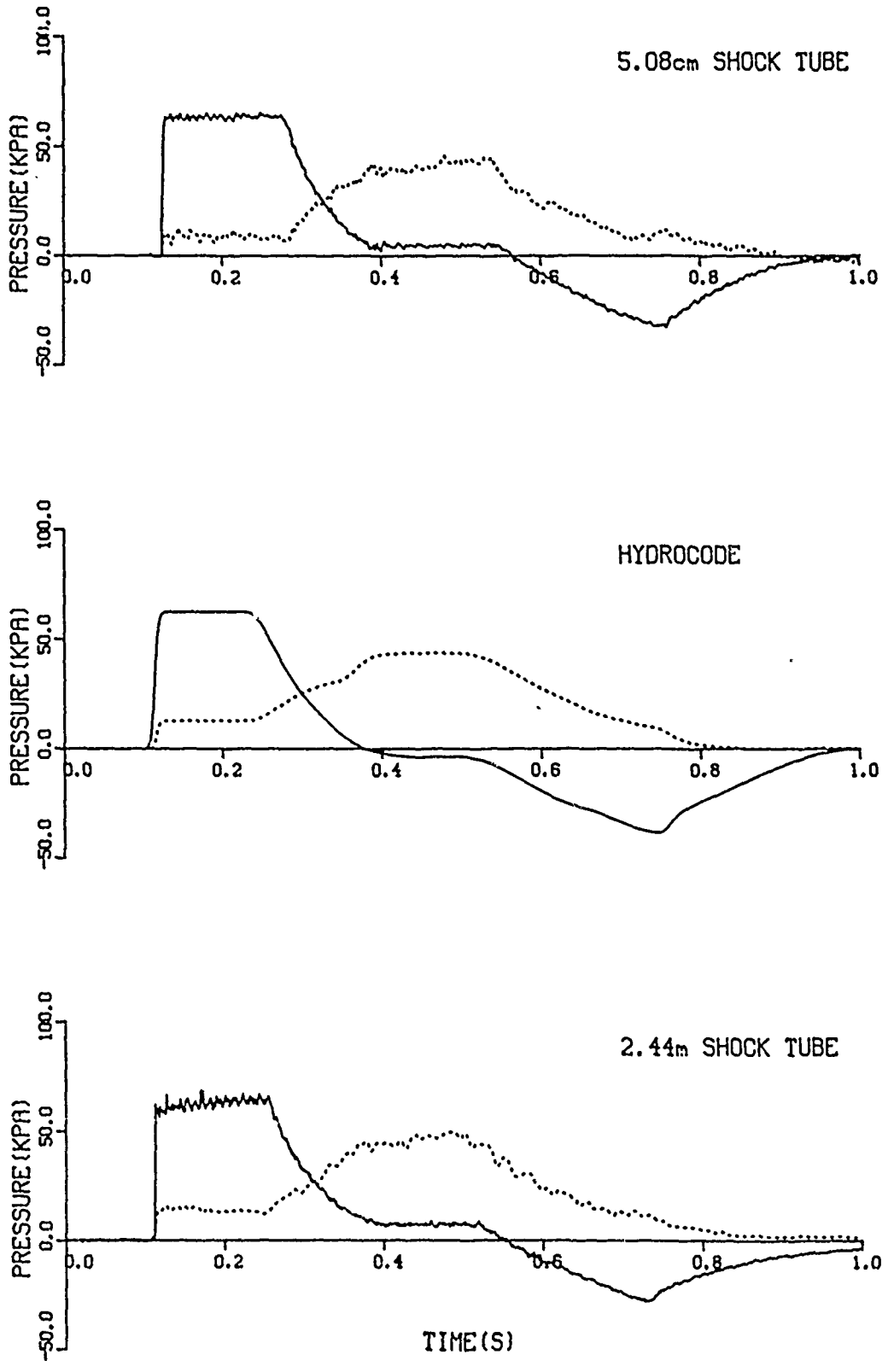

Figure 46. Comparison of results from 1/48 scale model and computer program output with full-scale results at Station 87 without RWE

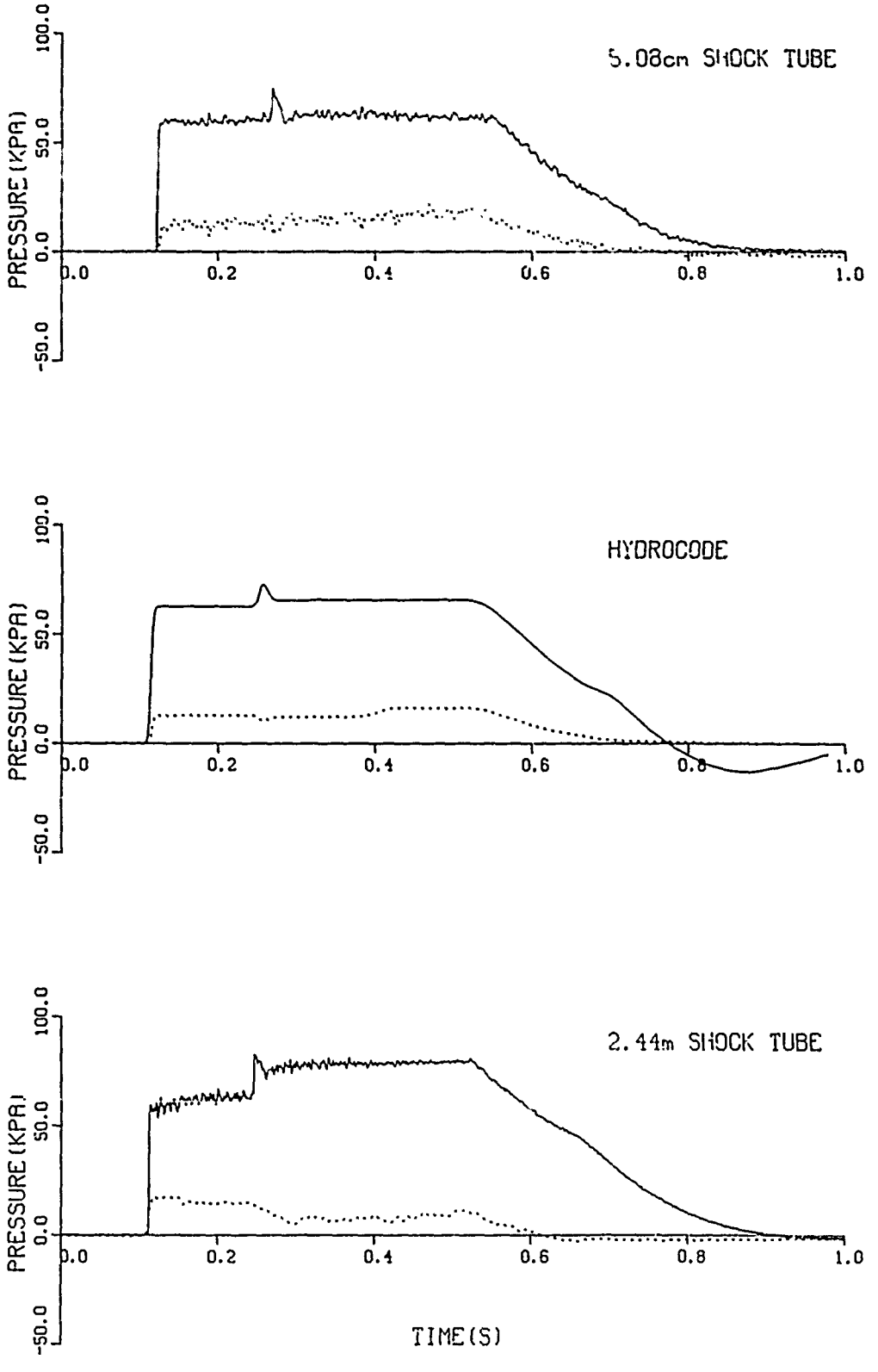

Figure 47. Comparison of results from 1/48 scale model and computer program output with full-scale results at Station 87 with RWE

VI. SUMMARY AND CONCLUSIONS

Three general types of rarefaction wave eliminators (RWEs) were designed and tested on a 5.08 cm I.D. shock tube to determine a suitable design of RWE for the BRL 2.44 m shock tube. The small shock tube had been modified from a standard calibration shock tube to represent 1/48th scale of the larger shock tube. Lengths of driver, test section, and transducer locations were scaled to match the larger shock tube.

The tests included parameter changes of input pressure, standoff distance, and plate opening shape and number of openings in a particular RWE plates used. Of the three types tested - solid plate, vented plate and lattice strips - the solid plate and vented plate types were found to be most suitable for use on the BRL 2.44 m shock tube. It was difficult to find the exact vented area ratio needed when the lattice RWE was tried.

Variations in the shape of the RWE plate opening did not seem to make any noticeable difference in the pressure-time records obtained. A rectangular hole, circular holes, and slats were used to set as a vent at the RWE end plate. Since the shape and number of holes did not change the resulting waveform at Station 3, the station of most interest, it is recommended that the currently used end flange assembly be used as a RWE directly on the BRL 2.44 m shock tube. Only slight changes will be needed for its use.

The NASA-Ames hydrocode was used to predict several shots that are compared to the corresponding experimental shots. The predictions compare favorably to the experimental data. Pressure-time records are shown with pertinent parameter tables for use of a rarefaction wave eliminator at the BRL 2.44 m shock tube.

Appendix B shows a sketch of the end flange assembly that might easily be adapted for use as a rarefaction wave eliminator by using either a solid plate or as a vented plate. The small 1/48th scale shock tube was found to produce waveforms representative of the large 2.44 m BRL shock tube at all positions where pressure-time records were obtained.

ACKNOWLEGEMENTS

The authors wish to thank Mr. Richard Thane for the shock tube modifications needed for the tests, Mr. George Watson for the electronic recording and Mr. Rodney Abrahams for writing the data reduction program. The authors also wish to acknowledge the assistance of Dr. Andrew Mark and Mr. Klaus Opalka whose work with the NASA-Ames hydrocode made possible the computer portions of this report.

REFERENCES

1. Andrew Mark, "Computational Design of Large Scale Blast Simulators," AIAA 19th Aerospace Sciences Meeting, January 12 - 15, 1981, St. Louis, Missouri.

2. J. J. Yagla and others, "The Waves System in Explosively Driven Conical Shock Tubes," Second MABS, DNA 2275P, The Naval Weapons Laboratory, Dahlgren, VA, 2 - 5 November 1970.

3. J. R. Crosnier and J. B. G. Monsac, "Large Diameter High Performance Blast Simulators," Fifth MABS, Stockholm, May 23 - 26 1977.

4. W. Haverdings, "Preliminary Design of the 2.0 m Diameter rOE - Driven Blast Simulator," Seventh MABS, Medicine Hat, Alberta, Canada, 13 - 17 July 1981.

5. George A. Coulter, "Dynamic Calibration of Pressure Transducers at the BRL Shock Tube Facility," BRL Memorandum Report 1843, May 1967 (AD 654508).

6. Brian P. Bertrand, "BRL Dual Shock Tube Facility," BRL Memorandum Report 2001, August 1969 (AD 693264).

7. C. Languin, "Simulation of Shock and Blast Expansion Wave Compensator for 2.40 m Diameter Shock Tube, Description, Report of Its Behavior in Response to Blast Waves," Centre d'Etudes de Gramat, Technical Note T-76-29, May 1976.

8. Patrick J. Roache, Computational Fluid Mechanics, Hermosa Publishers, Albuquerque, NM, 1972, pp 2 - 12, 204 - 286.

9. R. M. Beam and R. F. Warming, "An Implicit Factored Scheme for the Compressible Navier Stokes Equations," AIAA Journal, Volume 16, No. 4, April 1978, pp 393 - 402.

10. A. Weidermann, "Study of Grids in Shock Tubes," Proceedings of First Shock Tube Symposium, SWR-TM-57-2, Hq AFSWC, Kirtland Air Force Base, NM, 26-27 February 1957.

APPENDIX A

PRESSURE-TIME RECORDS

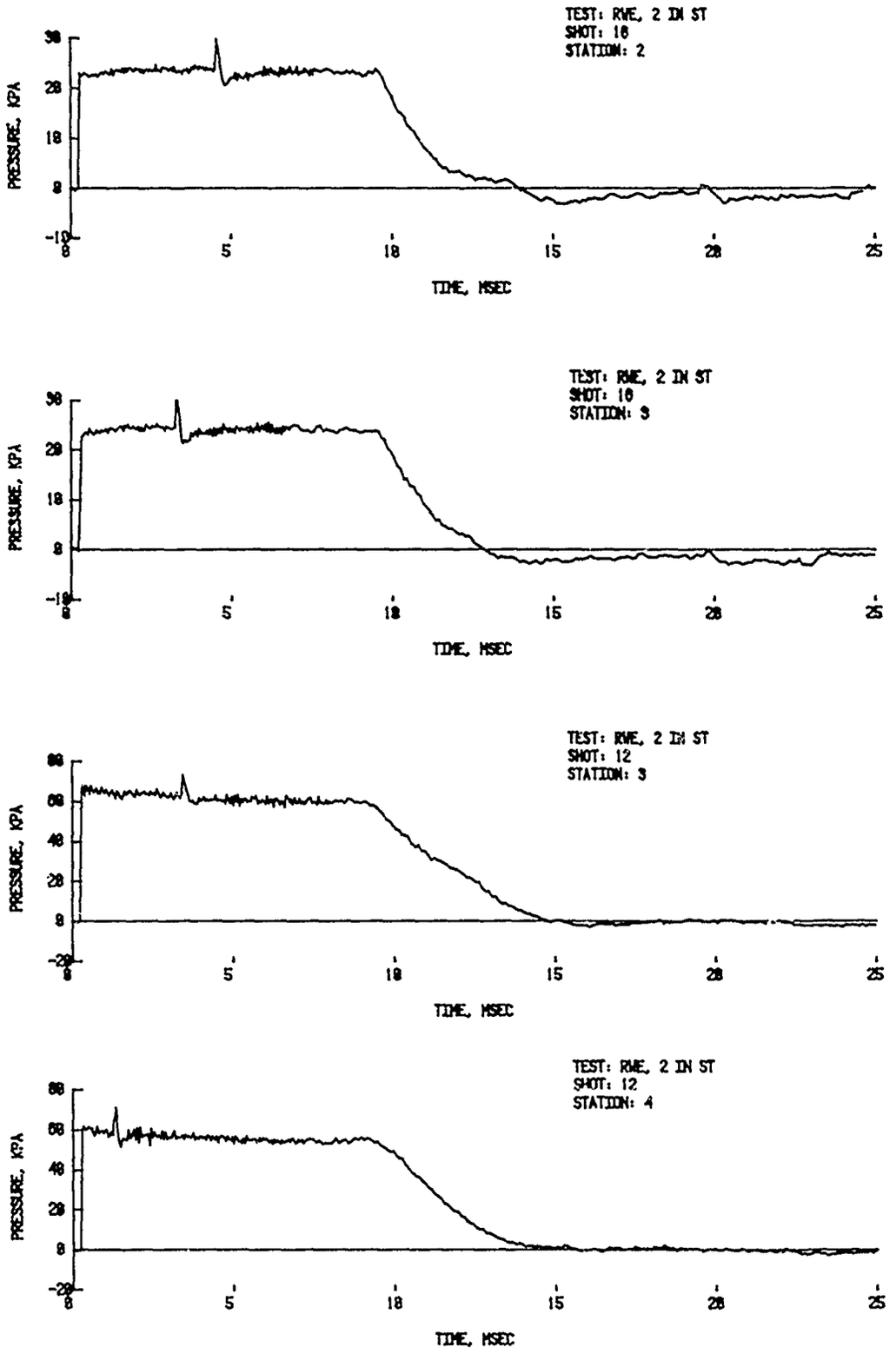

Figure A-1. Pressure-time records for solid plate RWE

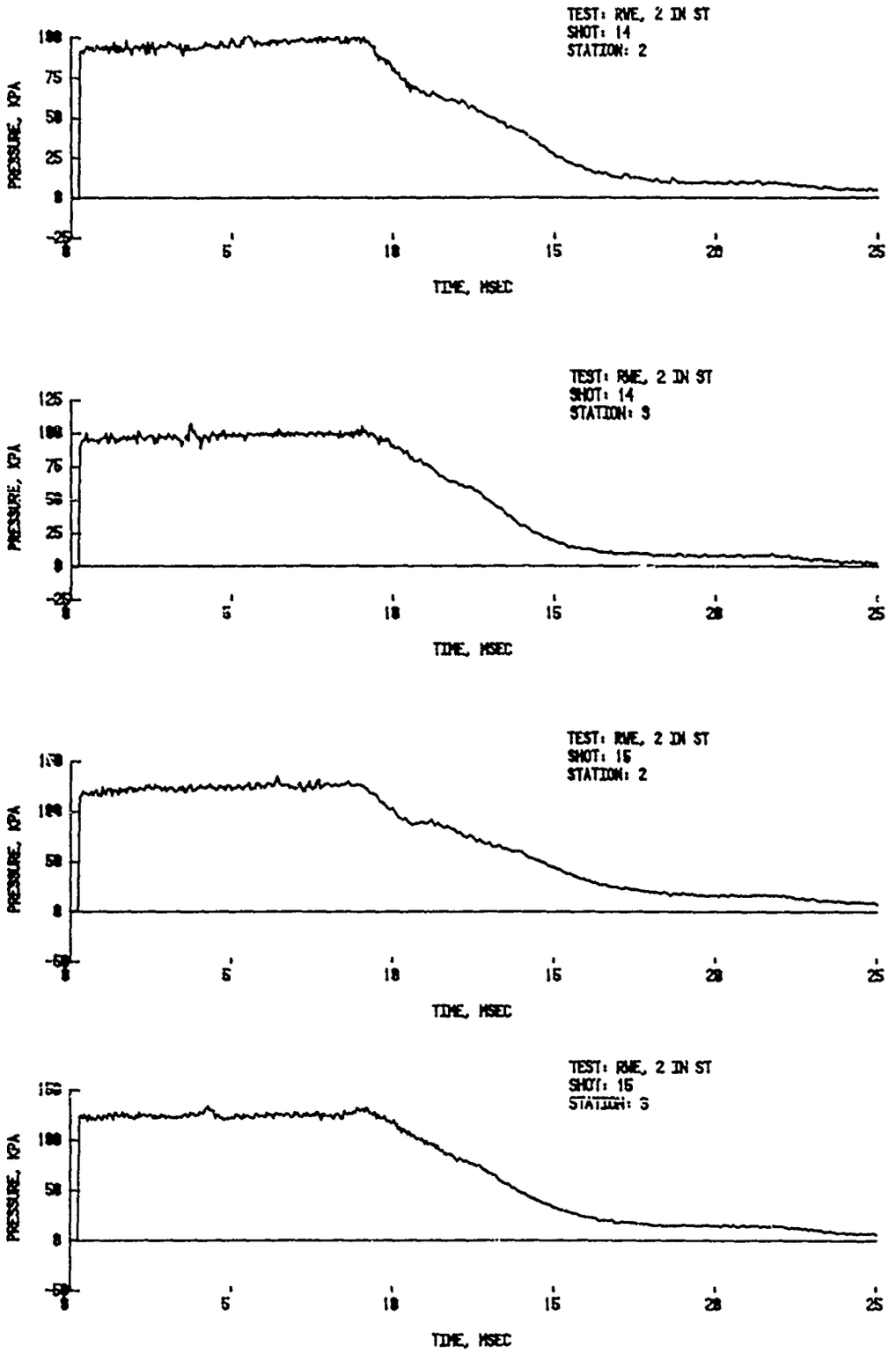

Figure A-1. (Continued) Pressure-time records for solid plate RWE

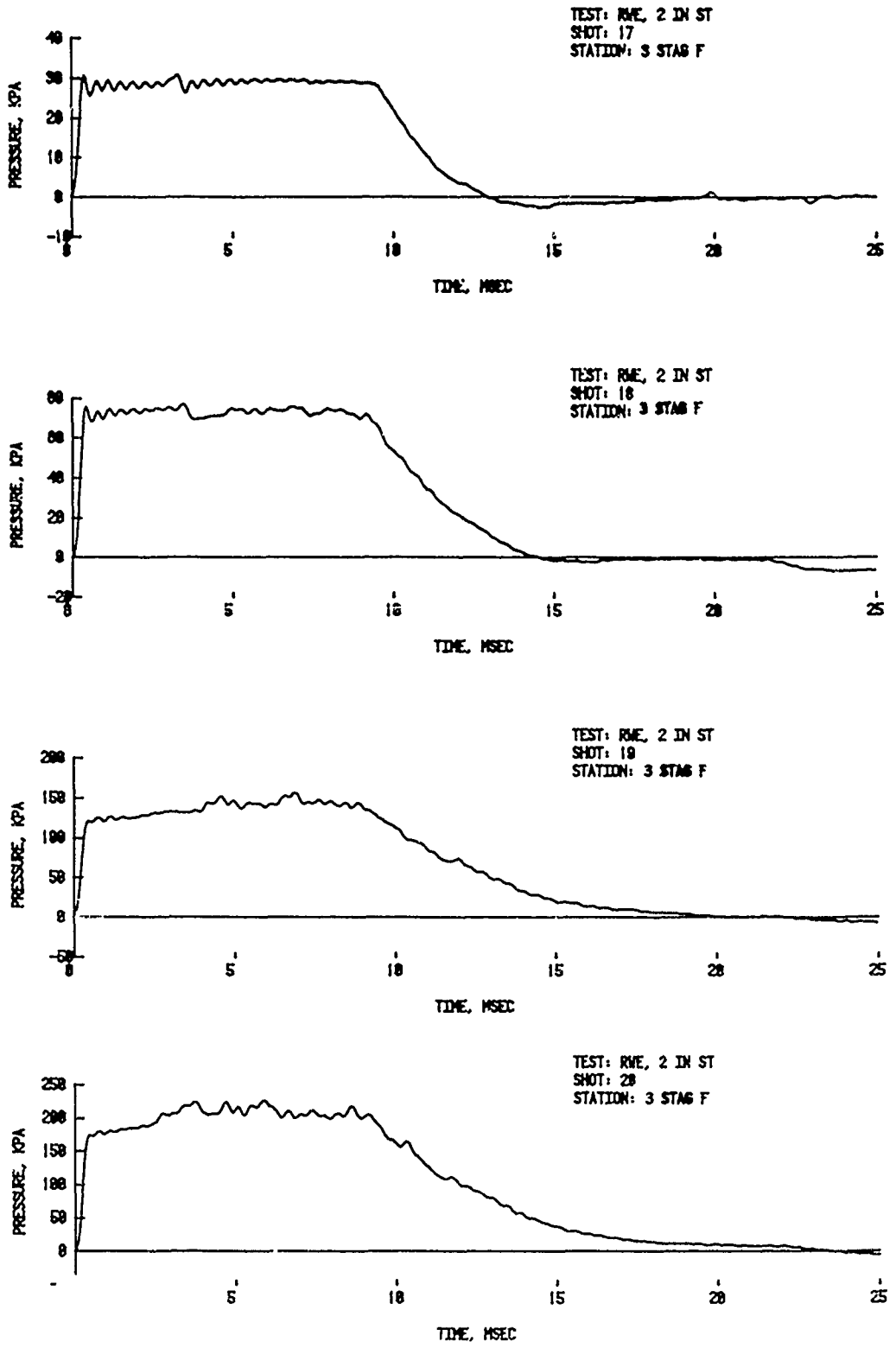

Figure A-1. (Continued) Pressure-time records for solid plate RWE

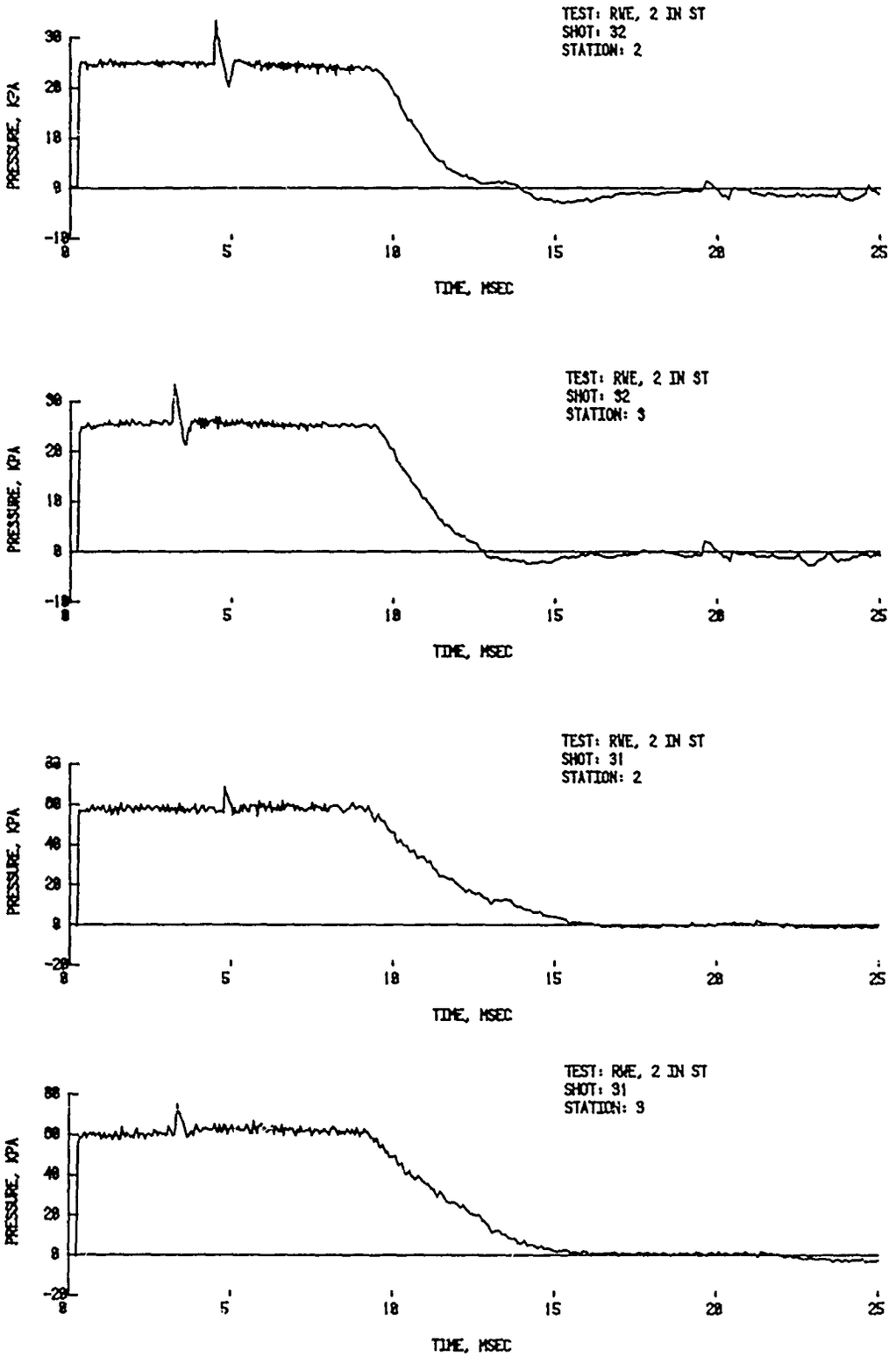

Figure A-2. Pressure-time records for rectangular vented RWE.

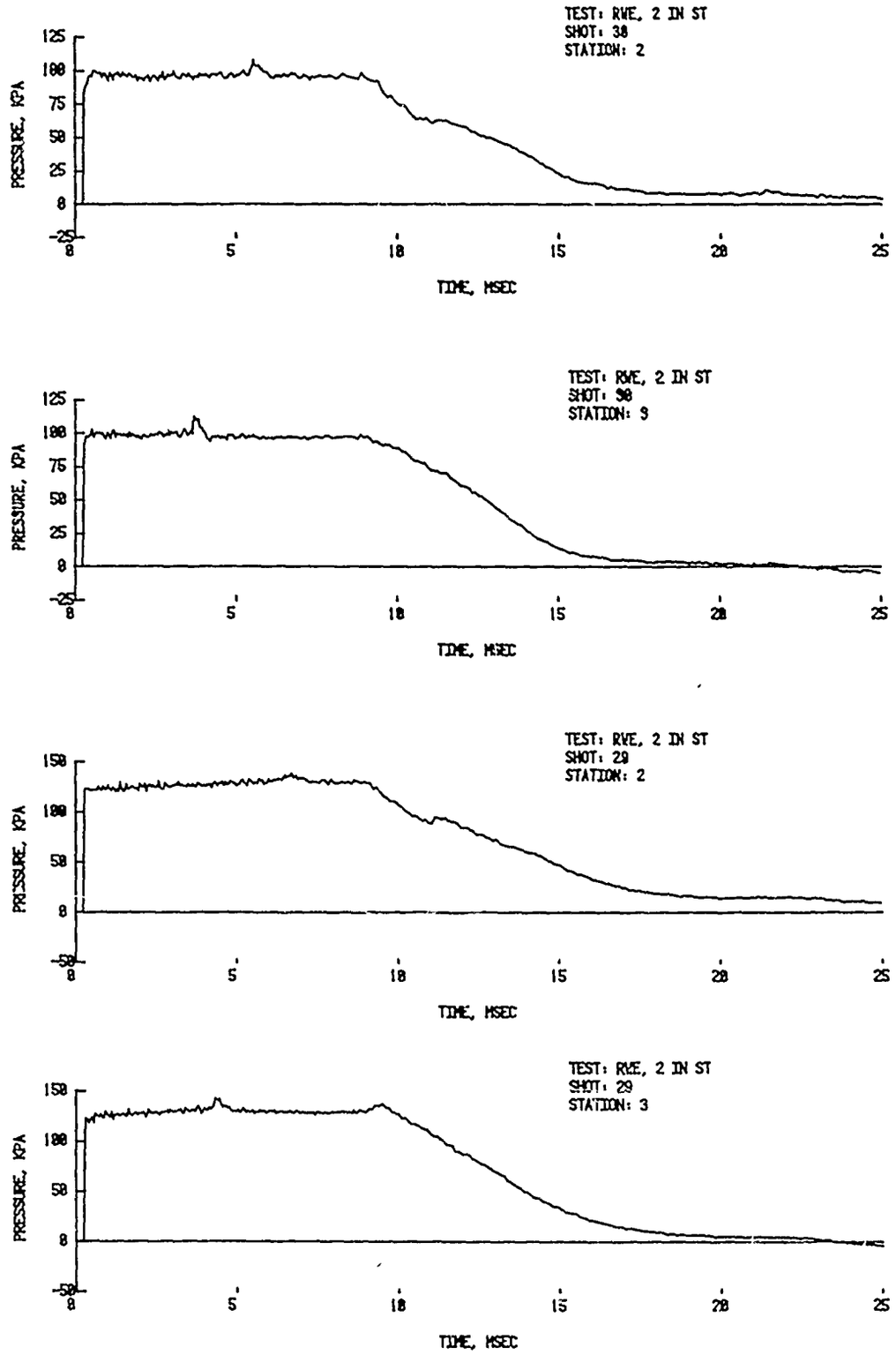

Figure A-2. (Continued) Pressure-time records for rectangular vented RWE.

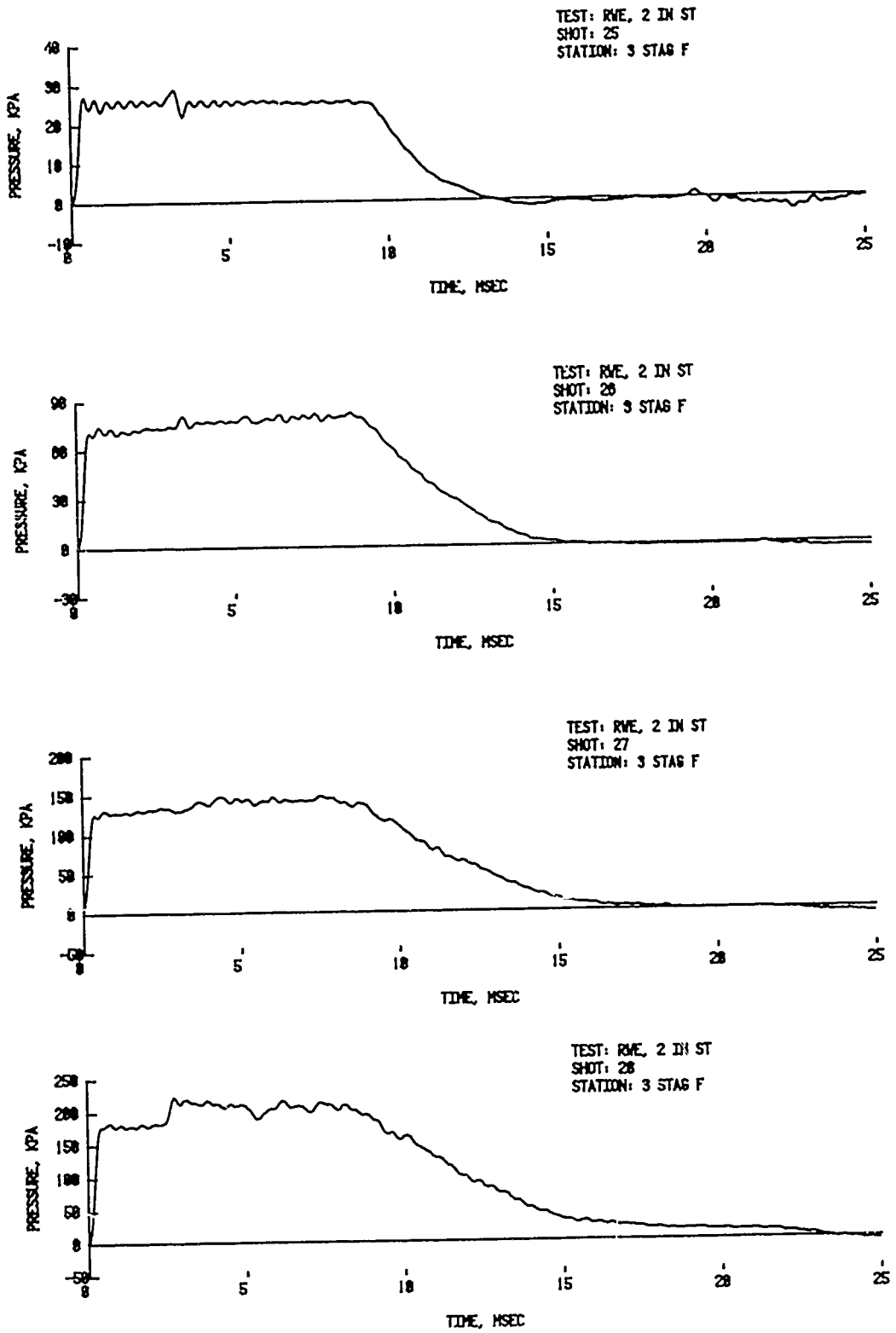

Figure A-2. (Continued) Pressure-time records for rectangular vented RWE.

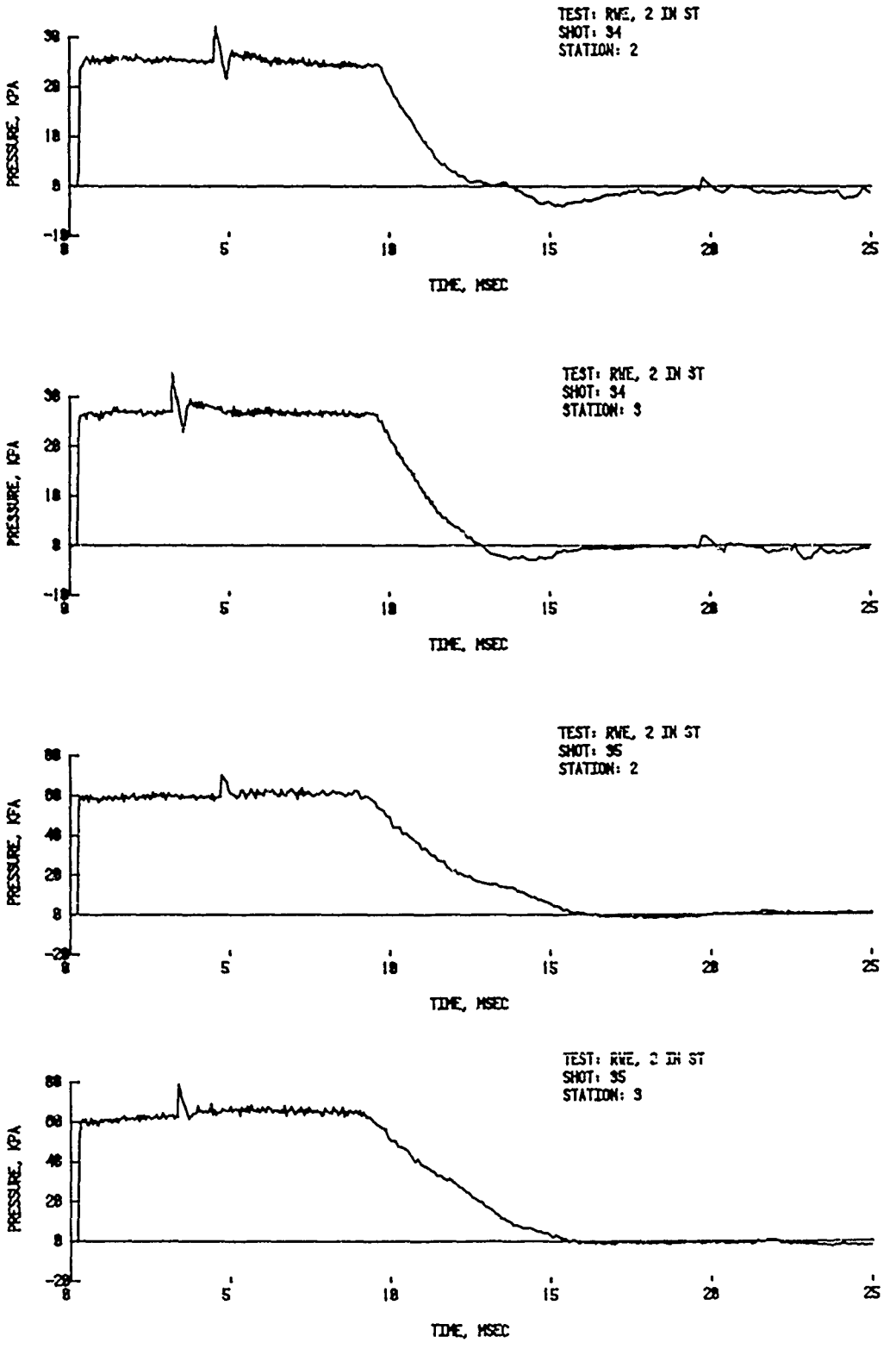

Figure A-3. Pressure-time records for a single circular hole vented RWE

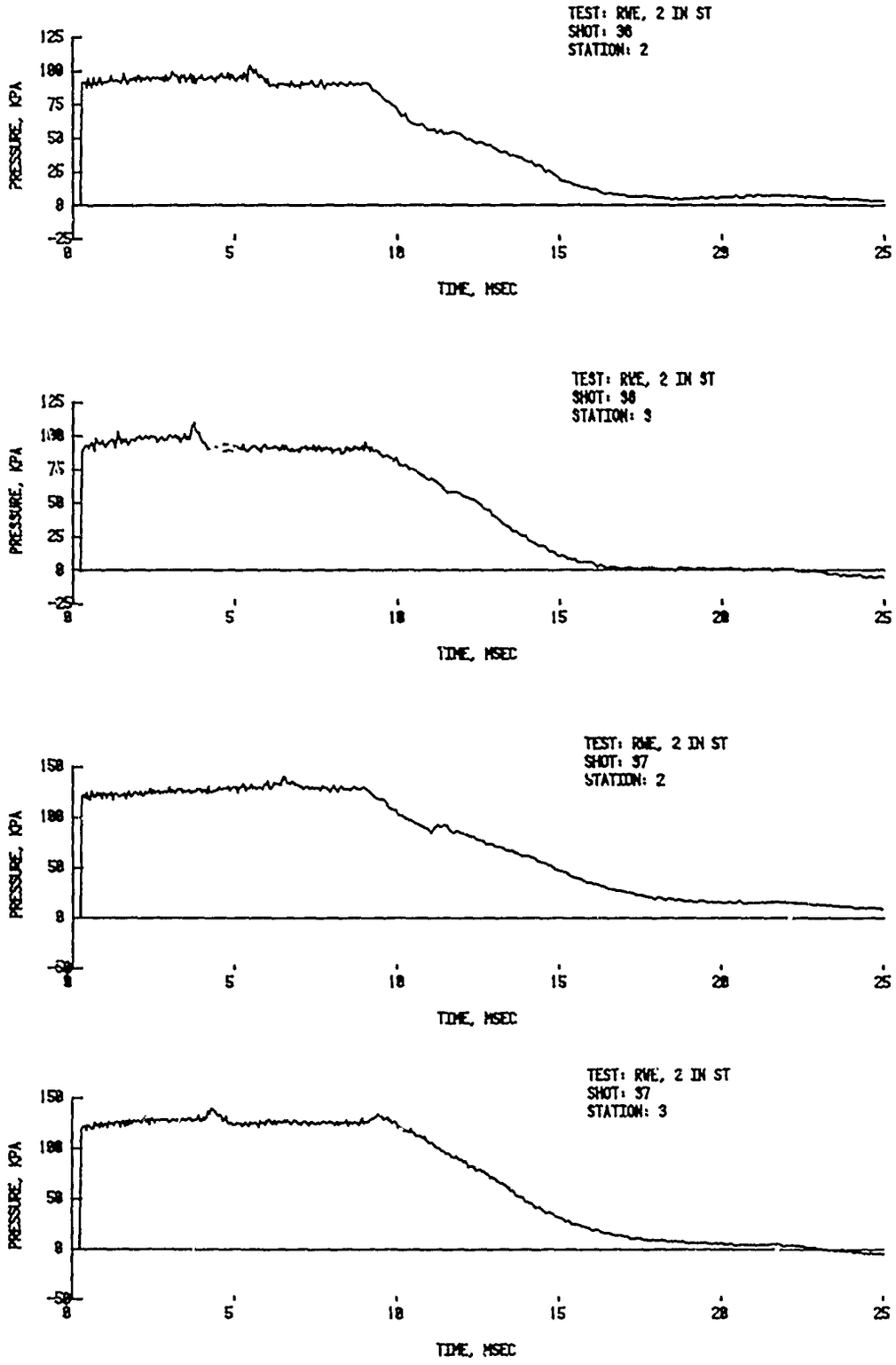

Figure A-3. (Continued) Pressure-time records for a single circular hole vented RWE

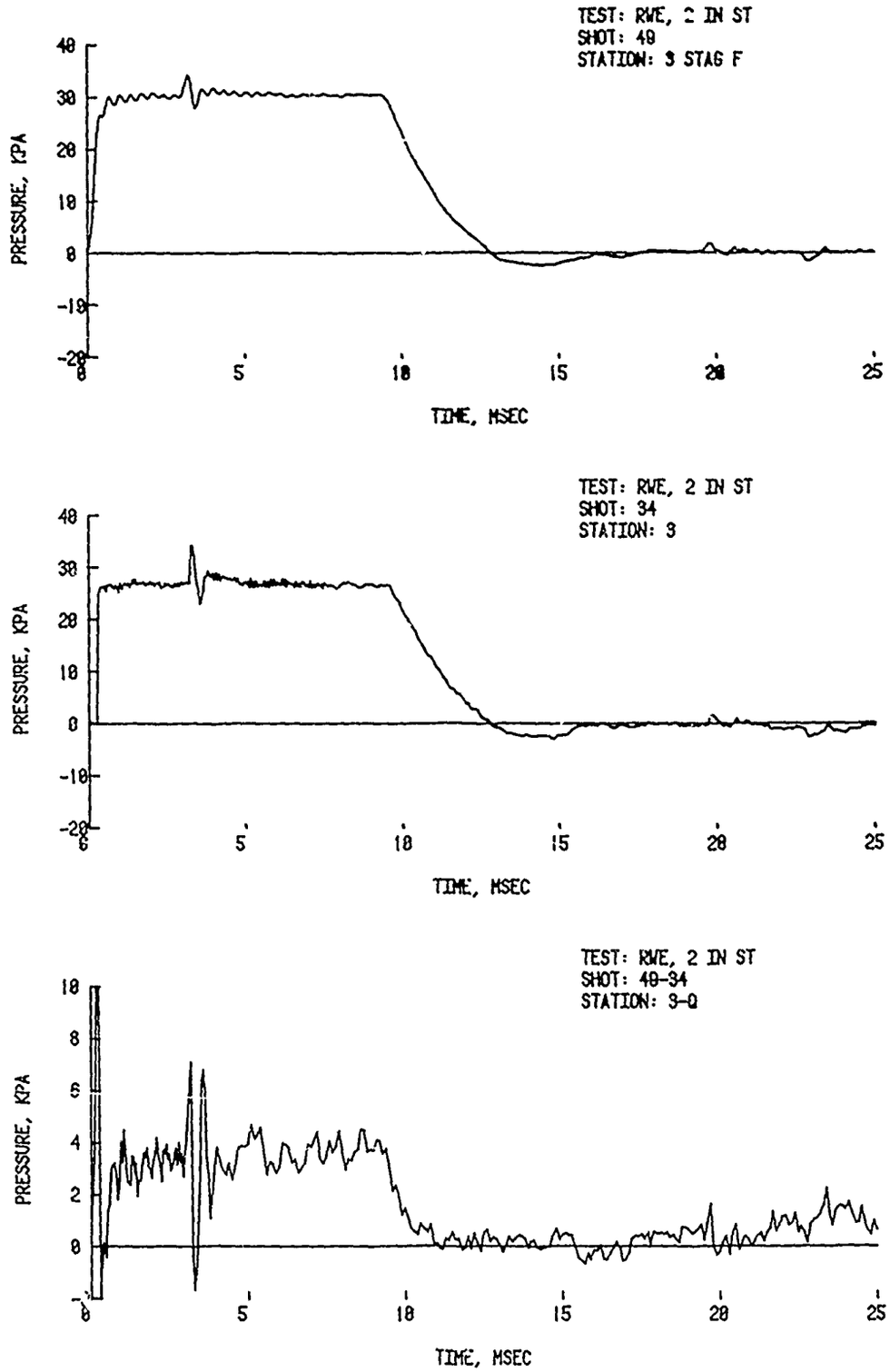

Figure A-3. (Continued) Pressure-time records for a single circular hole vented RWE

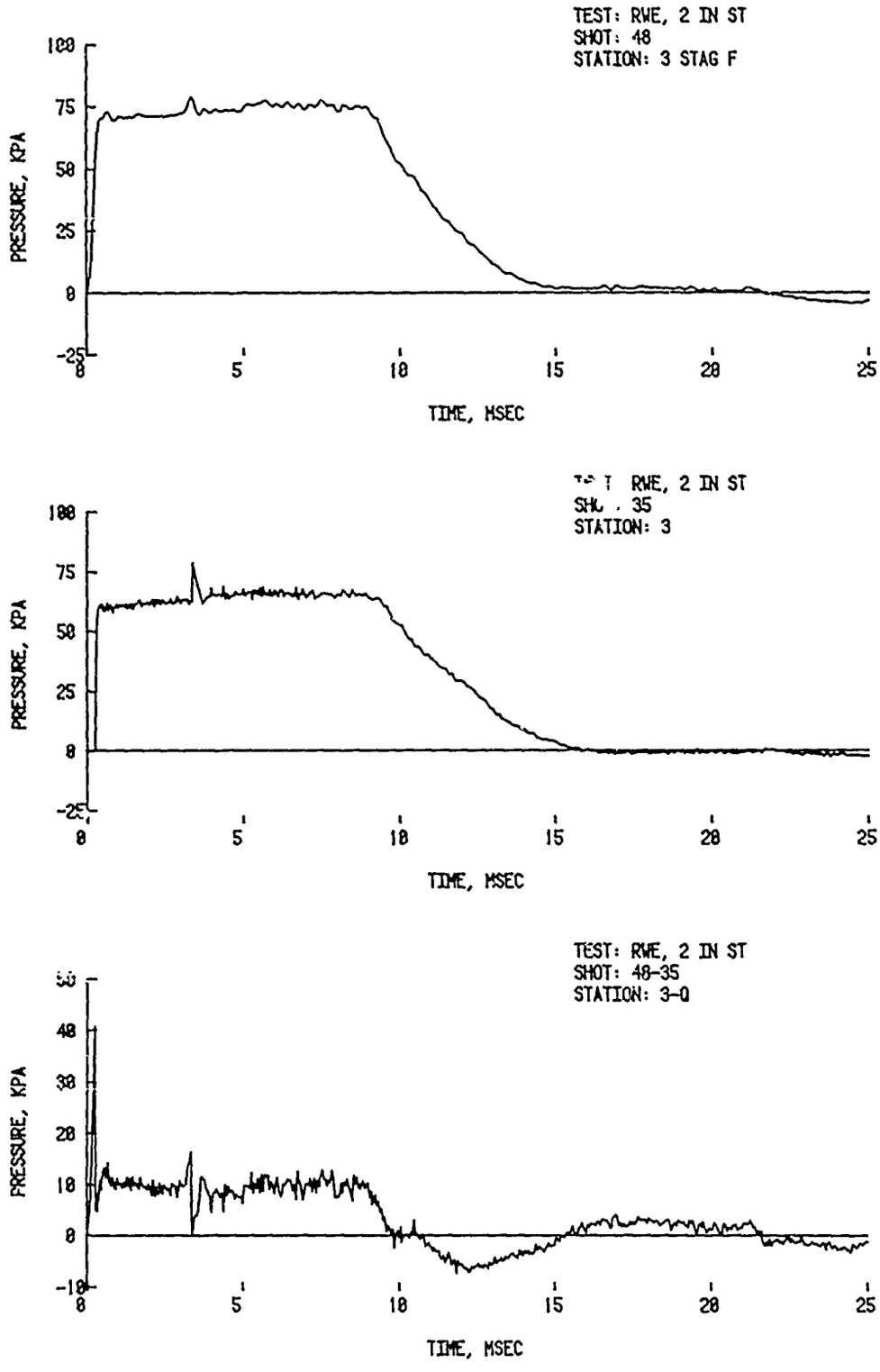

Figure A-3. (Continued) Pressure-time records for a single circular hole vented RWE

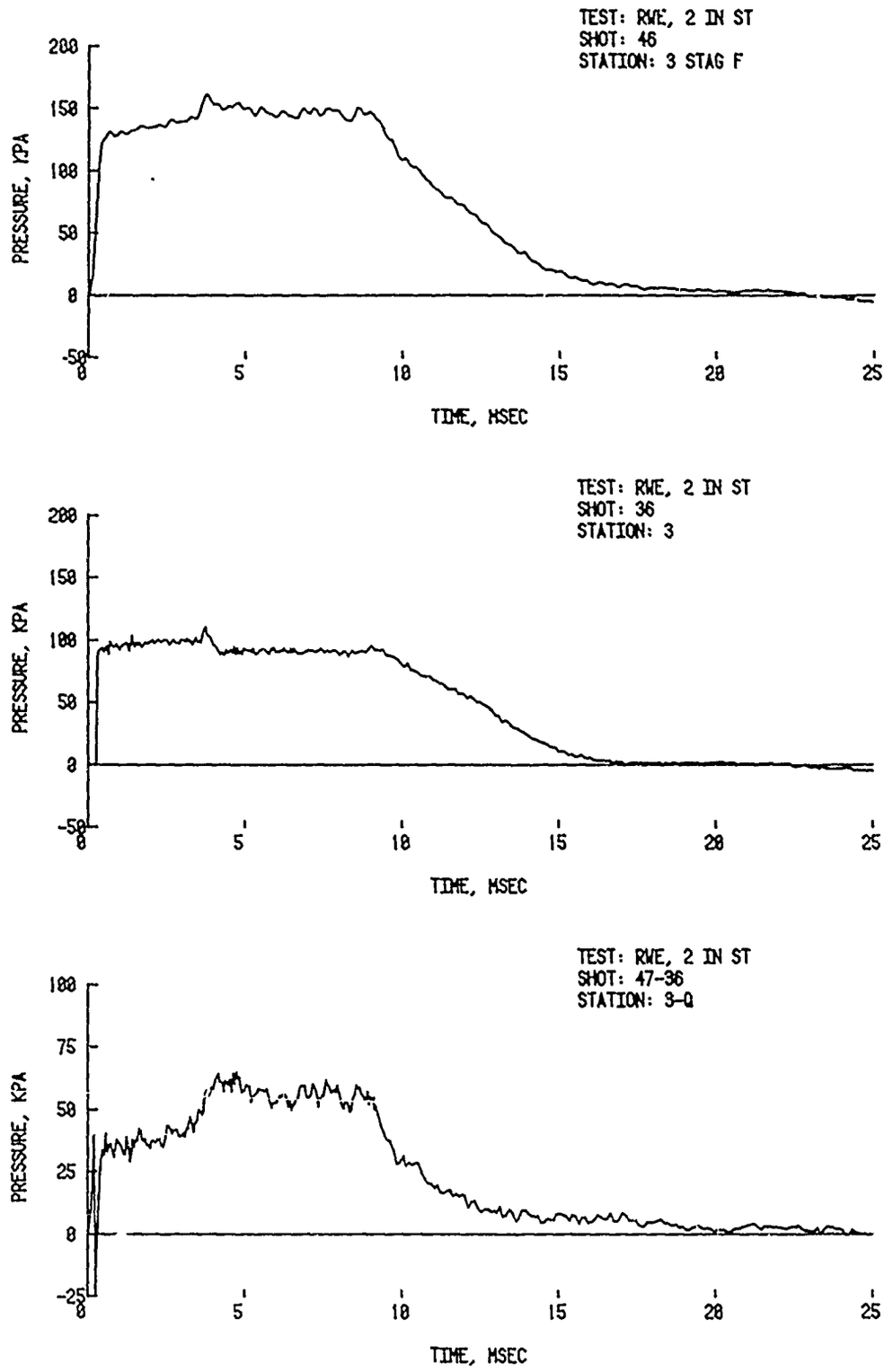

Figure A-3. (Continued) Pressure-time records for a single circular hole vented RWE

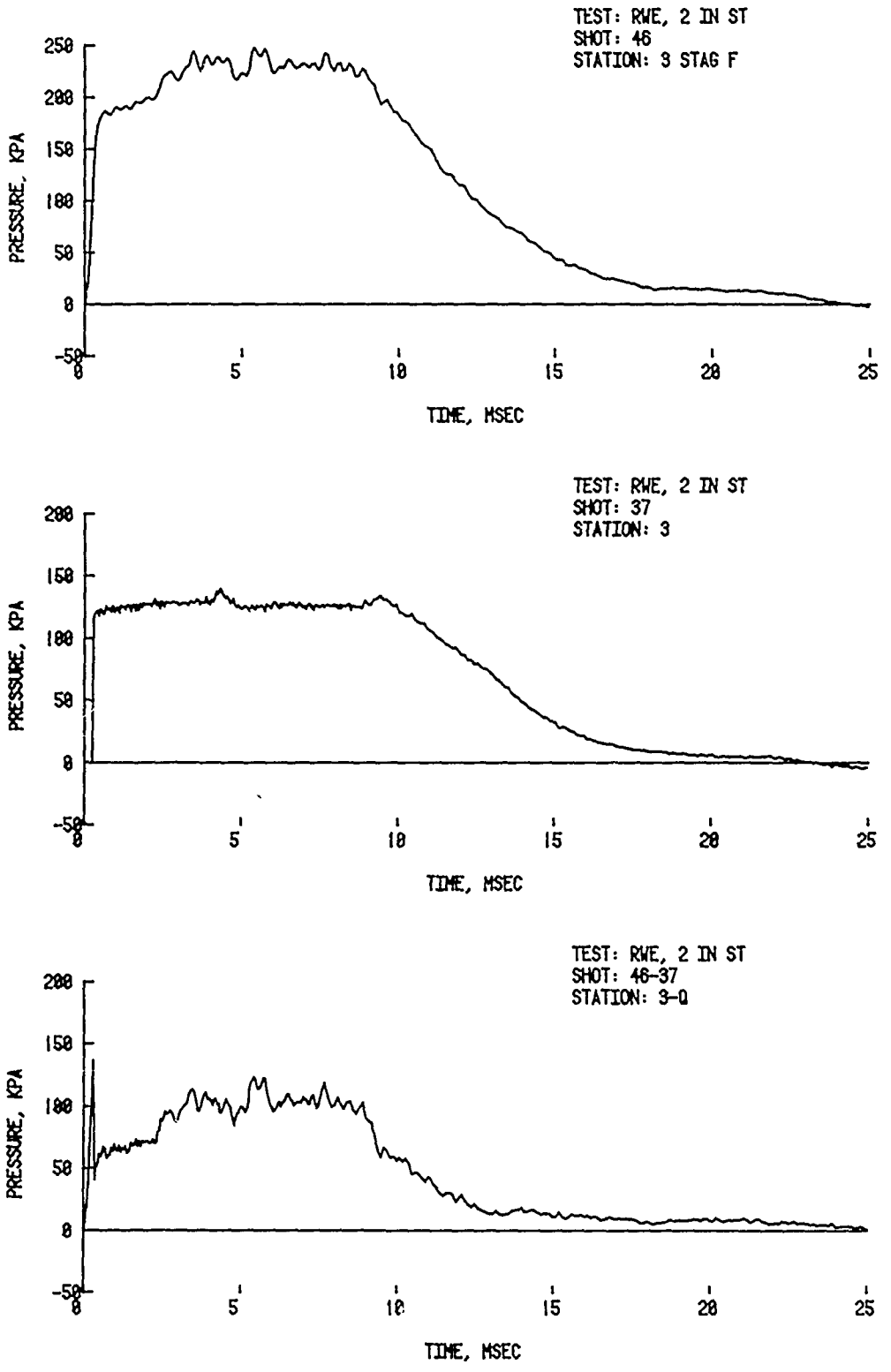

Figure A-3. (Continued) Pressure-time records for a single circular hole vented RWE

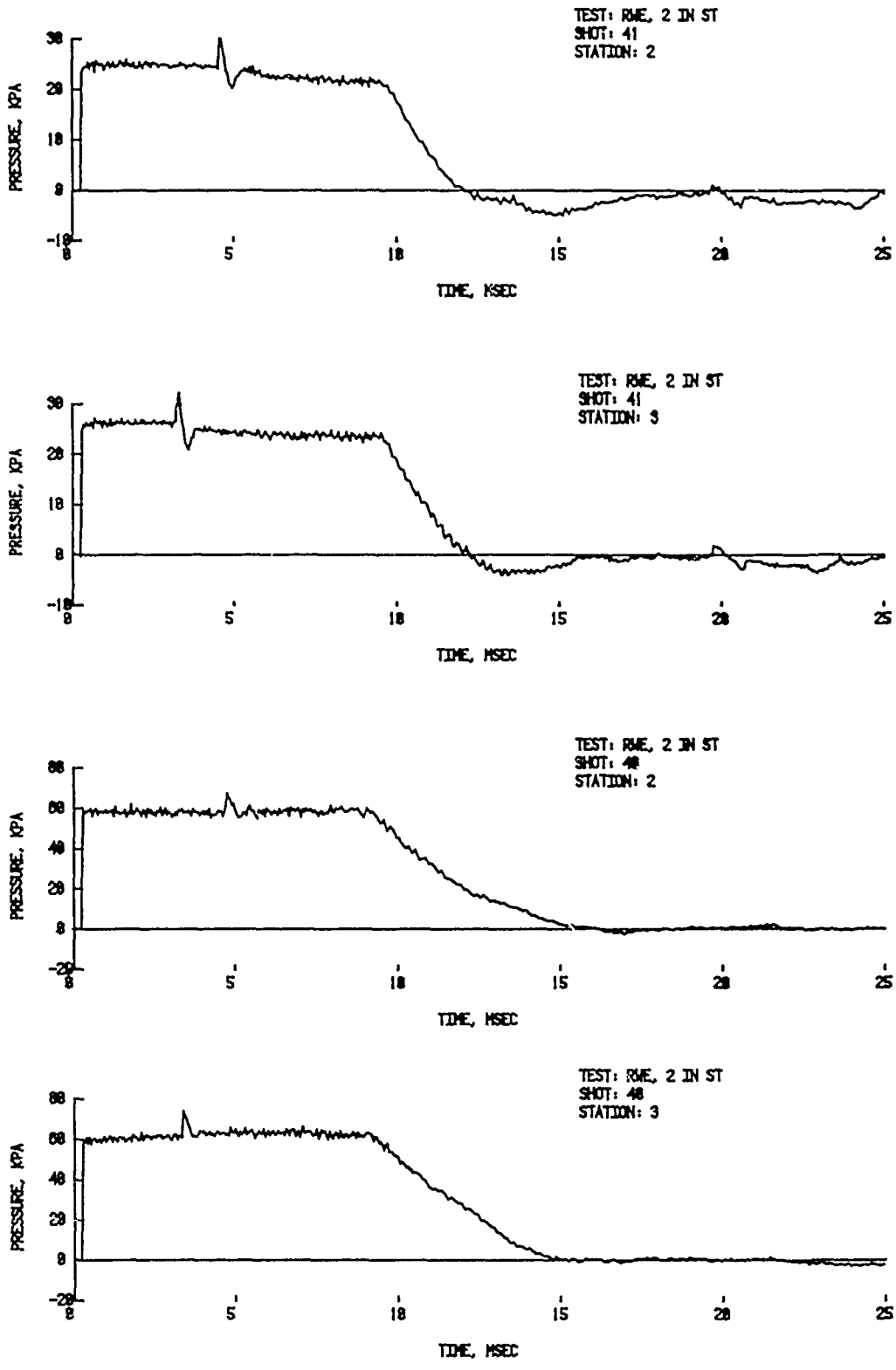

Figure A-4. Pressure-time records for circular vented RWE - 10 holes

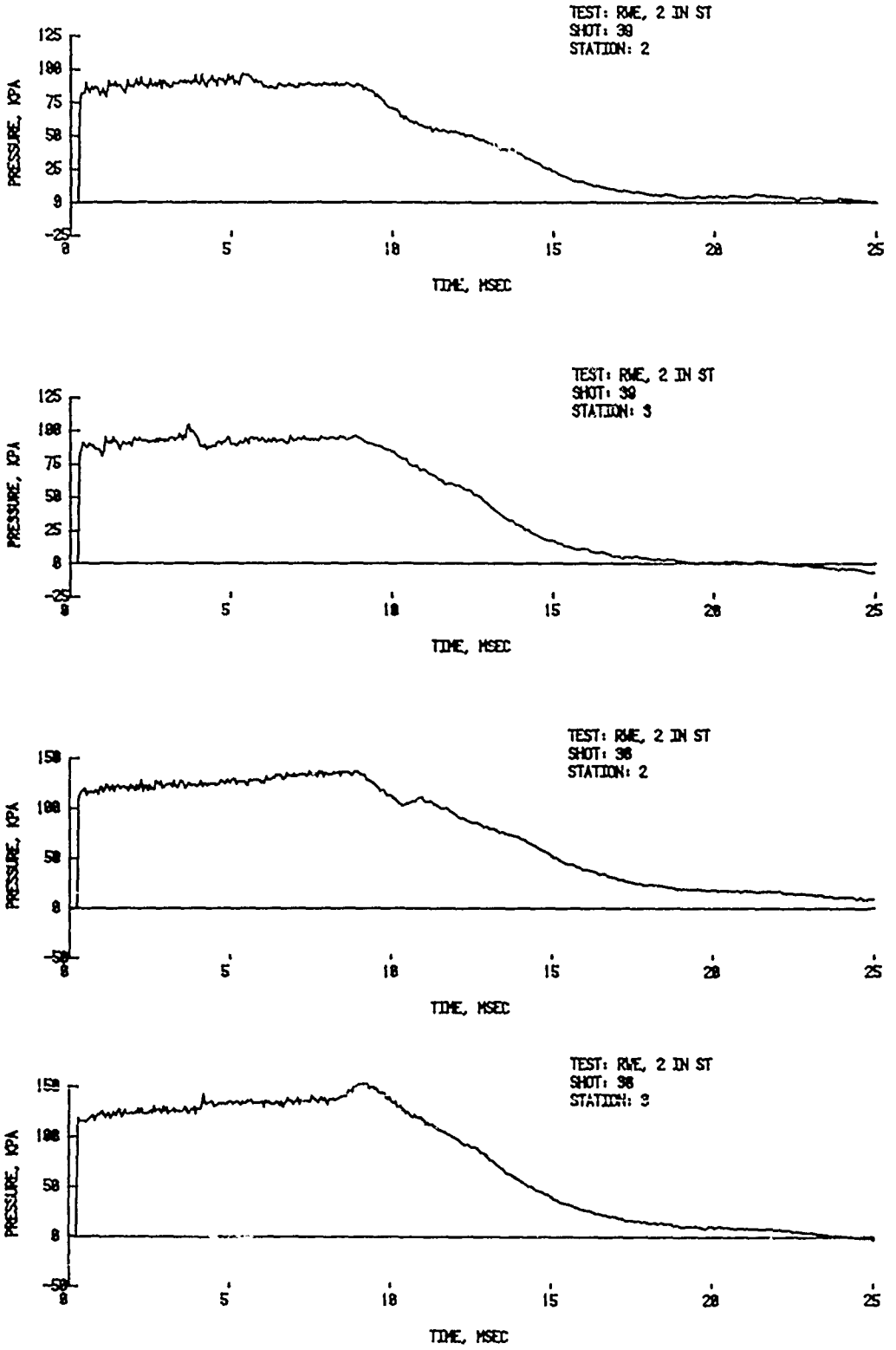

Figure A-4. (Continued) Pressure-time records for circular vented RWE - 10 holes

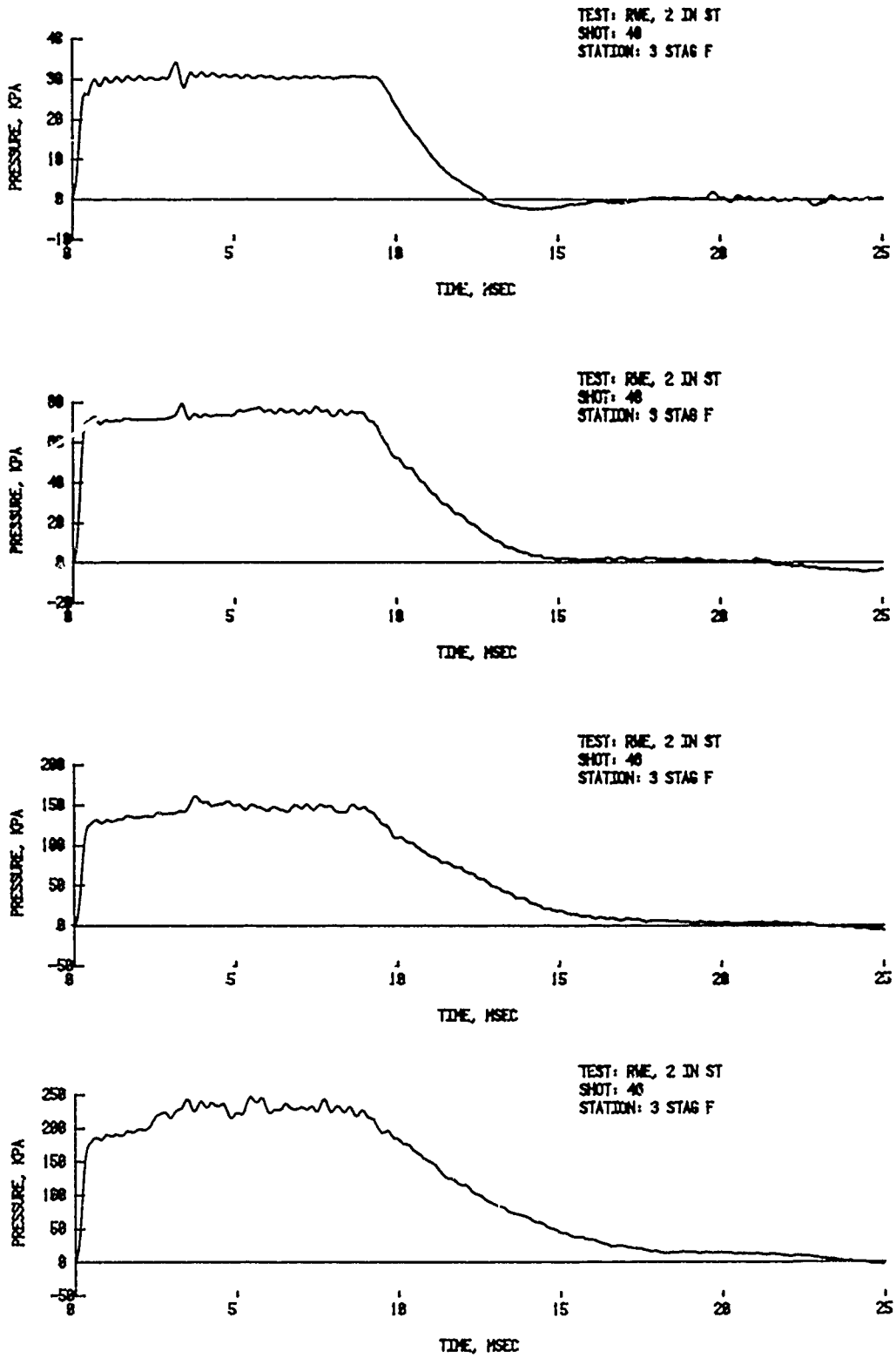

Figure A-4. (Continued) Pressure-time records for circular vented RWE - 10 holes

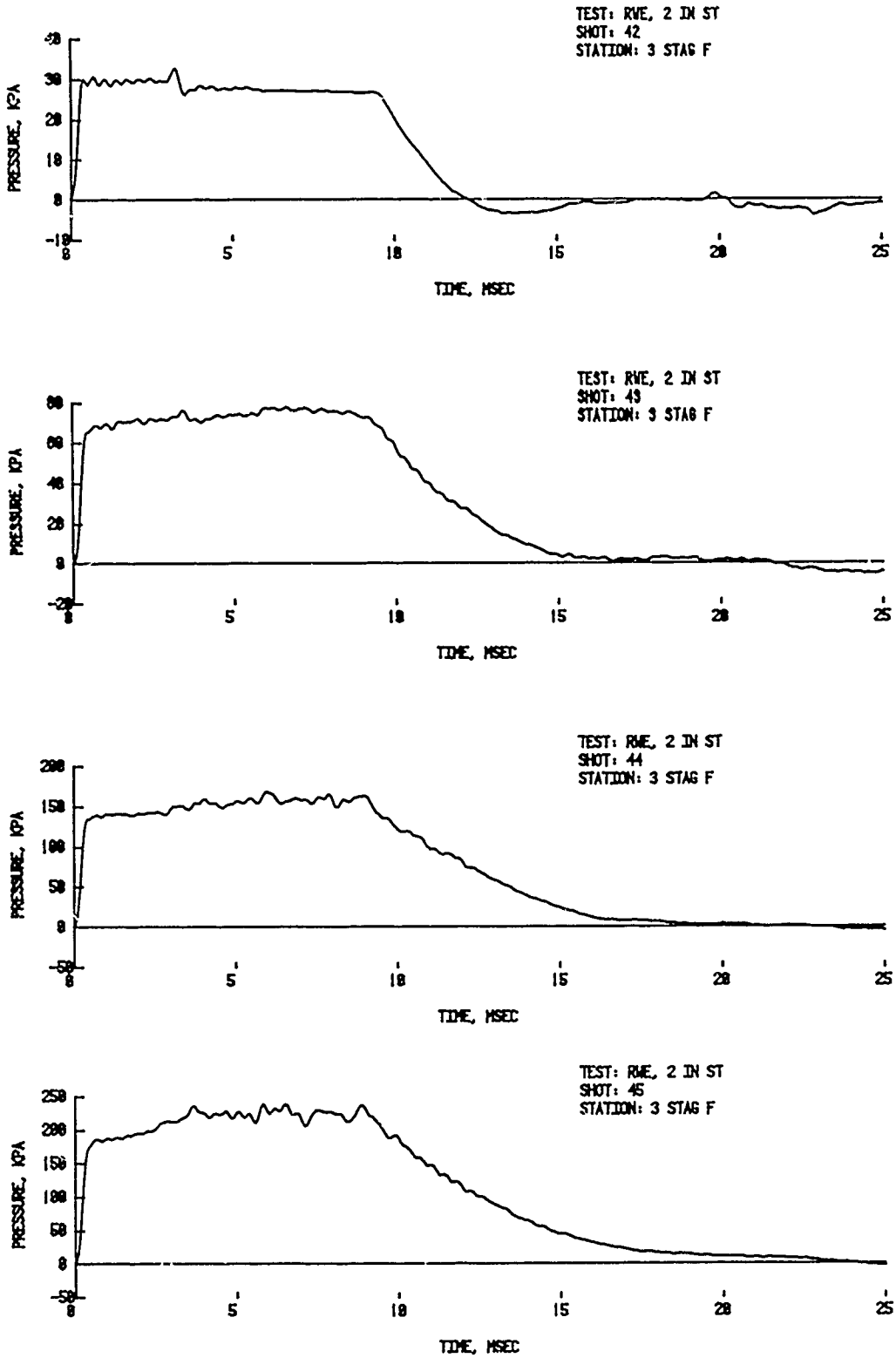

Figure A-4. (Continued) Pressure-time records for circular vented RWE - 10 holes

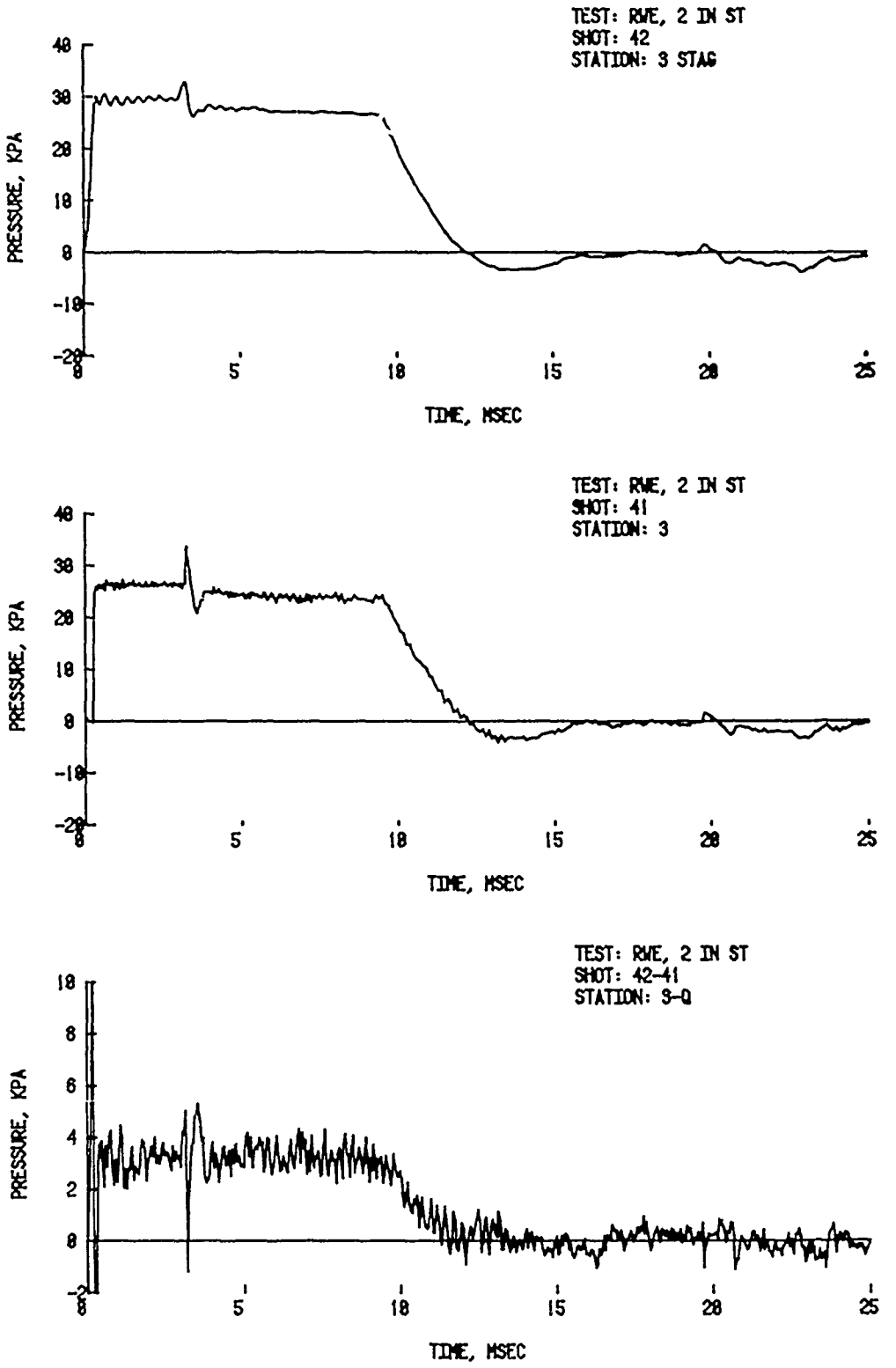

Figure A-4. (Continued) Pressure-time records for circular vented RWE - 10 holes

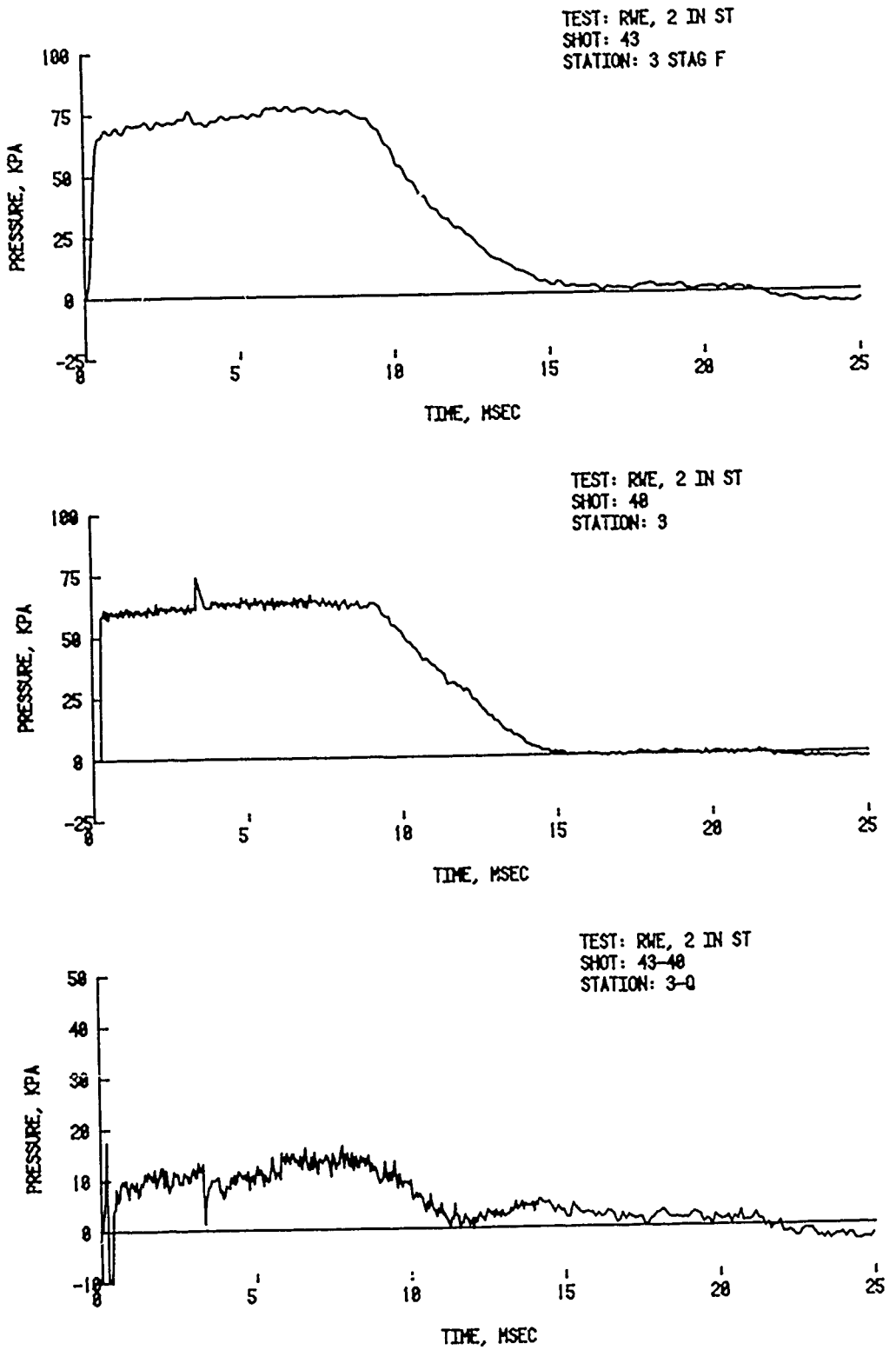

Figure A-4. (Continued) Pressure-time records for circular vented RWE - 10 holes

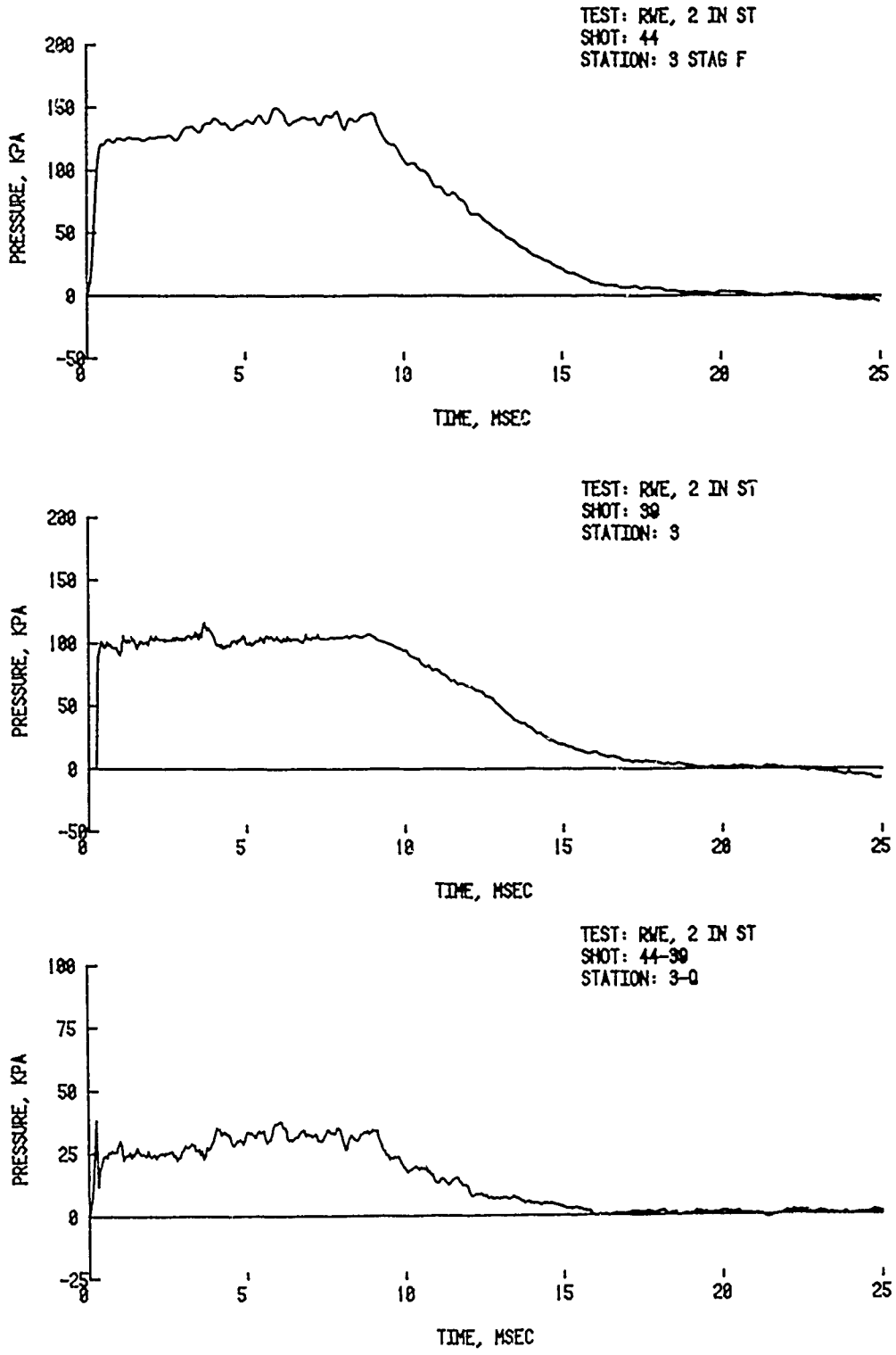

Figure A-4. (Continued) Pressure-time records for circular vented RWE - 10 holes

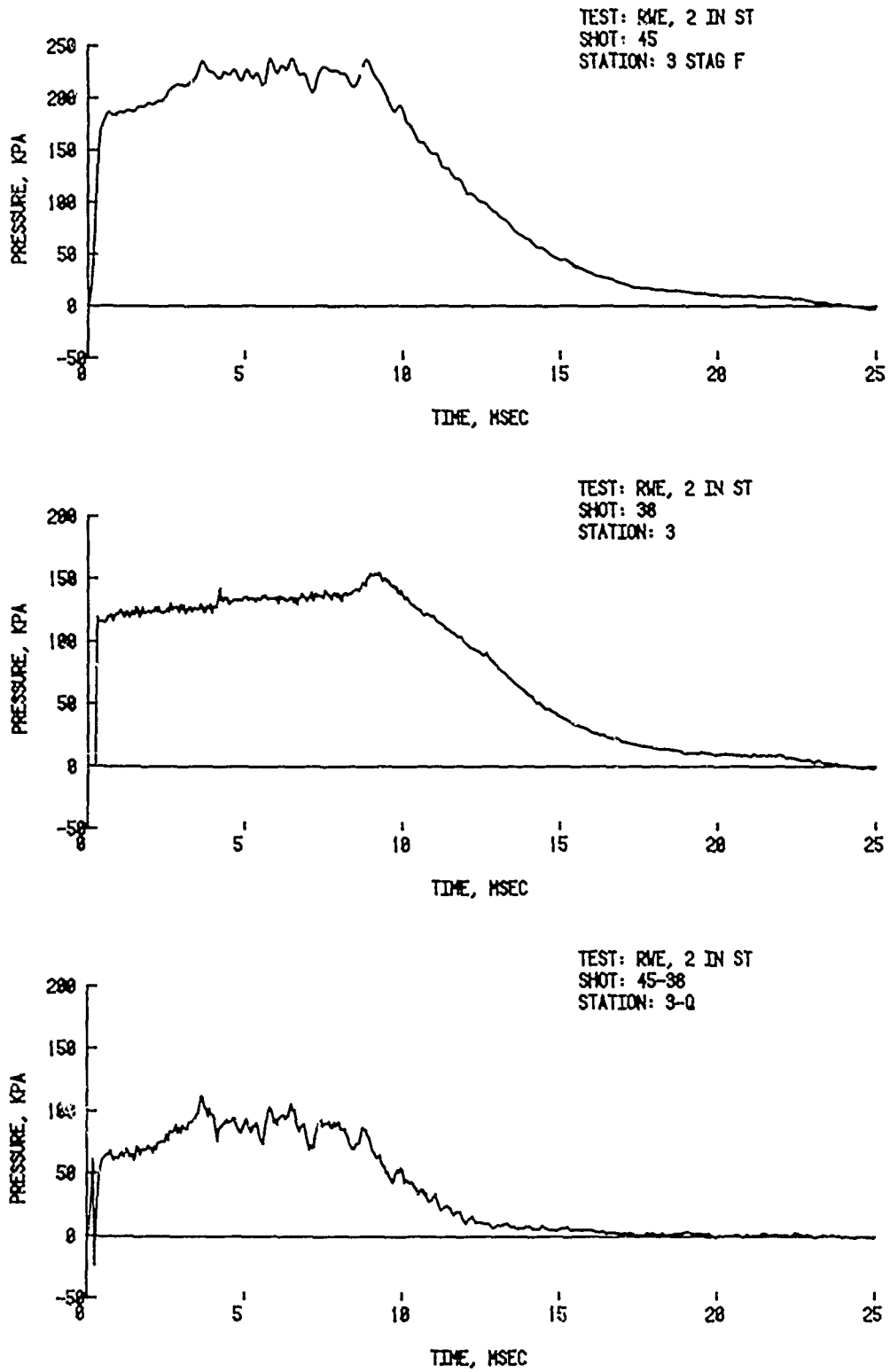

Figure A-4. (Continued) Pressure-time records for circular vented RWE - 10 holes

APPENDIX B

DRAWINGS OF ELIMINATOR FOR 2.44 m SHOCK TUBE

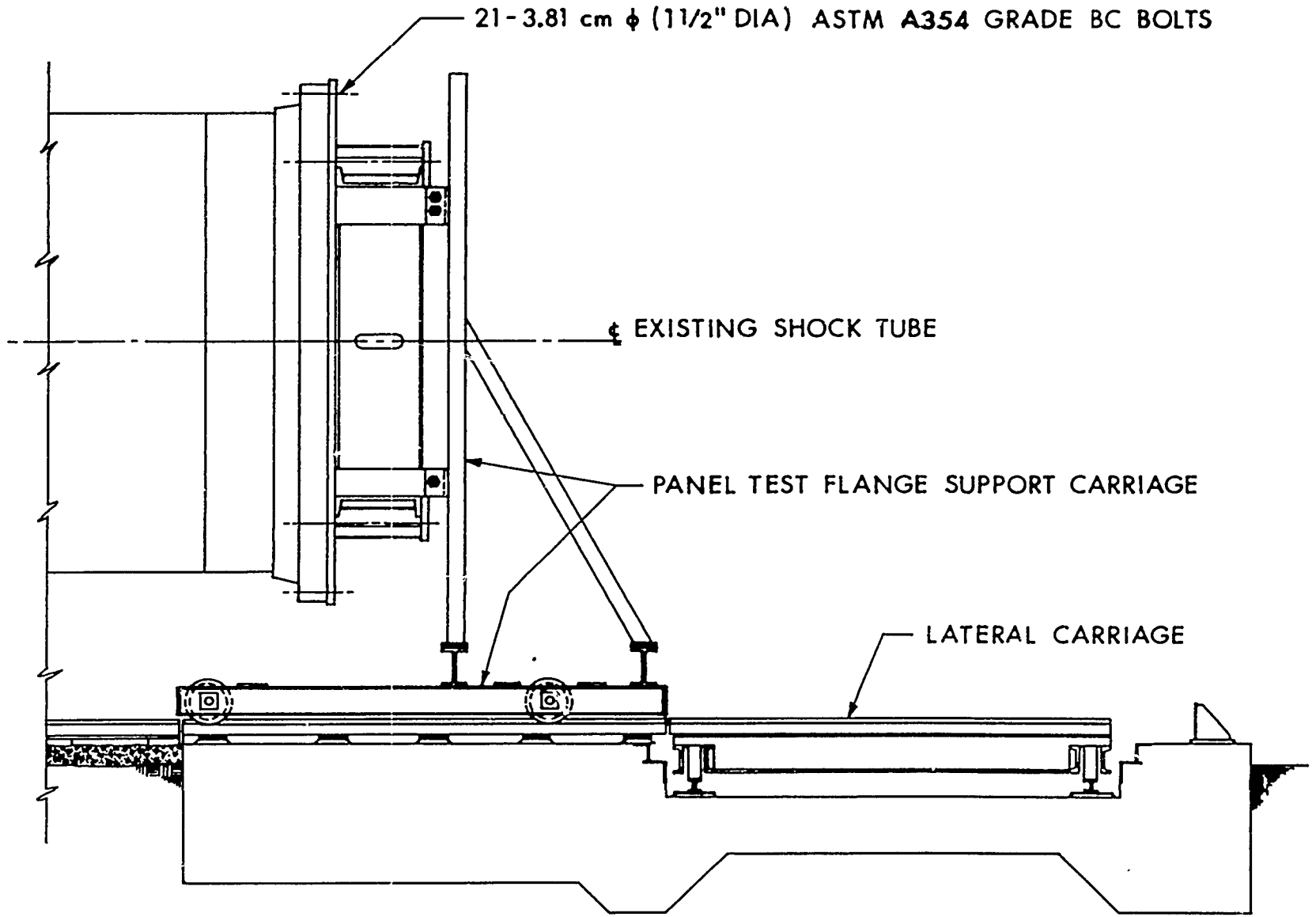

Figure B-1. Side View RWE

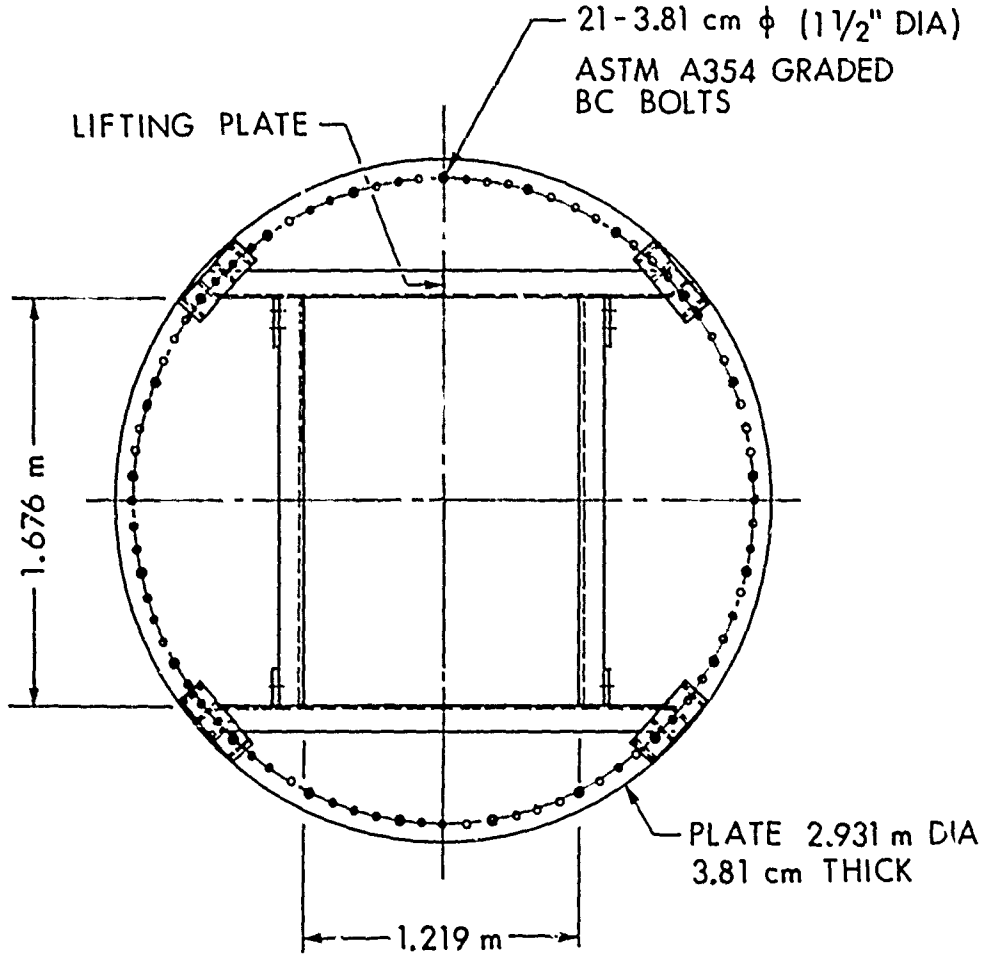

Figure B-2. End View RWE

DISTRIBUTION LIST

No. of Copies	Organization
12	Administrator Defense Technical Info Center ATTN: DTIC-DDA Cameron Station Alexandria, VA 22314
4	Director of Defense Research and Engineering ATTN: DD/TWP DD/S&SS DD/I&SS AD/SW Washington, DC 20301
3	Director Defense Advanced Research Project Agency ATTN: Technical Library NMRO PMO 1400 Wilson Boulevard Arlington, VA 22209
1	Director Defense Intelligence Agency ATTN: Mr. C. Wiehle Washington, DC 20301
8	Director Defense Nuclear Agency ATTN: STTL (Tech Lib, 2 cys) SPSS, Dr. K. Goering Dr. G. Ullrich DDST, COL Frankhouser (3cys) SPAS, Mr. D. Kohler Washington, DC 20305
2	Commander Field Command, DNA ATTN: FCTMOF Kirtland AFB, NM 87115
1	Commander US Army Armament Research and Development Command ATTN: DRDAR-TDC Dover, NJ 07801
1	Chairman DoD Explosives Safety Board ATTN: T. Zaker RM 856-C, Hoffman Bldg. I 2461 Eisenhower Avenue Alexandria, VA 22331
1	HQDA (DAMA-AR, NCB Division) Washington, DC 23010
1	Commander US Army Ballistic Missile Defense Program Office ATTN: DACS-SAE-S, J. Shea 5001 Eisenhower Avenue Alexandria, VA 22333
1	Commander US Army Ballistic Missile Defense Systems Command ATTN: SSC-DH P. O. Box 1500 Huntsville, AL 35807
3	Director US Army BMD Advanced Technology Ctr ATTN: Mr. B. E. Kelly Mr. M. Capps Mr. Marcus Whiteford P. O. Box 1500 Hunstville, AL 35804
2	Commander US Army Engineer Waterways Experiment Station ATTN: Library W. Flateau P. O. Box 631 Vicksburg, MS 39181
1	Commanding General Fleet Marine Force, Atlantic ATTN: G-4 (NSAP) Norfolk, VA 23511
2	Commandant US Army Infantry School ATTN: ATSH-CD-CSO-OR Fort Benning, GA 31905

DISTRIBUTION LIST

No. of Copies	Organization
1	Commander US Army Materiel Development and Readiness Command ATTN: DRCDMD-ST 5001 Eisenhower Avenue Alexandria, VA 22333
2	Commander US Army Armament Research and Development Command ATTN: DRDAR-TSS Dover, NJ 07801
1	Commander US Army Armament Materiel Readiness Command ATTN: DRSAR-LEP-L Rock Island, IL 61229
1	Director US Army ARRADCOM Benet Weapons Laboratory ATTN: DRDAR-LCB-TL Watervliet, NY 12189
1	Commander US Army Aviation Research and Development Command ATTN: DRDAV-E 4300 Goodfellow Blvd St. Louis, MO 63120
1	Director US Army Air Mobility Research and Development Laboratory Ames Research Center Moffett Field, CA 94035
1	Commander US Army Communications Rsch and Development Command ATTN: DRSEL-ATDD Fort Monmouth, NJ 07703
1	Commander US Army Electronics Research and Development Command Technical Support Activity ATTN: DELSD-L Fort Monmouth, NJ 07703
4	Commander US Army Harry Diamond Lab ATTN: DRXDO-TI/012 DRXDO-NP, F. Wimenitz J. Gaul J. Gwaltney 2800 Powder Mill Road Adelphi, MD 20783
1	Commander US Army Missile Command ATTN: DRSMI-R Redstone Arsenal, AL 35898
1	Commander US Army Missile Command ATTN: DRSMI-YDL Redstone Arsenal, AL 35898
1	Commander US Army Tank Automotive Command ATTN: DRSTA-TSL Warren, MI 48090
1	Commander US Army Foreign Science & Technology Center ATTN: Research & Data Branch 220 7th Street, NE Charlottesville, VA 22901
1	Director US Army Materials and Mechanics Research Center ATTN: Technical Library Watertown, MA 02172

DISTRIBUTION LIST

No. of Copies	Organization
3	Commander US Army Nuclear Agency ATTN: ATCN-W CDINS-E Technical Library 7500 Backlick Rd., Bldg. 2073 Springfield, VA 22150
1	Director US Army TRADOC Systems Analysis Activity ATTN: ATAA-SL White Sands Missile Range NM 88002
2	Chief of Naval Research Department of the Navy ATTN: T. Quinn, Code 461 J. L. Warner, Code 461 Washington, DC 20360
4	Commander Naval Surface Weapons Center ATTN: Code 1224, Navy Nuclear Programs Office Code 241 Code 730, Tech Library J. Pittman Silver Springs, MD 20910
1	Commander Naval Weapons Evaulation Fac ATTN: Document Control Kirtland AFB, NM 87117
1	Officer in Charge (Code L31) Civil Engineering Lab Naval Construction Battalion Center ATTN: Dr. W. A. Shaw, Code L31 Port Hueneme, CA 93041
3	Commander Naval Research Laboratory ATTN: M. Persechino G. Cooperstein Tech Lib, Code 2027 Washington, DC 20375
1	HQ USAFSC/SDOA (DLCAW, Tech Lib) Andrews AFB Washington, DC 20334
1	AFOSR (OAR) Bolling AFB, DC 20332
1	RADC (Document Lib, FMTLD) Griffiss AFB, NY 13440
5	AFWL (CA, Dr. A. Guenther; DYT, 4 cys) Kirtland AFB, NM 87117
1	SAMSO (Library) P.O. Box 92960 Los Angeles, CA 90009
2	AFTAC (K. Rosenlof; G. Leies) Patrick AFB, FL 32925
2	AFML (G. Schmitt, MAS; MBC, D Schmidt) Wright-Patterson AFB, OH 45433
2	Headquarters Energy Research & Development Administration Dept of Military Application ATTN: R&D Branch Library Branch, G-043 Washington, DC 20545

DISTRIBUTION LIST

No. of Copies	Organization
2	Director Los Alamos Scientific Lab ATTN: Dr. J. Taylor Technical Library P.O. Box 1663 Los Alamos, NM 87545
1	Director National Aeronautics and Space Administration ATTN: Code 04.000 Langley Research Center Langley Station Hampton, VA 23365
1	Director NASA Scientific & Technical Information Facility ATTN: SAK/DL P.O. Box 8757 Baltimore/Washington International Airport, MD 21240
1	President National Academy of Sciences Advisory Committee on Civil Defense ATTN: Dr. Donald Groves 2101 Constitution Avenue, NW Washington, DC 20418
1	Aerospace Corporation ATTN: Tech Information Svcs Building 105, RM 2220 P.O. Box 92957 Los Angeles, CA 90009
1	Agbabian Associates ATTN: Dr. J. Malthan 250 N. Nash Street El Segundo, CA 90245
1	AVCO Government Products Grp ATTN: Dr. W. Bade 201 Lowell Street Wilmington, MA 01887
1	AVCO-Everett Research Lab ATTN: Technical Library 2385 Revere Beach Parkway Everett, MA 02149
1	John A. Blume & Associates ATTN: Dr. John A. Blume Sheraton-Palace Hotel 100 Jessie Street San Francisco , CA 94105
1	Center for Planning and Research Inc. ATTN: John R. Rempel 2483 East Bayshore Road Palo Alto, CA 94303
1	Effects Technology, Inc. ATTN: E. Anderson 5383 Holister Avenue Santa Barbara, CA 93105
1	General Electric Co. - TEMPO ATTN: DASIAC 816 State Street; Drawer QQ Santa Barbara, CA 93102
1	General Electric Co. - TEMPO 7800 Marble Avenue, NE Suite 5 Albuquerque, NM 87110
1	H-Tech Laboratories, Inc. ATTN: B. Hartenbaum P.O. Box 1686 Santa Monica, CA 90406
1	Hughes Aircraft Company Systems Development Lab ATTN: Dr. A. Puckett Centinela & Teale Streets Culver City, CA 90230

DISTRIBUTION LIST

No. of Copies	Organization
1	Ion Physics Corporation ATTN: Technical Library South Bedford Street Burlington, MA 01803
1	Kaman-Nuclear ATTN: Dr. D. Sachs 1500 Garden of the Gods Road Colorado Springs, CO 80907
1	Kaman Avidyne, Division of Kaman Sciences ATTN: Dr. J. Ray Ruetenik 83 2nd Ave, NW Industrial Park Burlington, MA 01830
1	KTECH Corporation ATTN: Dr. Donald V. Keller 911 Pennsylvania NE Albuquerque, NM 87110
1	Lockheed Missiles & Space Co, Inc. Div of Lockheed Aircraft Corp ATTN: J. Nickell P.O. Box 504 Sunnyvale, CA 94088
1	Management Science Associates ATTN: Kenneth Kaplan P.O. Box 239 Los Altos, CA 94022
1	Martin Marietta Aerospace Orlando Division ATTN: A. Ossin P.O. Box 5837 Orlando, FL 32805
1	Maxwell Laboratories, Inc. ATTN: A. Kolb 9244 Balbao Avenue San Diego, CA 92123
1	McDonnell Douglas Astronautics Corporation 5301 Bolsa Avenue Huntington Beach, CA 92647
2	Merrity Cases, Inc. ATTN: J. L. Merritt Technical Library P.O. Box 1206 Redlands, CA 92373
1	H. L. Murphy Associates Box 1727 San Mateo, CA 94401
3	Physics International Company ATTN: Document Control Emil Kovtun (2 Cys) 2700 Merced Street San Leandro, CA 94577
3	R&D Associates ATTN: Technical Library Jerry Carpenter Allen Kuhl P.O. Box 9695 Marina del Rey, CA 09291
1	Sandia Laboratories ATTN: Dr. J. Kennedy Albuquerque, NM 87115
2	Science Applications, Inc. ATTN: Joseph McGahan Dr. John Cockayne 1710 Goodridge Dr., P.O. Box 1303 McLean, VA 22102

DISTRIBUTION LIST

No. of Copies	Organization
1	Systems, Science and Software ATTN: Technical Library P.O. Box 1620 La Jolla, CA 92037
1	Teledyne-Brown Engineering Cummings Research Park Huntsville, AL 35807
1	Union Carbide Corporation Oak Ridge National Lab ATTN: Technical Library P.O. Box X Oak Ridge, TN 37830
1	Battelle Memorial Institute ATTN: Technical Library 505 King Avenue Columbus, OH 43201
1	Director Applied Physics Laboratory The Johns Hopkins University Johns Hopkins Road Laurel, MD 20707
1	Lovelace Research Institute ATTN: Dr. D. Richmond P.O. Box 5890 Albuquerque, NM 87115
1	Massachusetts Institute of Technology Aerophysics Laboratory 77 Massachusetts Avenue Cambridge, MA 02139
1	New Mexico Institute of Mining and Technology ATTN: Mr. P. McClain Socorro, NM 87801
1	Northwestern Michigan College Traverse City, MI 49584
1	Southwest Research Institute ATTN: Dr. W. Baker 8500 Culebra Road San Antonio, TX 78228
1	Research Institute of Temple University ATTN: Technical Library Philadelphia, PA 19144
1	Texas Tech University Dept of Civil Engineering ATTN: Mr. Joseph E. Minor Lubbock, TX 79409
1	University of Arkansas Department of Physics ATTN: Prof O. Zinke Fayetteville, AR 72701
1	University of California Lawrence Livermore Lab Technical Library Division ATTN: Technical Library Dr. Donald N. Montan P.O. Box 808 Livermore, CA 94550
2	University of Denver Denver Research Institute ATTN: Mr. John Wisotski P.O. Box 10127 Denver, CO 90210
1	J. D. Haltiwanger Consulting Svcs B106a Civil Engineering Bldg. 208 N. Romine St. Urbana, IL 61801

DISTRIBUTION LIST

No. of Copies	Organization
1	University of Maryland Department of Physics College Park, MD 20742
1	The University of New Mexico Eric H. Wang Civil Eng'g Res Fac ATTN: Technical Library University Station, Box 188 Albuquerque, NM 87131
1	University of Oklahoma Department of Physics ATTN: Prof. R. Fowler 440 W. Brooks, Rm 131 Norman, OK 73069

No. of Copies	Organization
	Aberdeen Proving Ground
	Director, USAMSAA ATTN: DRXSY-D DRXSY-MP, H. Cohen Mr. R. Norman, GWD
	Cdr, USATECOM ATTN: DRSTE-TO-F
	Dir, USACSL Bldg E3516, EA ATTN: DRDAR-CLB-PA DRDAR-CLN DRDAR-CLJ-L

USER EVALUATION OF REPORT

Please take a few minutes to answer the questions below; tear out this sheet, fold as indicated, staple or tape closed, and place in the mail. Your comments will provide us with information for improving future reports.

1. BRL Report Number _____

2. Does this report satisfy a need? (Comment on purpose, related project, or other area of interest for which report will be used.)

_____

_____

_____

3. How, specifically, is the report being used? (Information source, design data or procedure, management procedure, source of ideas, etc.) _____

_____

_____

4. Has the information in this report led to any quantitative savings as far as man-hours/contract dollars saved, operating costs avoided, efficiencies achieved, etc.? If so, please elaborate.

_____

_____

5. General Comments (Indicate what you think should be changed to make this report and future reports of this type more responsive to your needs, more usable, improve readability, etc.) _____

_____

_____

_____

6. If you would like to be contacted by the personnel who prepared this report to raise specific questions or discuss the topic, please fill in the following information.

Name: _____

Telephone Number: _____

Organization Address: _____

_____

_____

FOLD HERE

Director
US Army Ballistic Research Laboratory
ATTN: DRDAR-BLA-S
Aberdeen Proving Ground, MD 21005

NO POSTAGE
NECESSARY
IF MAILED
IN THE
UNITED STATES

OFFICIAL BUSINESS
PENALTY FOR PRIVATE USE, $300

BUSINESS REPLY MAIL
FIRST CLASS PERMIT NO 12062 WASHINGTON, DC
POSTAGE WILL BE PAID BY DEPARTMENT OF THE ARMY

Director
US Army Ballistic Research Laboratory
ATTN: DRDAR-BLA-S
Aberdeen Proving Ground, MD 21005

FOLD HERE